OSLO METROPOLITAN UNIVERSITY
STORBYUNIVERSITETET

Master's Degree in
Structural Engineering and Building Technology
Department of Civil Engineering and Energy Technology

MASTER THESIS

TITLE	DATE
Modal identification and finite element model updating of railway bridges considering boundary conditions using artificial neural networks	June 9, 2021
	NUMBER OF PAGES
	86
AUTHOR	SUPERVISOR
Mohammadreza Salehi	Emrah Erduran

SUMMARY

Two-part study, with the evaluation of the variation in modal identification of two railway bridges located in Northern Norway based on free decay responses after the passage of different types of trains. In addition, performing the neural network based finite element model updating considering both rotational and translational stiffnesses of the boundary conditions to present the aging and constraining effect of the boundary conditions. The modal parameters of the finalized calibrated model were compared with the field-measured modal parameters to quantify the success of the model updating process.

KEYWORDS
Operational modal analysis
Railway bridge
Model updating
Boundary conditions

List of Contents

List of Figures

List of Tables

ABSTRACT

The accuracy of different operational modal analysis (OMA) methods and the variation of the identified modal parameters through the different excitation sources is of utmost importance in vibration based health monitoring and safety assessment of the structures. Also, since structural properties and the constraining effect of boundary conditions often change during the service life of the structures, improving the simulation ability of the finite element (FE) models considering these changes plays a vital role in the development of FE models to reflect the real behavior of the existing structure. Therefore, this thesis aims, firstly, to identify the modal parameters of the railway bridges using different OMA techniques and to evaluate the sensitivity of the identified modal parameters to the various train-induced excitation sources. Secondly, it tries to create an accurate FE model of the existing bridge using the artificial neural networks (ANNs) based model updating considering the additional rotational stiffness of the boundary conditions.

The case study structures are two railway bridges in Northern Norway, located on the Ofot line (*Ofotbanen),* as a part of a railroad carrying the iron ores mined in Kiruna, Sweden to the harbor in Narvik, Norway. Thus, the bridges are subjected to very high axel loads induced by iron ore trains. The first bridge is single-span with a length of 50 m, while the second has two spans with a total length of 85m.

To identify the modal parameters, two OMA techniques, FDD and SSI-COV, have been conducted on the various free vibration responses of the bridges caused by different train crossings including lightweight railway vehicles, loaded and unloaded iron ore trains to evaluate the variation of the identified modal parameters with the different methods and the various excitation sources.

The bridge properties, like material properties and boundary conditions, tend to alter due to aging, deterioration, and damage, and a high level of complexity and uncertainty may arise for parameter estimation tasks. As such, to perform the FE model updating (FEMU) ANN is used, as a powerful technique to find the hidden relationships, to estimate the modified properties of the bridge while the behavior of the boundary conditions is simulated by the use of both rotational and translational stiffnesses.

It was found that the results from FDD and SSI-COV, generally, were in a satisfactory agreement, while the identified modal parameters may differ from one train crossing to another, particularly frequencies were affected by the mass of the passing trains. The study also indicated the significance of the detailed behavior of the bridge supports, considering the rotational stiffness, in the success of the FE model updating.

ACKNOWLEDGMENTS

---

[1] https://www.banenor.no/

CHAPTER 1

Introduction

1.1   Preface

Safety assessments and requirements in the regulatory framework of structural engineering have created new engineering challenges for understanding the behavior of existing structures in the last few decades. During this time, the development of technology has led to an increase in traffic volumes and speeds, and heavier road and railway freight. This transportation development applies additional loads to the transportation network and infrastructure. Bridges, as a vital component of this infrastructure and one of the key transportation network elements, need to be reviewed and investigated under these new transportation situations. On the other hand, from the environmental point of view, it is of utmost importance to retain and use what we currently have rather than building and investing in new structures and projects. For example, instead of demolishing the old bridges and replacing them with new ones, we can preserve and upgrade them by using efficient monitoring, safety assessment, and rehabilitation methods.

In the Norwegian context, characterized by low seismic risk, some factors like aging, deterioration, the increased loads and traffic intensities are the major portion of problems that have adverse impacts on the durability and serviceability of the bridges. Numerous existing bridges are several decades old and being deteriorated, and their serviceability is also affected because of country developments and the growing need of society. Therefore, it is necessary to monitor the existing

bridges over time and correctly identify their dynamic behavior in order to assess their safety conditions.

Before doing anything else, a brief description of the research aim can help the readers to understand why OMA and FEMU are performed in this research. The cases studied are two railway bridges located on the Ofot line *(Ofotbanen)* a pivotal railroad that carries iron ore from Kiruna, Sweden to the harbor in Narvik, Norway. A new project is described to increase the axel load of trains crossing the bridges and carrying the iron ore, which means the bridges will be supposed to the new load patterns and higher traffic loads. Therefore, the main purpose of this thesis is to identify the dynamic characteristics of the bridges and calibrate the FE models reflecting the real behavior of the bridges. The updated FE model provides the opportunity for a reliable bridge safety assessment under current conditions and new serviceability. Therefore, the accurate modal parameters identification and a calibrated FE model matching the real behavior of the bridges perfectly, play a vital role in the safety assessment of these bridges.

Modal identification using the information and assumptions considered in the design procedure of the structures may not lead to identifying the real dynamic behavior of the existing structure, since some of these assumptions do not correspond perfectly to the characteristics of the constructed structures. Also, some structural characteristics will change gradually in the long run or due to damages. Therefore, a study is required to evaluate the current structural responses and identify the dynamic characteristics accurately. For this, operational modal analysis is highly beneficial to extract the modal parameters of the existing structures. After identification of the dynamic parameters, the finite element (FE) model updating technique can calibrate the FE model to match the existing structure. The accurate identification of the dynamic parameters and precisely calibrated FE model are necessary application tools for bridge safety assessment.

During the last few decades, modal analysis has increasingly been used in structural engineering to conduct identification processes and monitoring the dynamic characteristic of the structures. Modal analysis is aimed to determine the inherent dynamic characteristics of the structures in terms of natural frequency, damping ratio, and mode shapes. A particular type of modal analysis considered in this thesis is operational modal analysis (OMA). In the last few years, OMA has attracted attention in the identification of the modal parameters since it does not require excitation equipment and a controlled excitation and it can be performed under operational conditions without interrupting the use of the structure. During the measurements and vibration tests for

OMA, the structure is subject to its natural excitation, therefore the structure functionality is not compromised. In the case of bridges, the natural excitation can be lightweight vehicular traffics or wind. Based on this basic assumption, OMA does not require shaker or impact tests, and this advantage allows the test and analysis to be conducted over a long period without interrupting the operability of the structure and it makes it possible to perform a long term monitoring of the structure.

In this thesis to perform the OMA, the covariance-driven stochastic subspace identification (SSI-COV) method and the Frequency Domain Decomposition (FDD) method are utilized. They are popular methods of OMA that operate in the time and frequency domain respectively.

The model updating attempts to match the initial FE model with the results extracted from field measurements. The FE model updating calibrates the mathematical model prior to and after structural parameter changes and the damages. The model prior to damage can be a benchmark for following safety assessment and damage detection. In order to update the FE model, many methods and algorithms have been developed by researchers. Due to some simplifications, assumptions, modeling errors, and uncertainties, achieving an accurate updated FE model is not easy. In some structures, particularly complicated structures with several parameters to be updated, high level of uncertainties and complexity, in the case of using the manual calibration strategy, analytical results from the FE model are less likely to match perfectly the results extracted from field-measured results. Therefore, in this thesis, an attempt is made to apply an advanced FE model updating method using Artificial Neural Networks (ANNs), which is composed of numerous interconnected processing elements working parallelly together with weighted connections to solve specific problems. ANN is a robust technique that can be used reliably and efficiently for estimation tasks under a high level of complexity and uncertainties, in the case of structures these uncertainties and complexities can stem from aging and deterioration of the structures. Network training is implemented to adjust the weight connections between neurons. A training dataset is required to train the network which is generated by performing several FE simulations and changing the values of the critical structural parameters identified by a sensitivity analysis.

Thus, by means of tools and methods discussed widely later in the following chapters, the modal identification procedure of two concrete railway bridges is performed, and the modal calibration of the FE model is carried out to match the results obtained experimentally.

1.2 Problem definition and research question

The studied bridges in this research are two prestressed concrete bridges, built in the 1980s, on the Ofot line *(Ofotbanen)* a crucial railroad that carries iron ore from Kiruna, Sweden to the harbor in Narvik, Norway. Therefore, the bridges are subjected to the very high axel loads induced by the iron ore trains. A new project has been described to increase the axel load of trains carrying the iron ore, which means higher traffic loads and a new load pattern for the bridges. This higher axel load can have adverse impacts on the bridge properties especially boundary conditions and change them in the long term. Also, with respect to the age of the bridges, it is predictable that bridge properties and boundary conditions have been affected by aging and deterioration. For this purpose, evaluation of the current conditions of the bridges is required to show that the safety of the bridges will be satisfied under the new load pattern. That is why this study is undertaken to identify the modal parameters of the existing bridges and generate the updated FE model considering the real behavior of the boundary conditions.

To identify the bridge modal parameters, although OMA can be highly beneficial, this technique suffers from some limitations on input excitation. On the on hand, using different types of excitation sources may lead to significant variation in identified modal parameters, and estimation of modal parameters may exhibit variability between results from different OMA methods. On the other hand, in OMA the input force or excitation is assumed to be uniform random white noise that has a uniform distribution all over the structure [1] and this assumption is not always true and can have adverse impacts on the modal identification process.

During the FE model updating process, determining the proper updating parameters plays a crucial role in the success of the model updating process. On the one hand, inserting extra parameters cause more computational cost and may lead to error. On the other hand, missing some key parameters probably results in the estimation of unrealistic values for other parameters. To update the FE model successfully and reliably, considering the actual behavior of the boundary conditions is one of the critical parameters. The boundary conditions of the studied bridges have been definitely affected by aging and high axel loads of iron ore trains. Therefore, it is very difficult, if not impossible, to create an accurate updated FE model without a proper boundary conditions simulation.

With respect to the above-mentioned deficiencies and drawbacks, the main concerns of this thesis are focused on the variation of identified modal parameters of the railway bridges, and choosing the proper parameters for FE model updating focusing on the boundary conditions. The main research questions can be presented as follows;

– *Is there any significant variation in the identified modal parameters by the use of different input excitations and OMA algorithms?*

– *Can we trust the initial FE model based on the design assumptions and drawings to perform the safety assessment of the existing structures?*

– *What are the real boundary conditions of the actual railway bridges affected by aging, deterioration, or unaccounted factors of bridge construction?*

1.3 Aims of research

The outstanding aim of the present thesis is to evaluate the variation of the identified modal parameters and choosing the most effective parameters of the railway bridges to be used in FE model updating. It can be divided into three distinct parts.

– Evaluation of the variation in modal identification of the railway bridges using different free vibration responses caused by train passage.

– Evaluation of identified modal parameters extracted from the different OMA algorithms.

– Calibration of FE model considering boundary conditions behavior with a focus on the rotational stiffness of the supports.

1.4 Limitations

Almost all experimental researches involve limitations and difficulties. The most important limitations in this study can be mentioned as:

– *Limited number of sensors.* The optimum location and number of sensors on the instrumented structure are of substantial importance in the quality of the identified modal parameters. In this study, just five triaxial accelerometers were deployed on the bridges, between two bridge ends. Despite the importance of sensor installation at the supports to monitor the responses at these points, no sensor was installed at this location due to mentioned limitation.

- *Quality of the data recorded.* The quality of the identified parameters is often compromised by poor signal-to-noise ratios. During the data recording in this research, the acceleration responses have suffered from poor signal-to-noise ratios and the ambient excitation is completely dominated by noises.

- *The period of data recording.* Although data recording was performed for a period of 24-hour for each bridge including ambient and train-induced vibration, a large portion of this recording is unusable due to the low quality of the data that is mentioned above.

- *Lack of design documentation and drawings.* This limitation caused deficiencies in the FE model updating since documents and drawings of the design level can be beneficial for initial computer simulation and initial estimation of the updating parameters values. Also using an initial FE model can be helpful for the modal identification process since it can provide a quick first insight into the modal parameters.

1.5 Overview of chapters

Chapter2 offers an overview of modal identification and FE model updating methods and their applications to the bridges. Then, there is a description of the OMA focusing on Frequency Domain Decomposition (FDD) and Covariance-driven Stochastic Subspace Identification (SSI-COV) methods. In the following, the ANNs method and FE model updating using the ANNs technique are described.

Chapter3 provides the description of the methodology aimed at performing the operational modal analysis and choosing the free vibration responses of the bridges as the excitation in OMA. Also, it describes the methodology of selecting the updating parameters and suitable neural network architecture.

Chapter4 describes the studied bridges and provides detailed information about the identified modal parameters, in both vertical and transverse directions, extracted by FDD and SSI-COV methods. The variation of the extracted modal parameters using different train crossings is evaluated, also this chapter evaluates the effect of train properties in terms of mass on the OMA results.

Chapter5 consists of the finite element model updating process using artificial neural networks. The sensitivity of the natural frequencies of the bridge to different parameters is evaluated to identify the most sensitive parameters in model updating. The model updating process is performed with a focus on boundary conditions behavior considering the rotational stiffnesses in addition to the translational stiffnesses.

Chapter6 presents general conclusions and observations obtained through the research carried out during the master thesis. Concurrently, a few suggestions for future research works are briefly pointed out.

CHAPTER 2

Overview of Modal Parameter Identification and Finite Element Model Updating

2.1 Introduction

Every structure is subjected to degradation, whether it is a building, a bridge, or other types of structures. Some damages occur in the long run such as corrosion-induced cracks in concrete and some are caused by accidents like the earthquake. In all damage cases, the key structural parameters affecting the structural behavior, such as material property and boundary conditions, often change during the structure's service life, even these changes can be caused by rehabilitation of the structures. On the other hand, changes in serviceability of the structures might alter the type of excitations involving the structures, in terms of characteristics and intensity, and cause unexpected structural behavior. These unknown phenomena make it difficult to identify and predict the actual behavior of the existing structure based on previous numerical modeling and computer simulation. Information obtained from the original design of the structures, testing of the materials in the laboratory, and visual inspections hardly provide enough and perfect information of current structure situations to develop a numerical model that presents the real structural behavior to fulfill the aim of safety assessment.

To satisfy the need to have access to the real information of the actual behavior of the structure, modal identification through dynamic measurements and the finite element (FE) model updating

method using identified modal parameters have been developed and become popular methods that can update the initial FE model based on the identified modal parameters to permit reliable simulation for structural performance assessment.

2.2 Modal parameters identification

Over time, evaluation of the dynamic responses of the structures has become increasingly necessary in different parts of engineering applications. Dynamic analysis and evaluation of the modal parameters can be utilized in different professional aspects of structural engineering including design of the structures, structural health monitoring (SHM), and damage detection. The evaluation of the structural dynamic response becomes more complex regarding the big and complex structures like bridges. One of the main aims of the structural dynamic analysis is the modal parameters identification including natural frequency, mode shapes, and damping ratio. Modal parameters are inherent characteristics of the structures which can be used as the indicators presenting the current safety condition of the structure [2,3].

2.2.1 Modal analysis

Modal analysis is the determining process of inherent dynamic characteristics of a structural system in terms of natural frequencies, mode shapes, and damping ratios. A modal model presents the structural dynamical behavior as a linear combination of different resonant modes. Each resonance mode is characterized in the form of modal parameters. Modal analysis embraces theoretical and experimental techniques. A theoretical modal analysis uses a physical model of the structural system consists of the mass, stiffness, and damping ratio. Finite element analysis can be the most used physical modal analysis technique. The experimental-based modal analysis is performed by use of data obtained from experimental tests and developing mathematical relationships to extract the modal parameters [4]. In some experiments in the laboratories and in-situ tests, input data are known, and they can be adjusted and measured. Therefore, by measuring the dynamic responses of the structure, all input and output data are available and it is possible to find the relation between them. But it should be considered that in many practical projects, measuring the input data is difficult, if not impossible, and the only available data is dynamic responses of the structure. In these types of tests with unknown inputs, in order to identify the

modal parameters, an analysis is required using just the output data (response of the structure) to identify the modal parameters [5].

Experimental Modal Analysis (EMA) and Operational Modal Analysis (OMA) are two techniques using the structural dynamic responses to identify the modal parameters. The type of excitations, or input data, is the key difference between these two techniques. EMA or classical modal analysis requires both measured input data and dynamic responses. Some excitation devices such as impact hummers or shakers provide controlled excitation forces and these excitations are measurable. Conversely, in OMA the excitation forces are unavailable and they are not measured and this is the most outstanding feature of operational modal analysis. This advantage of OMA can be of great importance when it comes to the testing of massive structures like bridges and high-rise buildings since these types of structures are not easily excited artificially and they need a large excitation to be vibrated efficiently [5].

2.2.2 Experimental modal analysis (EMA)

EMA identifies the modal parameters of the structures using the known input excitation and measured dynamic responses (see Figure 1). The excitation can be induced by shakers or impulse hammers as shown in Figure 2. Although using these devices has the benefit of providing wide-band input frequencies that allow different modes to be excited and identified [6], there are some critical drawbacks. Firstly, the use of shakers and other excitation devices may apply the additional load on the lightweight structures and cause the error in the results. Secondly, since these artificial excitations are not able to reflect completely the real operational conditions, in some cases the results obtained in the lab or by artificial excitation may differ from the results under operational conditions. Thirdly, it is difficult, if not impossible, to excite large size of structures efficiently since input excitation has insufficient energy to excite all modes [7,8].
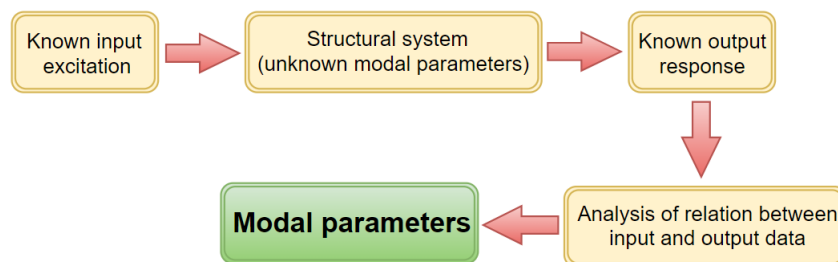
Figure 1. Experimental Modal Analysis [8].

In the vibration test, there is a set of input and output measurements. These signals are transformed from the time domain to frequency domain, and linear spectra of the input excitation and output responses are calculated. Power spectra are obtained from linear spectra, and averaging is performed on them. To calculate the modal parameters, two crucial functions of Frequency Response Function (FRF) and coherence function are computed from the relation between the controlled applied inputs and measured outputs. The coherence function is used to assess the data quality, which identifies how much of the output signals are related to the measured input signal. The FRF is a relationship between vibration response at one location and excitation at the same point or different location as a function of the excitation frequency. A complete set of frequency responses (FRFs) is formed by a combination of the excitations and responses at different locations. FRFs can be presented in matrix form which is usually symmetric and illustrates the reciprocity of the structure under test. FRF provides important information regarding the frequency and damping of the system, and mode shapes can be obtained from a set of FRFs at measured locations [9].
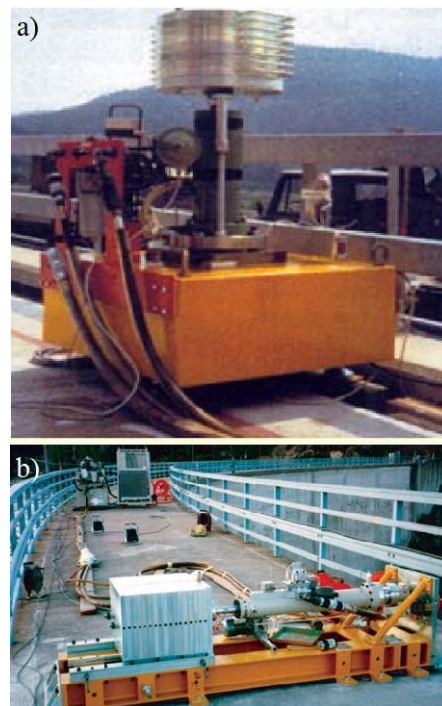
Figure 2. Application of hydraulic shakers to excite the: a) bridges; b) dams [6].

2.2.3 Operational Modal Analysis (OMA)

Although EMA can be performed as an efficient method to identify modal parameters, controlled excitation in this test requires equipment that makes it costly, and to excite the large-size structures an impossibly large amount of excitation force is required. Since in OMA no specific excitation equipment is required, this method has been developed rapidly and paid attention increasingly to apply to the vast range of structures, therefore over the past two decades, EMA has been replaced by OMA in many engineering applications [10]. Since OMA aims to identify the modal parameters of the structures using only structural responses in operational conditions, it is also known as the output-only modal identification method (see Figure 3).

Some advantages of OMA can be mentioned as follows [11]:

- OMA does not need excitation tools and it is less expensive in comparison to EMA.
- OMA enables obtaining the dynamic characteristics of the whole system in the actual environment and operational condition.
- Since ambient excitation can be caused by different sources, OMA is a very suitable technique for modal characteristic identification of complex structures since the analysis is Multi-Input Multi-Output (MIMO), and close modes are identified easily.
- OMA does not interfere in the functionality of the structure and is suitable for long-term vibration-based health monitoring and damage detection of the structures.
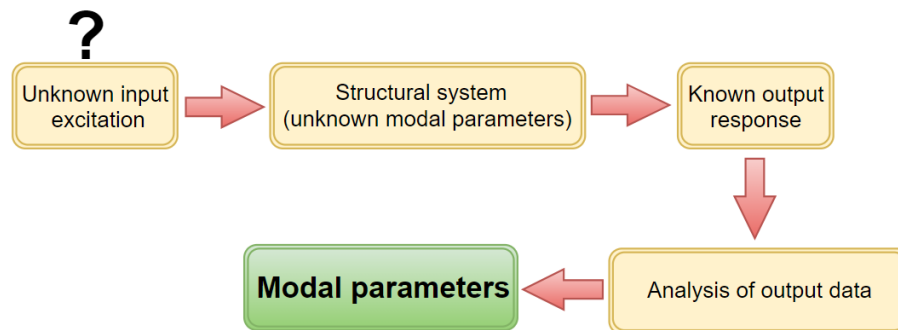
Figure 3. Operational Modal Analysis [8].

The theoretical basis of the OMA has been studied largely and developed in both the frequency- and time-domain. Historically the OMA method has been derived from the EMA technique so that basic equations in OMA are similar to EMA mathematically. OMA method in time-domain approach is based on analysis of the time histories response or the correlation functions, while frequency-time approach identifies the modal parameters by using the power spectrum density

(PDS) functions of output responses [12]. As mentioned before, input excitation data is unknown in OMA and it is mostly impossible to be measured, unlike EMA. Therefore, for simplicity, OMA needs some assumptions that should be considered. OMA is performed under assumptions of stationary excitation, system linearity, the lightly damped structure, and broadband white noise input signals with a Gaussian distribution that has a constant power spectrum density and this excitation is applied to the structure uniformly [12,13].

Several OMA techniques in both time and frequency domain have been developed. The peak picking (PP), the frequency domain decomposition (FDD), and the enhanced frequency domain decomposition (EFDD) methods can be mentioned as the most common techniques in the frequency domain. Regarding time domain, Natural Excitation Technique (NEXT), Stochastic Subspace Identification (SSI), Auto-Regressive Moving Average (ARMA), and Eigensystem Realization Algorithm (ERA) comprise the most common techniques in the time domain [14,15].

2.2.3.1 Frequency domain decomposition (FDD) method

FDD algorithm is an improved version of the Peak Picking (PP) method. The PP method is the simplest frequency-domain method and one of the first OMA methods that identify the modal parameters as the peaks of the output response spectrum [16]. The main assumption in PP and FDD is that in the vicinity of peaks or response frequencies, the cross-spectra or power spectral density (PDS) is dominated by the contribution of vibration modes so that each peak is representative of a vibration mode as shown in Figure 4., and the contributions of other modes are negligible in this peak.

The basic concepts behind the FDD method in form of Complex Mode Indication Function (CMIF) have been proposed by Shih et al. [17], then a complete definition of this method was proposed by Brinckler [18,19]. This method starts with the computation of the cross-spectral matrix and the key idea behind is the identification of the contribution of each vibration mode to the total spectral magnitude contained at the corresponding frequency. The singular value decomposition (SVD) method is the mathematical tool that enables such operation. The response spectra can be separated into a set of single degree of freedom systems (SDOFs) by introducing a decomposition of the spectral density function matrix. The associated mode shape of the resonance peak, or rather the natural frequency, is extracted as the corresponding first singular vector [19,20].
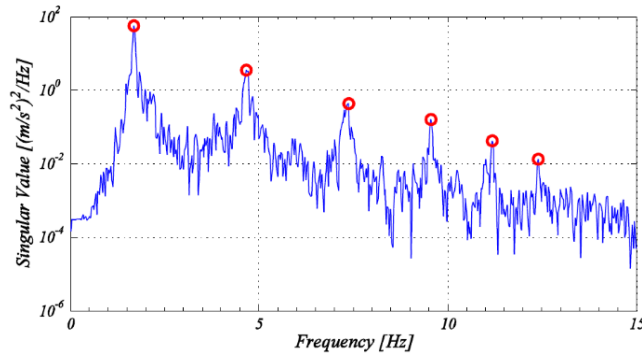
Figure 4. The first singular value of PDS matrix and the example of the peak selection [21]

It is necessary to define an indicator that is able to distinguish different vibration modes. For this purpose, identification of the modal domain can be helpful as it covers a frequency band around each resonance peak. The modal domain around each peak is described by the correlation between the singular vector of the resonance peak and singular vectors associated with frequencies around that peak [22]. The correlation can be done by Modal Assurance Criterion (MAC) that is a statical indicator and sensitive to differences in mode shapes. The MAC is also used to pair the mode shapes obtained from analytical models with those extracted experimentally. The MAC is calculated as the normalized scalar value of two vectors, $\{\varphi_A\}$ and $\{\varphi_B\}$, and the results are arranged into the MAC matrix [23]:

$$MAC = \frac{|\varphi_A{}^T \varphi_B|^2}{(\varphi_A{}^T \varphi_A)(\varphi_B{}^T \varphi_B)} \tag{1}$$

The MAC value ranges between 0 (representing no consistent correspondence) to 1.0 (representing complete consistent correspondence). To identify the acceptable neighboring values belonging to the modal domain, a threshold MAC level should be introduced. The small MAC values indicate the poor resemblance of the two mode shapes while values larger than 0.9 indicate consistent correspondence [23].

FDD is a user-friendly and fast identification method that can be used in many engineering applications especially for initial investigation due to low computational load, however, the FDD method suffers from a limitation that cannot identify damping ratio. For this purpose, the FDD technique is followed by the Enhanced Frequency Domain Decomposition (EFDD) method that is able to identify all modal parameters (natural frequency, damping ratio, and mode shape) [19].

In frequency-domain methods, measured signals are transformed from the time domain into the frequency domain through the Fourier transform. During this process, many data need to take the average value, which causes problems including overlapping and mixing, leakage, low resolution, and spectrum loss. The transformation of time-domain data into frequency-domain data will inevitably have an adverse impact on the accuracy of identification methods [24].

2.2.3.2   Covariance-driven Stochastic Subspace identification (SSI-COV) method

The time-domain methods identify the modal parameters using the time domain signal data directly. In comparison with the frequency domain methods, they have higher accuracy [25]. The stochastic subspace identification (SSI) method is a time-domain method considered as one of the most powerful OMA algorithms. The subspace method allows the identification of the state space matrices based on the measurements using numerical techniques such as singular value decomposition (SVD), least squares, and QR-factorization [26]. The covariance-driven stochastic based algorithm derives inspiration from the classical theory explained by Ho and Kalman [27]. Since it is beyond the scope of this thesis to explain details about the stochastic subspace identification method, the interested reader can refer to the literature [25,26].

SSI-COV method uses a stabilization diagram as a part of the modal identification process. The stabilization diagram is a plot of different model orders versus the identified frequencies in each model order, in this diagram frequencies are plotted in the x-axis and model order as y-axis, as shown in Figure 5.
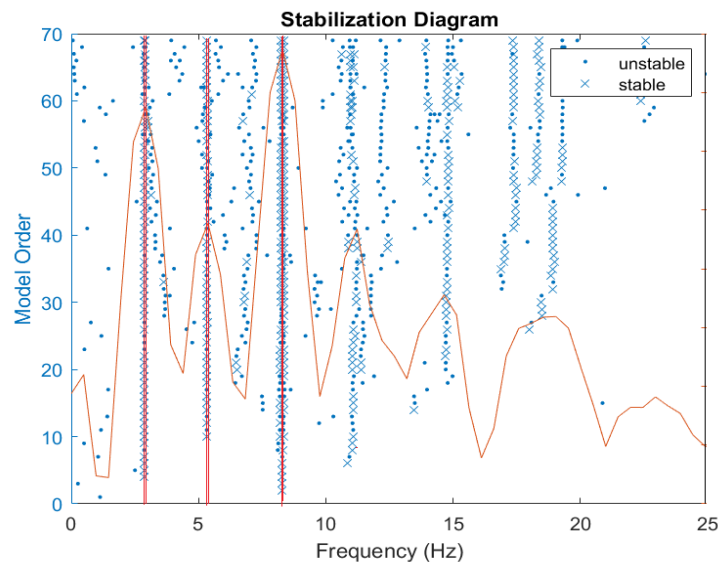
Figure 5. Stabilization diagram associated with the SSI-COV method.

In the stabilization diagram, the physical modes appear with consistent frequencies, damping ratios, and mode shapes at different model orders while spurious modes tend to be more scattered and show erratic behavior. This diagram is very valuable in separating the true system poles from the spurious numerical poles. Corresponding poles to a model order are compared with those of the former model order, then the stable and unstable poles are determined and plotted with different symbols depending on the following criteria [28]:

$$\frac{(f(n) - f(n+1))}{f(n)} \times 100\% < \delta_f$$

$$(1 - MAC(n, n+1)) \times 100\% < \delta_\emptyset \qquad (2)$$

$$\frac{(\xi(n) - \xi(n+1))}{\xi(n)} \times 100\% < \delta_\xi$$

Symbols of f, $\emptyset$ and ξ represent the frequency, mode shape, and damping ratio, and $\delta_f, \delta_\emptyset$ and δ_ξ are the stability limits of f, $\emptyset$ and ξ to separate the stable poles from unstable ones. Therefore, physical modes are identified from the alignments of stable poles as shown in Figure 5 with red lines.

Spurious modes can be categorized as noise modes and mathematical modes. Noise mode can arise due to physical reasons such as measurement noise and characteristics of excitation while mathematical modes are caused by an overestimation of the model order. Most of the spurious modes often do not fulfill the stabilization criteria, but some spurious modes may fulfill the stabilization criteria and have stable poles. In this case, spurious modes can be distinguished according to physical criteria, for instance, an expected range of damping ratio [28].

2.2.4 Application of OMA to the bridge structures

In recent years, a variety of OMA algorithms have been developed and numerous studies have been conducted on modal parameter identification of the bridges using different OMA techniques to compare their performance and evaluate their accuracy. A wealth of case studies of the application of OMA to bridge can be found in literature and only a small portion of them are presented here.

Chen et al. [29] investigated modal parameters of an eleven-span concrete bridge subjected to weak ambient excitation by measuring the acceleration responses. The main goal of their study

was the investigation of the reliability and feasibility of the modal identification under weak ambient excitation. They employed three OMA techniques, namely the peak picking (PP), the frequency domain decomposition (FDD), and the data-driven stochastic subspace identification (SSI-data) method. Despite the weak ambient excitation, nine lateral and three vertical modal frequencies below 10 Hz were extracted. Although there was no marked scattering in identified natural frequency values, related to damping ratios an outstanding dispersion was observed in the results. Comparison of the identified modal parameters with a numerical modal analysis demonstrated that several higher-order vertical modes were missed from all experimental results. In addition, FDD and SSI methods missed the fundamental lateral modes. They concluded that in order to obtain the preliminary results and quick evaluation, the PP and FDD methods can be useful and for detailed and comprehensive analyses both SSI and FDD can be used.

Lorenzoni et al. [30] evaluated five different types of road and railway bridges and used different identification methods including EFDD, SSI-COV, and SSI-UPC. They analyzed the results of the ambient and free vibration tests. It was observed that identification of the parameters is affected by the length of the acquired time history and the type of the structure. For railway bridges with a lightweight structure, the wight of the train may have a significant effect on the dynamic response, and modal identification is affected due to change in overall mass. All identification techniques had good accuracy and time-domain methods reflected less sensitivity to time history length. The coefficient of variation of standard deviation for damping estimation for the first mode in flexible bridges was between 10% and 25% and it was much higher, around 50%, for stiffer bridges, generally higher uncertainties were observed for stiff bridges and in the case of short acquired time history.

Silva and Neves [31] investigated a three-span concrete railway bridge under excitation caused by a group of people jumping over the bridge. They deployed 2 accelerometers in each span and one accelerometer at each end of the bridge, 8 accelerometers were mounted totally on the bridge. They compared the modal parameters extracted from the SSI method with numerical modeling developed in CSiBridge software. Due to the lack of simultaneous excitation in all three spans, identification of the high order modes was not possible that shows the importance of the excitation energy. Considering the small excitation caused by people, their study showed a reliable level of the results in modal identification using the SSI method.

Jin et al. [32] conducted a study on Songhuajiang River highway-railway bridge. They extracted the first ten natural frequencies of the bridge by using two OMA methods (ERA and SSI). Comparing the results with numerical simulation showed that identified modal frequencies by two time-domain methods are in good agreement with the results obtained from numerical analysis. The maximum difference between the results obtained by SSI and ERA with numerical analysis was 8% and 6% respectively and they presented two substantial reasons for these differences. The first is attributed to differences between numerical simulation assumptions and actual situations of the bridge such as boundary conditions. The second is related to the limitation in the number of measuring points as they deployed just 6 sensors in order to measure the responses in this study.

Pedrosa et al. [33] assessed the safety condition of an old bridge, Portela Bridge, to find a reliable solution for rehabilitation. After modal parameters identification, the numerical simulation was calibrated based on identified modal parameters. Modal identification was performed by two methods namely EFDD and SSI with ARTEMIS commercial software. In comparison with numerical analysis, both methods had some missing modes and there was a good agreement between the extracted results from the two methods, and the difference between the results of the two methods was less than 2%.

Magalhaes et al. [34] applied four modal identification techniques in both frequency and time domain including PP, FDD, SSI-COV, and SSI-data to identify modal parameters of the international Guadiana cable-stayed bridge, which links Portugal and Spain. They compared the identified modal parameters with corresponding modal parameters obtained from a numerical model. They observed a low range of variation for frequency and mode shapes while a large scatter of damping ratios was found.

He et al. [35] identified modal parameters of Alfred Zampa bridge, by processing the accelerations data, the bridge was a newly built suspension bridge with no previous traffic loads or seismic excitation. Finally, the identified natural frequencies and mode shapes are compared with the bridge FE model. They applied three different identification methods, ERA, SSI, and EFDD. Two types of tests, ambient and forced vibration tests were performed and a very good agreement was observed between the natural frequencies and mode shapes obtained by using three types of techniques, except for the first antisymmetric vertical mode. This difference is caused by the low relative contribution of this mode to the measured vibration in both vibration tests. Regarding the identification of the damping ratio, higher values of damping ratio were obtained from the forced

vibration test compared with modal damping ratios identified from the ambient vibration test. The relative differences in the identified damping ratios by using three methods are larger than the relative differences of corresponding identified natural frequencies. The reason originates from the uncertainties involved in the identification of damping ratios which are higher than uncertainties of the corresponding natural frequencies.

Gönen and Soyöz [36] applied multiple methodologies for the modal identification of the masonry arch bridges with large stiffness and low signal-to-noise ratio. Since the frequency content was affected by a high level of noise, and spurious resonant peaks appeared in the frequency spectrum, preprocessing of the signal was highly required. Due to the high uncertainties, large stiffness, and inherent complexity of masonry bridges, they applied different identification algorithms in the frequency and time domain to have a better understanding of the modal parameters. The results revealed a satisfactory level of estimations for natural frequencies and damping ratio extracted from all methods, despite the fact that the estimation of the damping ratio tended to be relatively subjective. By contrast, mode shape identification was a demanding task of their study and they suggested a three-dimensional visualization to have better mode shapes.

2.3 Finite Element Model Updating (FEMU)

2.3.1 Safety assessment approaches

Understanding the capacity and performance of the structures during their serviceability plays a vital role in the safety assessment of the structures. To perform the structural safety assessment, two main approaches have been used [37]:

- non-model-based approach
- model-based approach

The non-model-based approach is based on the signal processing of data extracted from the in-situ and experimental tests. In this method, dynamic flexibility measurements, matrix update methods, modal analysis, and wavelet transform techniques are used to determine the structural vibration changes to identify the damage and assess the safety condition [37,38].

A model-based approach is based on the mathematical description and computer simulation of the structure such as a finite element (FE) model. The first step in the model-based approach is creating

an initial model according to the design level data and documents or initial investigation. In many cases, the initial structural model cannot reflect the actual responses of the real structure perfectly. These discrepancies between field-measured and computer simulation responses can be caused by the damages, errors in measurements and modeling, or the changes in structural properties that happen in the long run [39]. To avoid these shortcomings and improve the FE model precision, Finite Element Model Updating (FEMU) techniques were developed so that the updated FE model reflects the real structural behavior.

In the FEMU process, the experimental data and in-situ testing results are considered as the targets. Then, by changing the assumptions and parameters of the initial FE model, the results of the FE model are calibrated to obtain a high level of matching between the FE model output and the existing counterpart. This updated model, reflecting the real structural behavior, can be utilized for safety assessment [40]. In Figure 6 the general steps of modal parameter identification and finite element model updating are presented.

The presence of the errors in the FE model and data acquisition in experimental tests are inevitable and these errors have an adverse impact on model updating accuracy. In addition, choosing suitable structural parameters to be modified and updated is of great importance. By choosing those parameters that are not determinant of structural behavior, the model updating process is likely to drive some structural parameters to unrealistic values. For this purpose, a sensitivity analysis can be performed to determine the parameters with the least and highest sensitivity to structural responses [39].
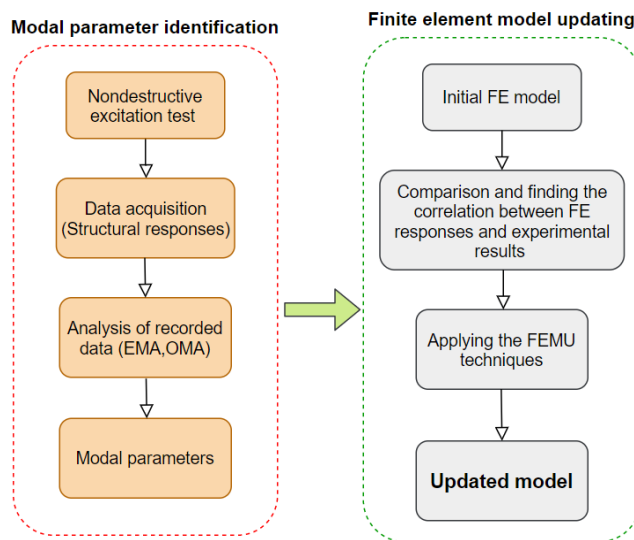
Figure 6. Process of modal parameter identification and model updating [38].

2.3.2 Finite Element Model Updating techniques

The finite element model updating can be categorized into two main classifications [41]:

- Non-iterative techniques (Direct)
- Iterative techniques (indirect)

Direct techniques can be used as a solution to update the model in just a single step. This non-iterative method can be efficient from the computational point of view, and it is of importance as a time-saving factor to reduce the computational cost [40]. Although this technique has some advantages, many drawbacks are making this technique difficult to use. The main drawback of these techniques is that they require accurate measurements and a high-quality modal testing and analysis procedure [41]. Iterative techniques update the structural parameters and material properties during each iteration to reduce the mismatch between responses of the experimental and FE model. The general algorithm for the iterative methods is presented in Figure 7.

For updating process, an error function is defined and minimized during each iteration step. The iteration process can be stopped when the difference between updated parameter values, in two iterations in a row, reaches an acceptable level. Since these methods require several iterative procedures, some problems related to divergence can arise during the iterative procedure. Also, these methods are computationally less efficient compared with direct techniques. Generally, iterative methods are utilized more for model updating [40].

The iterative technique emerged in 1974 by Collins et al. [42]. They developed an iterative eigendata sensitivity technique named Inverse Eigen Sensitivity Method (IESM). In the IESM technique, an error function is formed by modal data (damping ratio, eigenvectors, and eigenvalues). Modal analysis of measured FRFs is used for the extraction of modal data. So, the accuracy of the identified modal parameters is of great importance to avoid errors in modal identification results. For this, the measured FRFs can be used directly for model updating using Response Function Method (RFM). In RFM, unlike the IESM method, there is no need for modal extraction. In RFM, the results are highly affected by the existence of noises in signals. Therefore, RFM has inefficient performance in presence of noise [43].
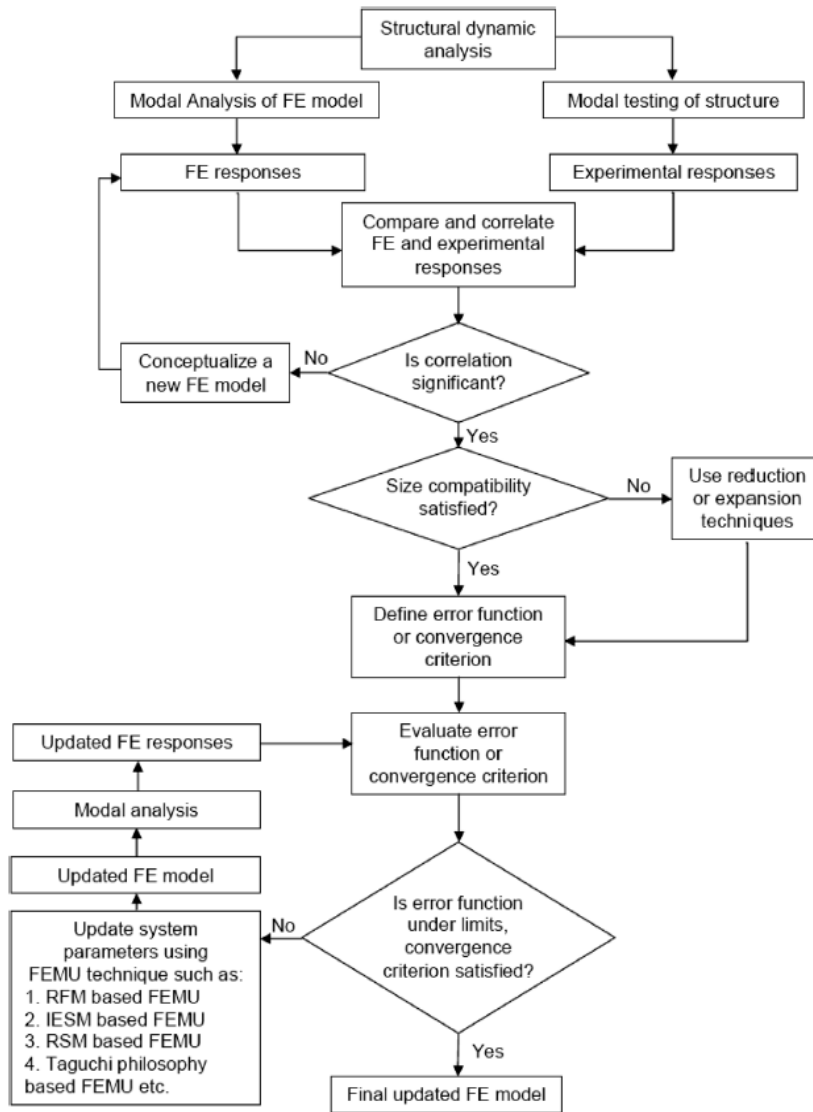
Figure 7. Algorithm for iterative model updating techniques [40].

In terms of complex and big structures like bridges, some problems make the model updating procedure difficult. Regarding the complicated conditions of the structure such as unknown damages, geometrical complexity, non-linearity effects, and measurement errors, some techniques may be inefficient for accurate model updating. For these types of structures, optimization and artificial neural networks (ANNs) methods can be efficient and more accurate. The most common optimization approaches are the methods based on the mathematical gradient or evolutionary algorithm such as the Genetic Algorithm (GA). ANN is also a robust technique for FE model updating of complex structures [40]. In ANN-based model updating, the network is trained and validated using responses of the different FE model simulations. When the training process is

performed by sufficient training data, the experimental responses can be used as the input of the network, and the trained network is able to estimate the updated parameters of the structure. The main limitation of ANNs is that it requires a large number of training data. For instance, if 'a' is the number of updating parameters and 'b' is the number of values that updating parameters can take, the number of training data will be 'ab' [40]. Since in this thesis ANN is used as the FE model updating technique, it is described more comprehensively as follows.

2.3.3 Artificial Neural networks (ANNs)

Artificial Neural Networks (ANNs) have been inspired by the biological nervous system. ANN has the ability to learn from events and experiences as the training data and to make a decision based on new observations. This feature of ANNs is of great importance to find the hidden relationships in a data set. A trained network can classify and examine new data sets that are in the same characteristics as the training dataset. ANNs can be highly beneficial, where extraction of the formula and explicit relationship between dataset data is difficult, if not impossible. This high potential capability of ANNs makes this technique suitable to be applied to various applications such as classification, identification, pattern recognition, and image processing [44].

During the last decade, ANNs have been developed as a powerful FEMU technique. The network learns from the existing patterns (training data) by capturing the relationships between a set of inputs and outputs, then the trained network can make a prediction for those patterns which are not considered during the learning procedure [45]. The most widely used network model in structural engineering applications is a multi-layered feed-forward neural network. A typical feed-forward neural network is formed from an input layer, an output layer, and one or more hidden (inner) layers as presented in Figure 8. Each layer consists of neurons that are interconnected in a feed-forward way. In a feed-forward way, connections are in a single direction and there is no connection between neighbor/other neurons in a layer. How to choose the number of hidden layers and neurons in these layers is still a question and open topic for research and there is no persuasive reason assuring that a network with two or more hidden layers has better performance than a network with one hidden layer. Also, using more neurons and hidden layers results in a high computational cost [46].

As shown in Figure 8, there are connections between each neuron in a layer to all neurons of the previous and subsequent layers except for the input layer that has connections just with the

subsequent layer. All connections are weighted and all neuron outputs from the previous layer are received as an input to each neuron in the subsequent layer. A nonlinear transformation of the weighted sum of the incoming inputs is performed by neurons and then outputs are produced and transformed to other neurons in the subsequent layer. Finally, in the output layer, these neurons' outputs are outside the network and they are considered as the final results [45,47]. The nonlinear transformation between neurons is conducted by activation functions. The activation function determines how the weighted sum of the input in a neuron is transformed into an output from the neuron [47]. In Figure 9 the most used activation functions in ANNs are presented.

The training process is implemented to adjust the weight connections between neurons. During this process, the training dataset (input data) is recurrently presented to the network. At each presentation, the network output is computed based on the current value set of weight coefficients, and the output of the network is compared with the desired output. The error between the desired and computed output is calculated and fed back to the network to adjust and update the weight coefficients [46]. The back-propagation algorithm, used in this process, is the most common and efficient algorithm of fine-tuning the weights of a neural network that is based on the rate of error obtained in the previous iteration and rearranging the error by spread to backward [46,47].
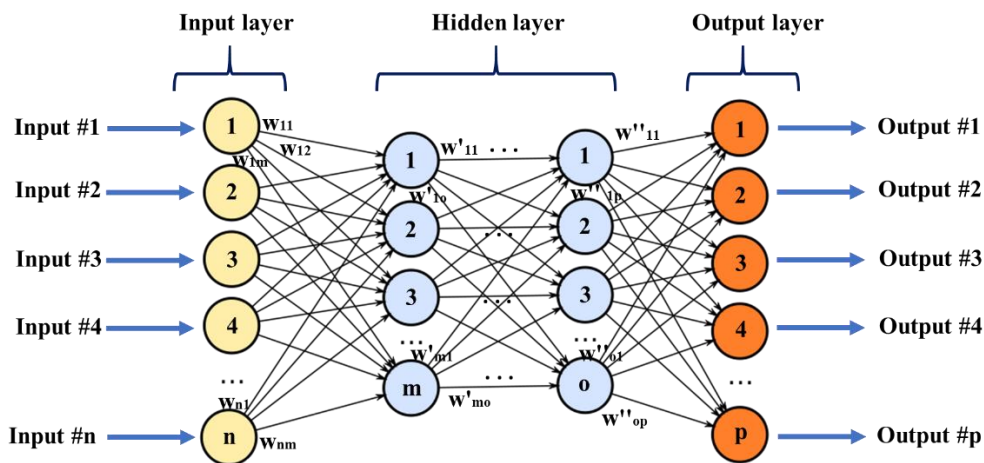
Figure 8. Neural network architecture.

The prediction performance of a network depends on many factors including the network architecture (number of layers and neurons), training process, network parameters, the complexity of the training dataset as well as the quality of the training dataset. Generally, an extensive parametric evaluation using a trial and error approach is required to reach the best performance of the network.
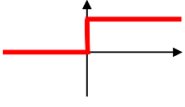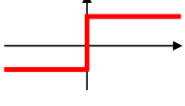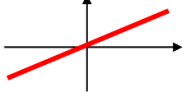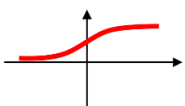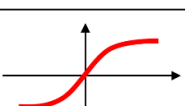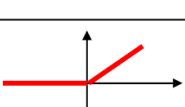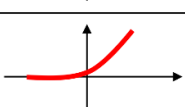
Activation function	Equation	Graph
Unit step (Heaviside)	$\phi(z) = \begin{cases} 0, & z < 0, \\ 0.5, & z = 0, \\ 1, & z > 0, \end{cases}$	
Sign (Signum)	$\phi(z) = \begin{cases} -1, & z < 0, \\ 0, & z = 0, \\ 1, & z > 0, \end{cases}$	
Linear	$\phi(z) = z$	
Piece-wise linear	$\phi(z) = \begin{cases} 1, & z \geq \frac{1}{2}, \\ z + \frac{1}{2}, & -\frac{1}{2} < z < \frac{1}{2} \\ 0, & z \leq -\frac{1}{2}, \end{cases}$	
Logistic (sigmoid)	$\phi(z) = \dfrac{1}{1 + e^{-z}}$	
Hyperbolic tangent	$\phi(z) = \dfrac{e^z - e^{-z}}{e^z + e^{-z}}$	
Rectifier, ReLU (Rectified Linear Unit)	$\phi(z) = max(0, z)$	
Rectifier, softplus	$\phi(z) = \ln(1 + e^z)$	

Figure 9. Neuron activation functions [48].

2.3.3.1 Selection of updated parameters and sensitivity analysis

Identification of updating parameters and their roles in the structural behavior is an important step for the model updating process. Due to damage, deterioration, aging, and even rehabilitation various parameters associated with the material and geometric properties of the structure tend to change over time. Therefore, there are differences between the values of the initial and current parameters. Although the change of almost all these parameters leads to some variations in the local response of the structure, a few of them change the response of the structure globally. The implementation of parametric analyses determines the critical parameters that considerably affect the global static and dynamic responses of the structure. Generally, these parameters are those that

have a significant effect on the mass or stiffness properties of the structure. They could be mentioned as the boundary conditions, size/thickness of the structural components, elasticity modulus of structural material, and mass of the structure [47].

The variation range of the parameters used in the model updating process should potentially contribute to the global response of the structure. It should be noticed that some selected parameters have high degrees of uncertainty. The uncertainty can be caused by changes in the structure from the construction time, differences between the engineering drawings and the as-built constructed structure, and non-structural parameters. To reveal the effective range of the most sensitive parameters for the model updating process, a sensitivity analysis is required to determine the effective range of these parameters. For this purpose, after careful consideration of the initial FE model, a sensitivity analysis should be conducted to evaluate the variation of the structural responses to the various parameter values [47,49].

2.3.3.2   Neural network based model updating

The process involved in a neural network based model updating can be described as follows:

1. Performing the parametric study to set the most sensitive parameters which are going to be estimated by the neural network.

2. Performing the sensitivity analysis to select the effective range of parameters.

3. Generating the training dataset using a sufficient number of FE analyses and obtaining the analytical responses by changing the parameters within their effective ranges.

4. Choosing a suitable neural network architecture and training the network using the provided training dataset to learn the inverse relationship between structural responses and parameters.

5. Obtaining the real responses of the structure from field tests.

6. Feeding the measured responses of the existing structure from the field test into the trained network to predict the parameters corresponding to real structural conditions.

7. Updating the structure parameters in FE analysis according to the network predictions.

8. Analyzing the updated FE model and comparing the results with field-measured responses to quantify the parameters estimation accuracy.

2.3.3.3 Application of ANNs to the structural health monitoring and model updating

ANNs have been successfully developed in structural health monitoring and model updating studies in the last decade. Hasancebi and Dumlupinar [47] employed ANN to develop an efficient technique for FE model updating of the concrete bridges. The network was trained according to datasets from non-linear and linear analyses separately. This study demonstrates that ANN can be used reliably for model updating and prediction of structural parameters under a high level of complexity and uncertainties. This study also evinces the importance of non-linear responses for parameter estimation so that consideration of dynamic responses based on linear analysis may lead to errors and less accurate results in parameter predictions. Park et al. [50] evaluated the bridge boundary condition using neural networks. They used ANN to find the relationships between bridge responses and the constraining effect of the boundary condition with a focus on the rotational stiffness of the boundary conditions.

Maity and Saha [51] employed the change of strains and displacements, as the static properties of the structure, for damage detection in a cantilever beam using a back-propagation algorithm in ANN. They trained the neural network with various possible damage scenarios. They observed the superiority of strain over displacement for the identification of damage. Chang et al. [52] proposed a model updating method for a steel bridge using an adaptive neural network to develop the structural health assessment methodologies. They used an iterative procedure, where the model updating process and training the network were repeated until a satisfactory agreement between the measured and calculated modal responses of the bridge. Zapico et al. [53] applied neural networks for the FE model updating of a small steel frame, where the network was employed to establish the relationship between the natural frequencies and some structural parameters. Tran-Ngoc et al. [44] presented a new approach for damage detection by applying the combination of ANN with cuckoo search (CS) algorithm. They tried to improve the ANN performance by improving the ANN training parameters.

CHAPTER 3

Methodology

3.1 Introduction

This chapter aims to describe the methodology to identify the modal parameters through the Operational Modal Analysis (OMA) and predict the structural parameters to calibrate the finite element (FE) model of the studied railway bridges. In this research, two prestressed concrete railway bridges were instrumented and studied. Five accelerometers were deployed on each bridge for a 24-hour period in August 2020. During the data recording, the ambient and different train-induced vibrations were recorded. Model parameter identification was conducted for both bridges while the model updating process is performed for one of them due to problems presented in CHAPTER 4.

In the previous chapters, it is mentioned that the reliability of the vibration based damage detection and safety assessment of the structures highly depends on the accuracy of the identified modal parameters. Since the changes in the structural modal parameters can be highlighted as a damage indicator, research on the modal identification process is required to reveal the variation of the identified modal parameters that stem from the use of various measured vibration data and different OMA algorithms. For this, one of the aims of this study is the use of different train-induced vibrations to identify the bridge modal parameters through the different free decay responses of the bridges using two OMA techniques implemented by the OoMA toolbox in MATLAB.

To evaluate the safety condition of the structures, FE model updating has become a popular approach since it can create a calibrated FE model reflecting the real behavior of the existing structures. The analytical results from the updated FE model may not perfectly match the identified modal parameters through OMA due to errors in modal identification and FE modeling inaccuracies. The errors in FE modeling can be caused by structural simplifications, idealized supports and boundary conditions, and uncertainties of material properties. Therefore, another substantial aim of this study is the determination of the crucial structural parameters used in the FE model updating process, with a focus on the boundary conditions behavior, to generate an accurate FE model.

One of the most important factors that highly affect the accuracy of the FE model updating is the boundary conditions. Without proper assumptions for boundary conditions, it is very difficult to match the FE model with the results obtained through the vibration test. The real boundary conditions behavior is often complex and different from idealized hinged or fixed supports, and it may differ from the design assumptions since the restraining effect of boundary conditions often change during the service life of the bridges due to deterioration, aging, and support damage. For this purpose, the model updating process is performed through training a neural network implemented by coding in Python to estimate the modified parameters of the bridge. In the end, in order to validate the updated FE model responses, the results from OMA analysis were compared with the analytical results of the FE model simulated in SAP2000 in terms of frequencies and mode shapes.

The simplified flowchart in Figure 10 presents the modal identification and model updating steps in this thesis.

3.2 Selection of different OMA algorithms

Over the past decade, many algorithms have been developed as reliable methods for modal identification to improve the performance of OMA. Although using one of these algorithms can identify modal parameters, the application of the additional algorithm can prove, or rather improve the results, as it is suggested in many studies [21,24,29]. Therefore, in this thesis, two modal identification algorithms in different domains, the time domain and frequency domain, have been utilized to evaluate the effects of using different OMA algorithms on identified modal parameters. In the time domain, the Covariance-driven Stochastic Subspace identification method (SSI-COV),

and in the frequency domain the Frequency Domain Decomposition (FDD) have been used as the two popular methods in the structural identification literature [21,24,29,30].
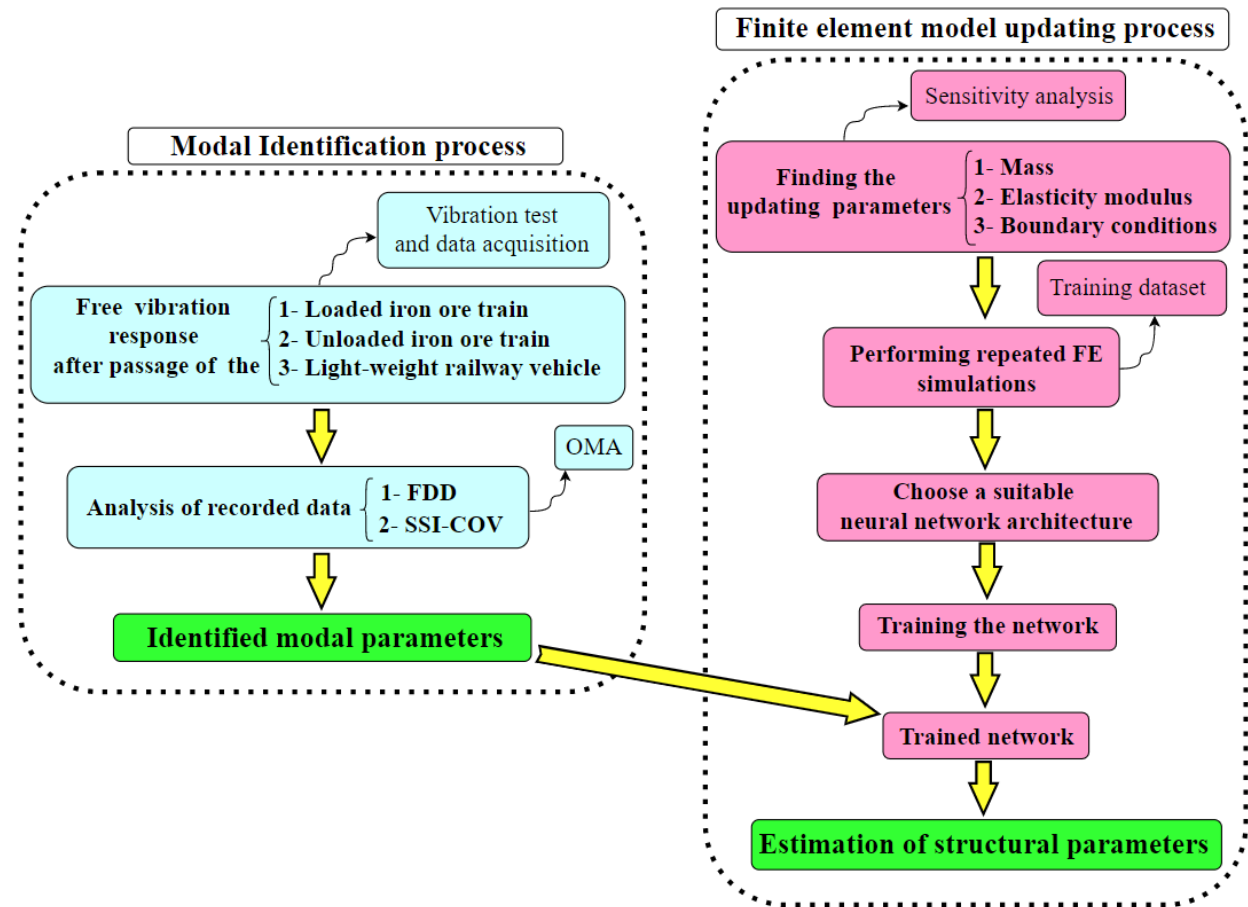
Figure 10. Modal identification and FE model updating steps.

3.3 Selection criteria for the type of excitation in OMA

Since in this study the vibration test was conducted under weak ambient excitation, the recorded acceleration time histories of the ambient vibration exhibited low signal-to-noise ratios which are dominated by noises. Therefore, the ambient vibration did not provide acceleration time histories to be usable in OMA.

OMA can be performed using different types of excitation caused by different sources. As reported in the modal identification literature [30,54], the free vibration recorded after the passage of the train can provide reliable data for modal identification since the amplitude of the accelerations is often higher than that of the ambient vibration. Therefore, the free decay response of the bridge, immediately after the train passage, was used as the excitation source to perform OMA in this

study. Totally, 23 train crossings were considered for each bridge classified according to their weight and categorized into 3 groups, a) Loaded iron ore train; b) Unloaded iron ore train; c) lightweight railway vehicles.

3.4 Parameter selection for model updating considering boundary conditions

To establish a more accurate FE model, considering the accurate behavior of boundary conditions is a crucial factor. In this research, to evaluate the aging and constraining effect of the boundary conditions, the rotational stiffness at each support is considered in addition to translational stiffness. For this, two rotational stiffnesses about the transverse and vertical directions, and three translational stiffnesses in the longitudinal, transverse, and vertical directions at each support are evaluated to present the behavior of the boundary conditions. Moreover, two other parameters, the elasticity modulus of the concrete and mass of the bridge deck were considered as the updating parameters which are directly affecting the stiffness and mass matrices. The elasticity modulus is assumed as a single uniform parameter for the whole bridge without considering the localized changes. Also, the mass parameter consists of concrete, ballast, sleepers, rails, and other railway equipment that are permanently on the bridge deck.

3.5 Suitable neural network architecture and training dataset

To select the most suited architecture for the network, there is no specific rule. Therefore, the bests performance of the network can be achieved by a trial and error approach. In this research different network architectures, including different layers and neurons, were analyzed and the best performance was selected based on the least error obtained between field-measured frequencies and results from the updated FE model.

To train the network, two types of the dataset were utilized. The first dataset was generated using a combination of the updating parameters so that just one parameter was changing in its effective range while others were constant. The second dataset was generated using a combination of different values of updating parameters selected randomly while all parameters were changing in their effective range.

CHAPTER 4

Application of OMA to Norddal bridges

4.1 Introduction

During this research, two concrete railway bridges located in Northern Norway located on the Ofot line (*Ofotbanen*) are instrumented and studied. In this chapter, after an overview of the bridges, detailed information is provided on the instrumentation and data acquisition, signal processing, choosing the type of excitation, and finally identification of modal parameters using different excitations and OMA algorithms. Two identification techniques, SSI-COV and FDD, used in this study are implemented using the OoMA toolbox in MATLAB.

4.2 Description of instrumented bridges

The instrumented bridges are two prestressed concrete bridges located on the Ofot line (*Ofotbanen*) which are part of a vital railroad that carries the iron ore mined in Kiruna, Sweden to the harbor in Narvik, Norway. As such, these bridges are exposed to very high axel loads from the iron ore trains that regularly operate on this line in addition to regular rail traffic such as the passage of passenger and freight trains.

The bridges are a single-span bridge with a span length of 50 m (B1) and a two-span bridge with a total length of 85m (B2), Figure 11 is showing the side view of the bridges. The one-span bridge is completely straight but the two-span bridge has a curvature in plan with a radius of 350 m. Both

bridges are T-beam concrete bridges with the same cross section and one traffic line in the middle of the deck. The only available drawing of the bridges suffered from a lack of dimensions and details, so the considered dimensions of the cross sections are obtained by measuring the drawing manually. The cross section of the bridge deck consists of a slab with 660 cm width and 35 cm depth as shown in Figure 12. The slab is supported by two webs, each web with 90 cm width and 250 cm depth. There are also secondary load-bearing elements, such as parapets and diaphragms that have a negligible contribution to the global stiffness of the bridge therefore, they are discarded in this study.
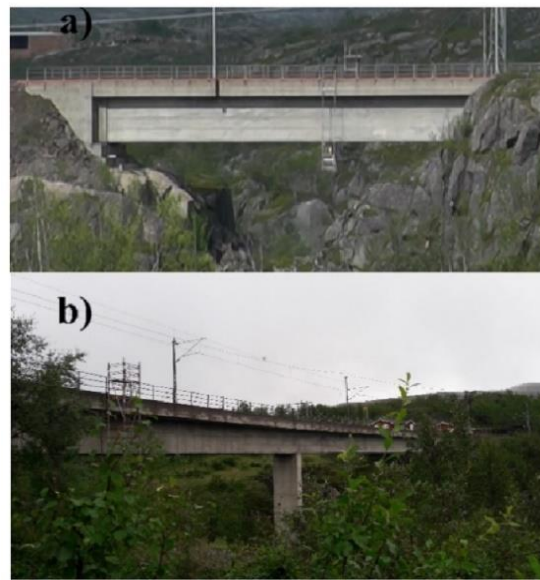
Figure 11. A side view of the: a) single-span bridge; b) two-span bridge.
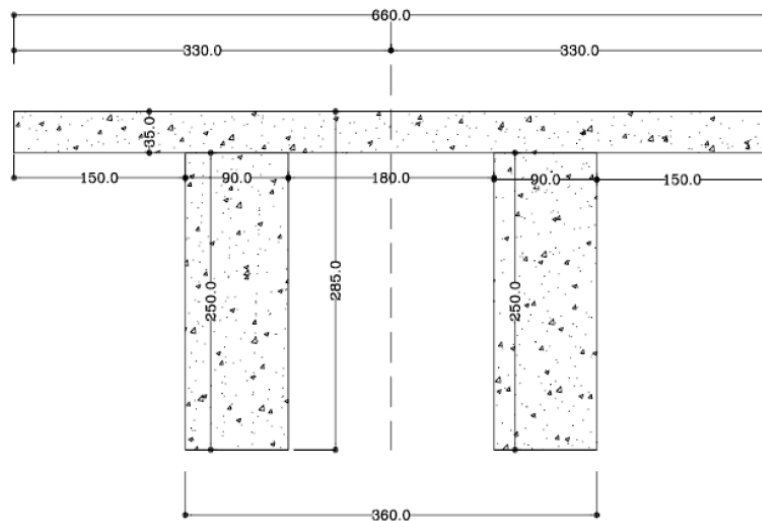
Figure 12. The bridge deck cross section (unit: cm).

4.3 Instrumentation and data acquisition

Each bridge was instrumented separately for a 24-hour period in August 2020. During the tests, six accelerometers were deployed on each bridge. During each measurement, data from one sensor was missing and the final locations of the deployed sensors with successful data recording are presented in Figure 13.
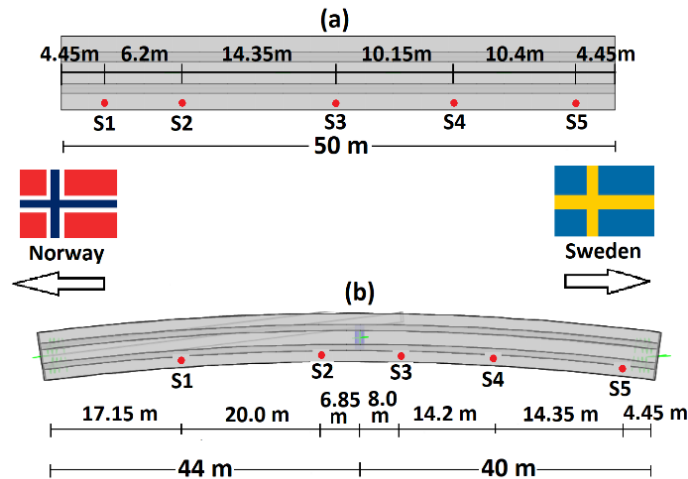
Figure 13. Location of the accelerometers installed on the: a) bridge B1, b) bridge B2.

The data acquisition was performed with a frequency range of 250 Hz that is more than adequate to identify the fundamental vibrational behavior of the bridges. The accelerometer used is a 20-bit Low Power, Low Noise, Low Drift, 3-Axis MEMS Digital Accelerometer. Also, GPS was used in order to synchronize multiple instruments. Figure 14 depicts one of the accelerometers and data loggers used in the test and their installation on the bridge deck.
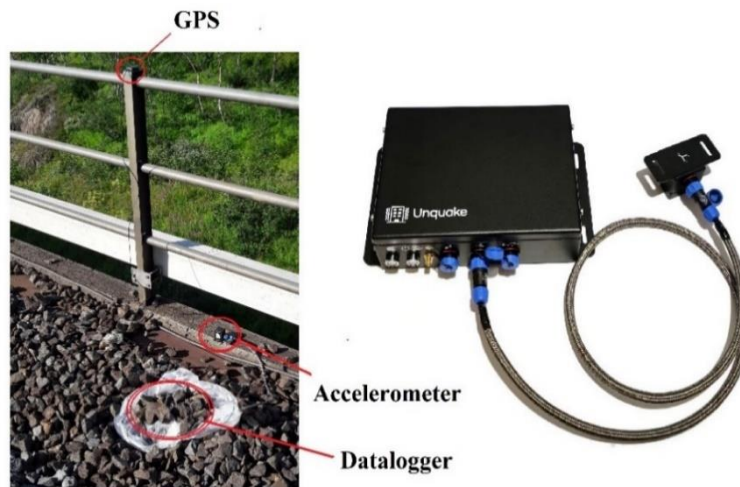
Figure 14. Equipment used in the vibration test.

4.3.1 Preliminary evaluation of the collected data

As mentioned before due to a 24-hours recording data, the data included different types of vibration induced by various trains passage in addition to ambient vibration. For the initial evaluation of the recorded data, the excitations induced by 3 different types of trains including heavily loaded iron ore trains, unloaded iron ore trains, and lightweight railway vehicles, different in terms of weight, are considered, in addition to ambient vibration. Figure 15 provides a better understanding of the different trains crossing the bridges.

Figure 15. Different trains crossing the bridges; a) Iron ore train, b) Lightweight railway vehicle.

In Figure 16 the unfiltered vertical acceleration time histories of different train crossings at the midspan of bridge B1 are presented, the duration of the excitation and the acceleration levels indicate the relative size of these trains. Totally, 23 train-induced excitations caused by 8 loaded iron ore trains, 7 unloaded iron ore trains, and 8 lightweight railway vehicles are considered for each bridge in the process of modal identification as presented in Table 1.
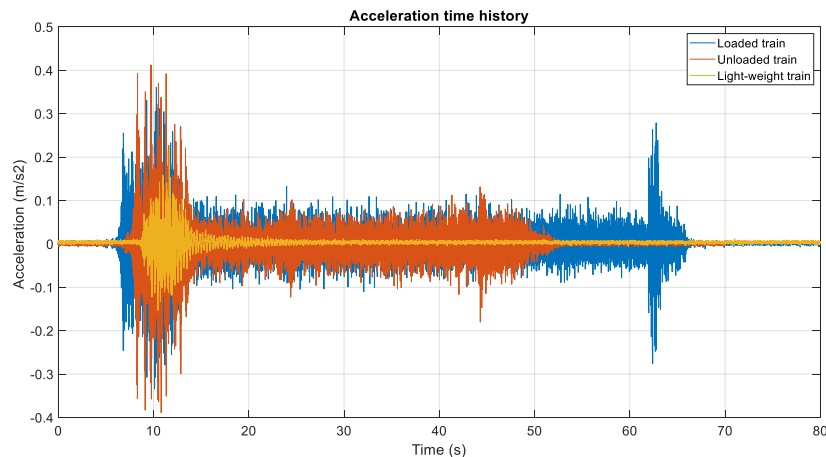
Figure 16. Unfiltered vertical acceleration time histories at the midspan of bridge B1 through different train crossings.

Table 1. The different groups of train crossings used in the identification process.

Loaded tarin	Unloaded tarin	Lightweight vehicle
T-9910	T-9909	LW-1
T-9912	T-9911	LW-2
T-9914	T-9913	LW-3
T-9916	T-9915	LW-4
T-9918	T-9917	LW-5
T-9920	T-9919	LW-6
T-9922	T-9921	LW-7
T-9924	-	LW-8

In addition to train-induced vibration, the ambient vibration was evaluated for both bridges. As it is illustrated in Figure 17 the ambient vibration for bridge B1 consists of very low acceleration amplitudes with low signal-to-noise ratios (SNRs). It turns out from a focused view of the FFT diagram, see Figure 17c, that ambient excitation is highly affected by noises, the presence of the abnormal peaks exactly in the frequencies with integer numbers can evince the contamination of the frequency content of the recorded ambient vibration. Based on the preliminary assessment of the recorded vibrations, train-induced vibrations seem to have adequate energy and acceleration amplitude to be used as the excitation sources, but in the case of ambient vibration more evaluation is required and presented in the following.
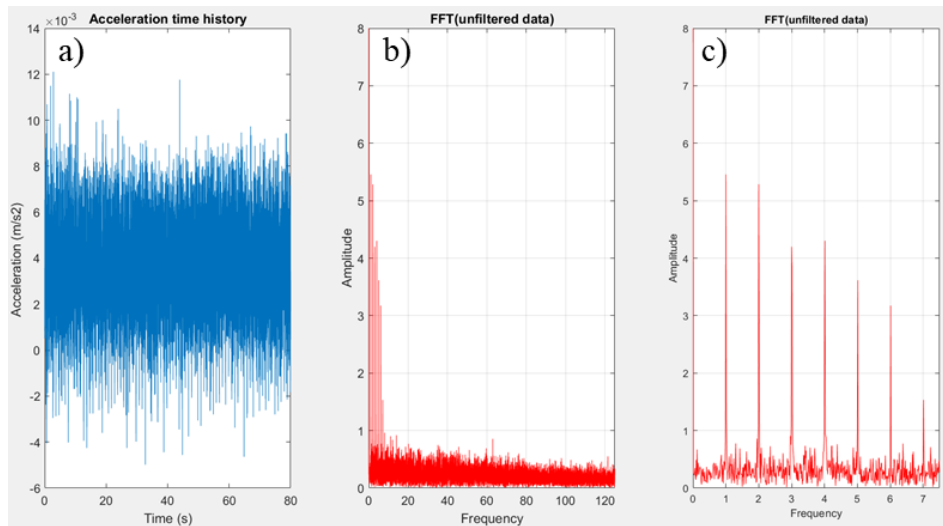
Figure 17. The ambient excitation in the vertical direction for bridge B1; a) Time history of the acceleration, b) FFT diagram, c) Focused view of FFT diagram.

4.3.2 Signal processing

To obtain more accurate identified modal parameters, regarding the contaminated data with a large amount of additional meaningless vibration data and noises, pre-processing of the recorded data is required. For this purpose, baseline correction (detrending), and filtration of the recorded data are performed. Detrending or baseline correction is the process of the subtraction of the mean or the best-fit line from acceleration time histories. In addition, in order to reduce the effect of the noise, a low and high pass filter was applied to the signals by a 4th order Butterworth bandpass filter with the cut-off frequencies at 0.1 Hz and 25.0 Hz, which are outside the frequency range of interest for the identification process. Figure 18 illustrates the unfiltered and filtered acceleration time histories from sensor 5 located on bridge B1 during the passage of train T-9910. After signal processing, clearer characteristics of the signals were available due to the elimination of unwanted data and noise. The difference between filtered and unfiltered data, specifically in the transverse direction, can imply the presence of a high level of noise.
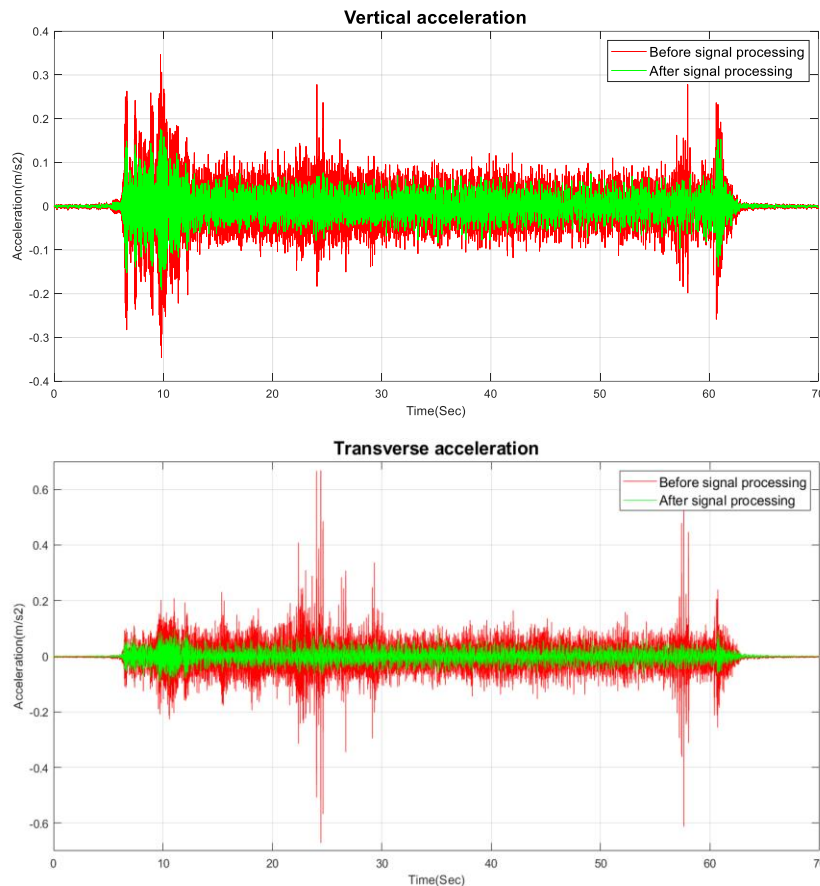
Figure 18. Train-induced vibration from sensor 5 caused by the passage of train T-9910 for bridge B1.

4.3.3 Choosing the suitable excitation as the input in OMA

As mentioned in CHAPTER 2, OMA should be performed under the assumption of stationary excitation [12,13]. Considering the entire acceleration time history of the train passage denies this basic assumption. In addition, the presence of the train on the bridge will apply an additional mass to the bridge and affect the identified natural frequencies. Therefore, to minimize the frequency content contamination of the recorded vibrations from the forcing frequency of the train, this type of excitation was discarded and it was decided the ambient excitation and the free decay response immediately after the train crosses the bridge in both vertical and transverse directions were selected as the input in OMA.

4.3.3.1 Ambient excitation

The ambient excitation is often affected by noises and the results extracted from OMA techniques highly depend on how close the ambient excitation is to the white noise assumption. Some drawbacks of using the ambient excitation can be mentioned as the low level of amplitude or narrow-band frequency content that leads to the identification of a limited number of modes. In the case of weak ambient excitation, it is advisable to perform hybrid vibration testing (HVT) through the application of weak ambient excitation besides an artificial force [55]. Since, in this study, it was impossible to perform HVT during the vibration test to improve the excitation levels and accuracy of the modal identification, it was decided to increase the length of the time history of the ambient vibration up to 60 minutes used for modal identification as shown in Figure 19, as the increase of the length of time history is recommended as an improvement factor of identified parameters [30].

Figure 20 shows the stabilization diagram, used in the SSI-COV method, in the frequency range of 0-35 Hz in both transverse and vertical directions extracted from ambient excitation for bridge B1. No alignment of the stable poles is observed in the frequency range of 0-20 Hz and only one alignment in the vertical direction and a few alignments in transverse direction appear in the frequencies higher than 25 Hz which are presenting noisy or mathematical modes and no one fulfills the modal validation criteria.
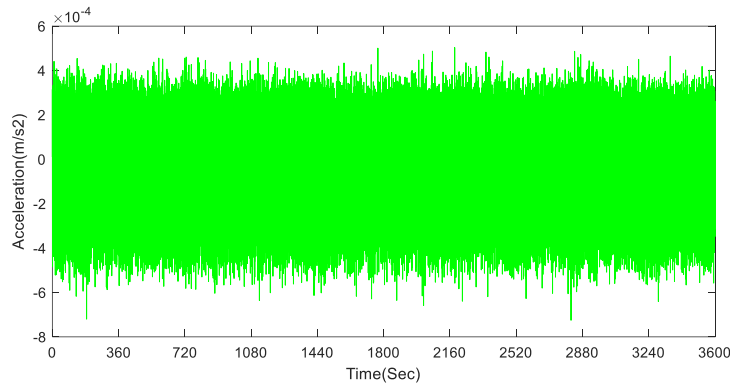
Figure 19. The ambient vibration at the midspan of bridge B1 with a duration of 60 minutes.
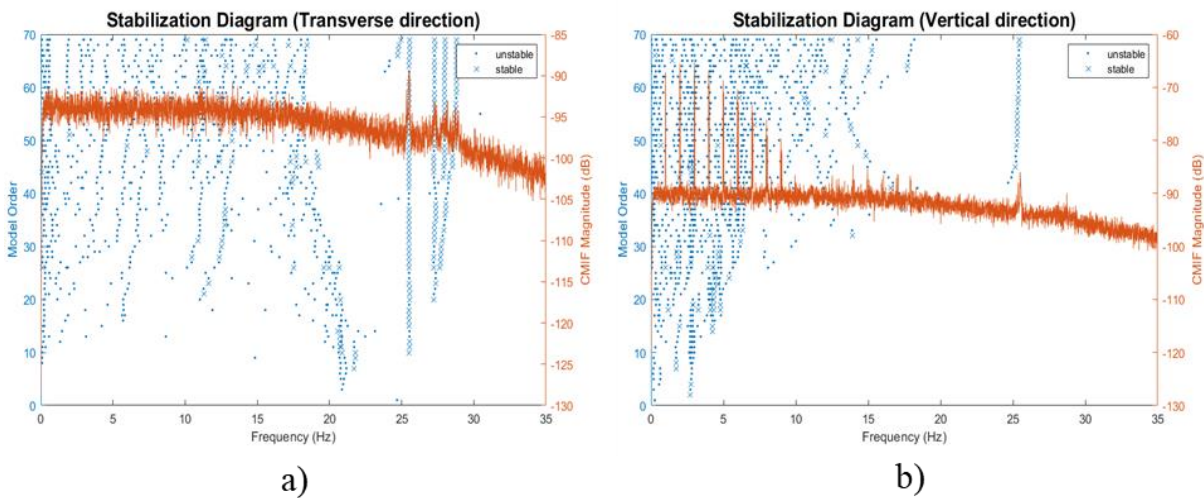
Figure 20. Stabilization diagrams using ambient excitation for bridge B1; a) transverse direction, b) vertical direction.

Figure 21 illustrates the CMIF plot, used in the FDD method, of the ambient vibration that depicts the energy content of the acceleration response at each frequency level. In the transverse direction, no clear peak is observed, while in the vertical direction the graph shows some peaks, as they appeared in the FFT diagram in Figure 17, and none of them produce physically meaningful mode shapes.

Also, by analyzing the ambient vibration for bridge B2 the same results were observed. With respect to the above-mentioned observations, the ambient excitation due to low SNRs and a high level of noise will not provide the opportunity for modal parameter identification.
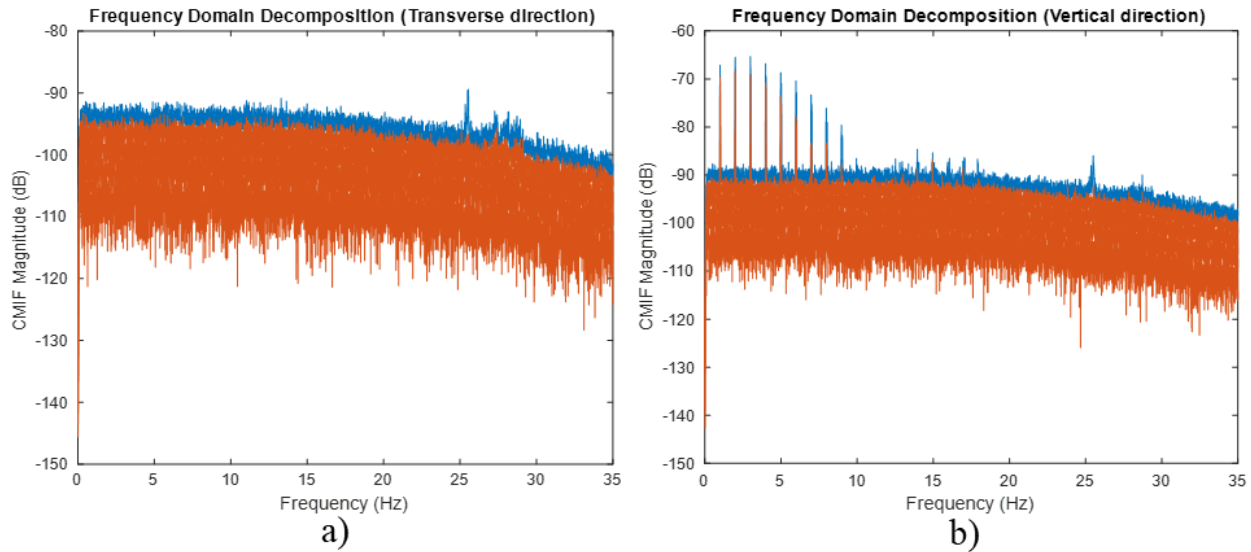
Figure 21. CMIF plot through the ambient vibration for bridge B1; a) transverse direction, b) vertical direction.

4.3.3.2 Free decay response

As observed in Figure 16 and Figure 18, the passage of the train is providing rather a strong excitation with sufficient quality to perform reliable modal parameter identification. Despite the fact that evaluation of just one free decay response induced by a random train can provide an initial insight into the bridge modal parameter, application of various types of the train crossings is required to evaluate the variation in the identified modal parameters due to the different properties of the excitation source. By use of train-induced vibration as the excitation source, the variation in the identified modal parameters can be explained by the influence of the train properties like the mass or velocity. Therefore, the modal identification is performed among 3 different groups of train crossings (see Table 1), for each bridge in total 23 train crossings are considered that providing free decay responses of the bridges.

The loaded iron ore train is approximately 700m in length with a 30t axel load. The train consists of 68 wagons with four axels on each wagon. The length of each wagon is approximately 10m and the presence of fully loaded wagons on the bridge adds 12 to 15t/m to the weight of the bridge that is approximately 55% to 70% of the bridge weight. Definitely, the unloaded iron ore train has the same properties as the loaded iron ore train just with less weight. Another type of railway vehicle, mentioned in Table 1 as the lightweight vehicle, was trafficking the bridge between the period of 2 AM to 8 AM while the line was closed in this period to the train traffic for maintenance and the only vehicles that were crossing the bridge were small maintenance vehicles (see Figure 15b).

Figure 22 and Figure 23 show the vertical acceleration of the free decay responses obtained from nearest and farthest sensors to the end of the bridges from where the train left. It can be observed that the acceleration values in the farthest sensor are less than those of the nearest sensor, and it is evident that this difference is more noticeable for bridge B2 (two-span bridge). The lowest amplitudes of the accelerations can be observed in the farthest sensor among the passage of the lightweight vehicle for both bridges. But it should be noted that the acceleration amplitude in the farthest sensor on bridge B1 is higher than that for bridge B2, with the comparison between Figure 22c and Figure 23c it can be seen that the maximum acceleration amplitude in the farthest sensor for bridge B1 is 0.032 m/s^2, i.e. almost two times that for bridge B2. The effect of these weak excitations can have an adverse impact on the identification process that is required to be evaluated. The more significant difference in acceleration values between the nearest and farthest sensors on bridge B2, compared with bridge B1, can be caused by the longer length of bridge B2 and the column in the middle of this bridge that can dissipate the energy of the excitation.
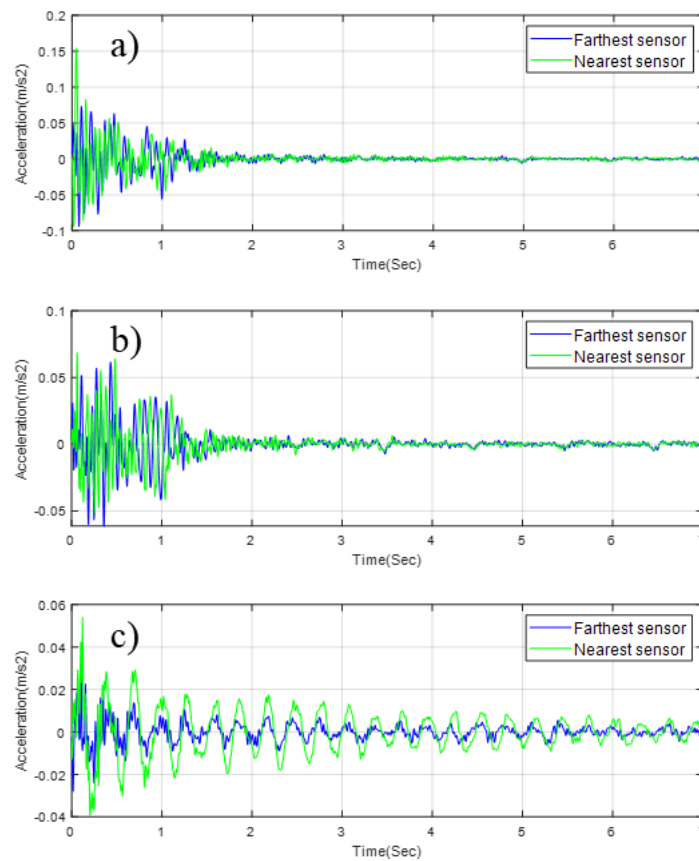
Figure 22. Free decay responses from the nearest and farthest sensors to the point where the train left bridge B1; a) T-9910 (Loaded iron ore train), b)T9921 (Unloaded iron ore train), c) T-LW2 (Lightweight vehicle).
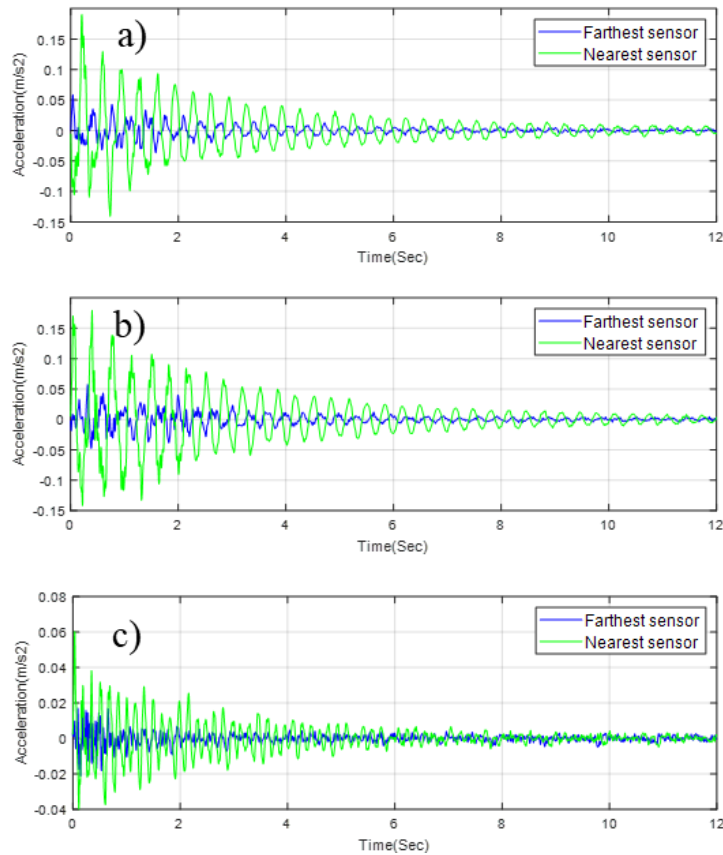
Figure 23. Free decay responses from the nearest and farthest sensors to the point where the train left bridge B2; a) T-9912 (Loaded iron ore train), b) T9917 (Unloaded iron ore train), c) T-LW4 (Lightweight vehicle).

4.4 Identification of modal parameters

It was mentioned that this thesis aims to evaluate the variation of the identified modal parameters caused by different OMA algorithms and various excitation sources. The different algorithms used in this thesis are the SSI-COV and FDD techniques, and various excitations are free vibration responses caused by the passage of different trains categorized into 3 groups of train crossings, different in weight. Each single train crossing, as an excitation source, provided independent information about the modal parameters. The final parameters were obtained by averaging the values provided by the train crossings from the same group of the train crossing. It means that the mean values are presented in 3 categories, each category is representative of a specific type of train crossing. Then, the standard deviation was calculated to show how widely the results were dispersed from the mean value. Finally, the comparison of the results is conducted based on the mean values identified through two OMA methods. For each bridge, the first six modes of

vibration including three vertical and three transverse modes were identified. Due to the limited number of sensors, identification of the higher modes did not provide the high quality of the mode shapes.

In the application of the SSI-COV method stabilization diagram was used to identify the modal parameters. The determination of the maximum model order is a challenge in the SSI technique since a high order of the model leads to the identification of spurious modes. Therefore, a model order of 70 was selected as the maximum model order in this study. To build the stabilization diagram, a series of modal parameters are identified across increasing model orders. If two consecutive poles had a change in frequency within 1%, change in damping ratio within 5% (a looser criterion was used due to relatively large variability for damping ratios), and the modal assurance criterion (MAC) more than 98%, these poles were kept and known as the stable poles. If the poles did not meet the above-mentioned criteria, the first one was discarded and the second one was compared to the subsequent pole.

Identification of the modal parameters using the FDD method was performed by Complex Mode Indicator Function (CMIF) that shows the resonant peaks and returns the singular values (SV) of the cross power spectrums as a function of frequency. FDD uses the singular value decomposition (SVD) of the spectral matrix and each value corresponds to a single degree of freedom [18].

The length of time histories of free vibration responses was selected 7.0 s and 12.0 s for bridges B1 and B2 respectively as shown in Figure 22 and Figure 23. At the end of these time histories, the train-induced excitations were completely damped and ambient excitation was the predominant vibration. In the case of considering longer time histories, the results were affected by noises from ambient vibration.

4.4.1 Identified frequencies of the bridges

The FDD technique was performed using 256 points for the spectra calculation. It should be noted that if the number of points is not well chosen, the results can present high bias. In this study, the increase in the number of points did not provide more accurate results. In Figure 24 and Figure 25 the CMIF plots used in the FDD technique are presented. These plots show the results extracted from free decay responses caused by the passage of the trains T-9924, T-9919, and T-LW8 (as the representative of each group of the train crossing) for bridge B1 and B2 respectively. The CMIF plots show several peaks, some of which (indicated by frequency values) were confirmed to

correspond to transverse and vertical modes. Other peaks were discounted as the modal frequencies since they did not fulfill the clear mode shapes and they can be considered as the resonant peaks caused by noise contamination or oven they could be components of dominant modes in another direction [29]. The range of identified frequencies is approximately between 2.5 Hz and 19 Hz for bridges B1, and between 2.2 Hz and 10.5 Hz for B2.

Although the FDD technique provided an initial insight into modal frequencies and mode shapes of the bridges, the application of an additional identification technique was required to prove, or rather improve, the identified results. Therefore, the results were extracted from the SSI-COV technique and presented in the following.

Figure 26 and Figure 27 depict the stabilization diagrams and alignments of the stable poles extracted from free decay responses caused by the train crossings of T-9924, T-9919, and T-LW8 for bridges B1 and B2 respectively. For bridge B1, the identified frequencies among SSI-COV lie between approximately 2.5 Hz and 19 Hz, and for bridge B2 between 2.2 and 10.5 Hz, the same as the range of the identified frequencies through the FDD method. In the stabilization diagrams, more alignments of stable poles can be observed, but they were discounted as corresponding to modal frequencies since they did not provide modal validation criteria and had unclear mode shapes and negative and high damping ratios. They could be the feature of ambient excitation, components of dominant modes in another direction, and caused by noises, as mentioned for identified results from FDD. Figure 24-27 show a rather correspondence of the identified natural frequencies between the two techniques, although in some cases, a noticeable difference was observed between results extracted from the two techniques.
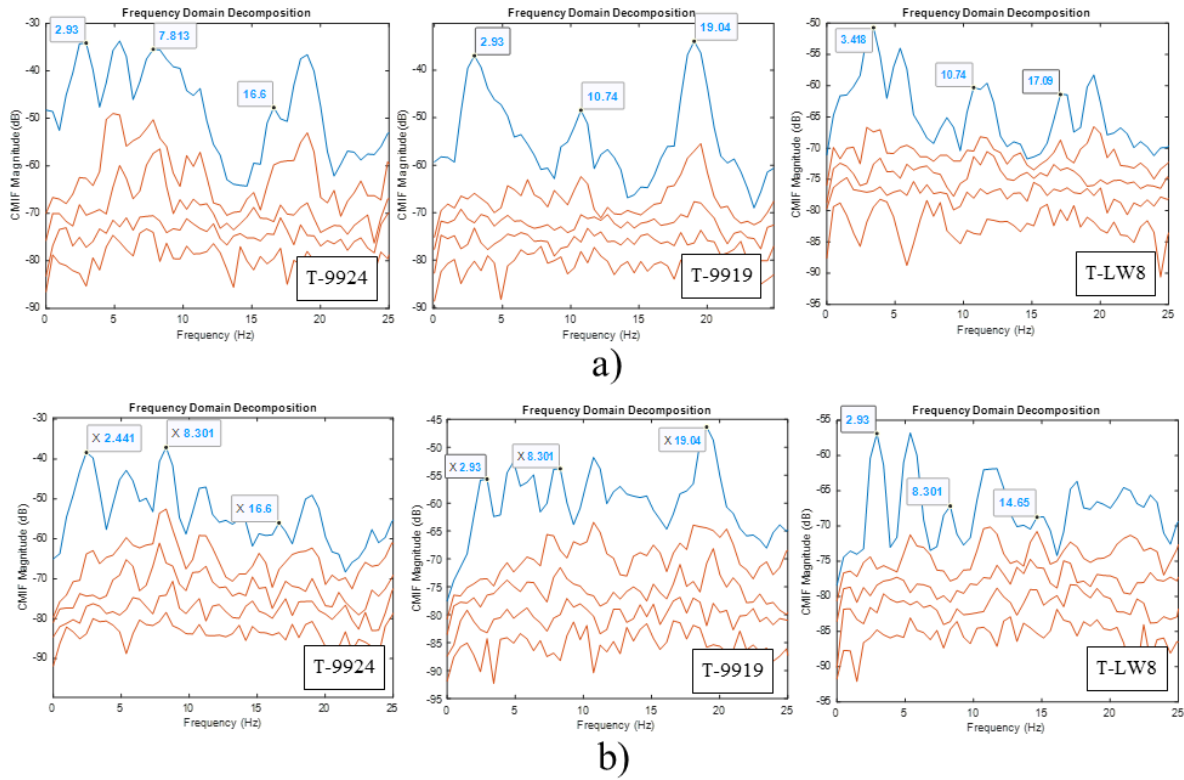
Figure 24. CMIF plots associated with the FDD technique through the free decay measured of bridge B1 after the train passage; a) Vertical direction, b) Transverse direction.
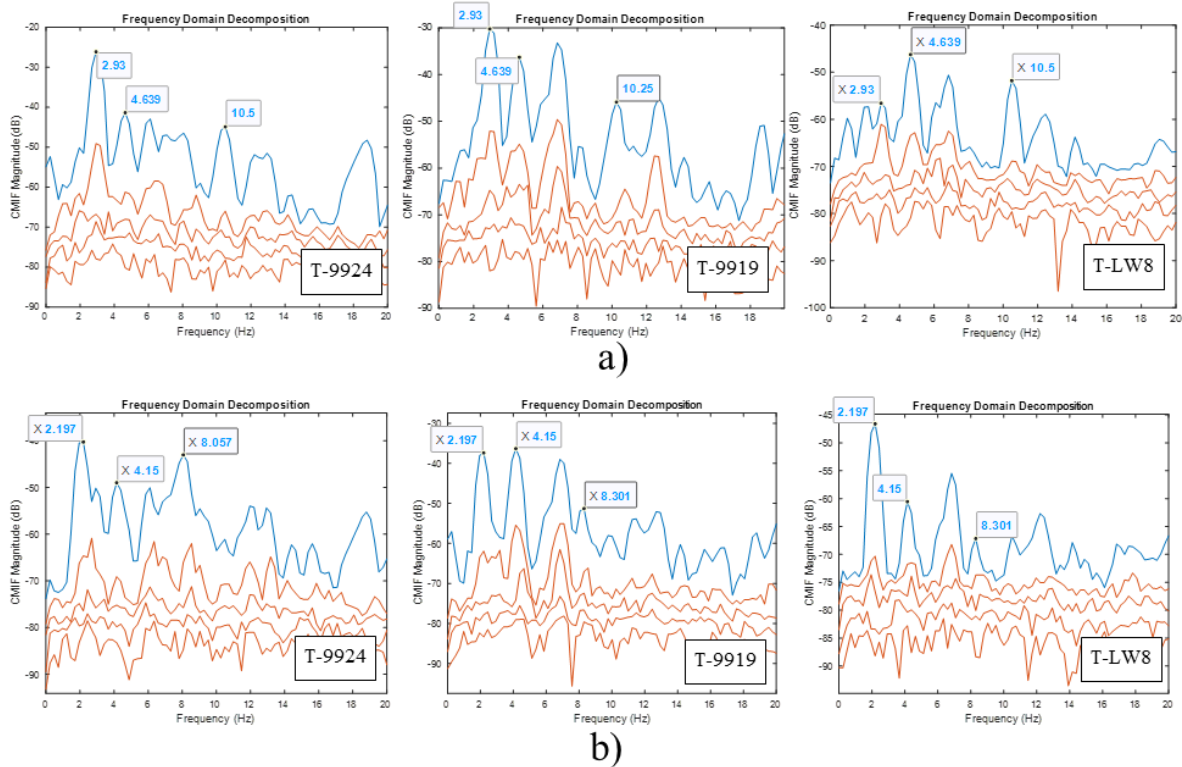
Figure 25. CMIF plots associated with the FDD technique through the free decay measured of bridge B2 after the train passage; a) Vertical direction, b) Transverse direction.
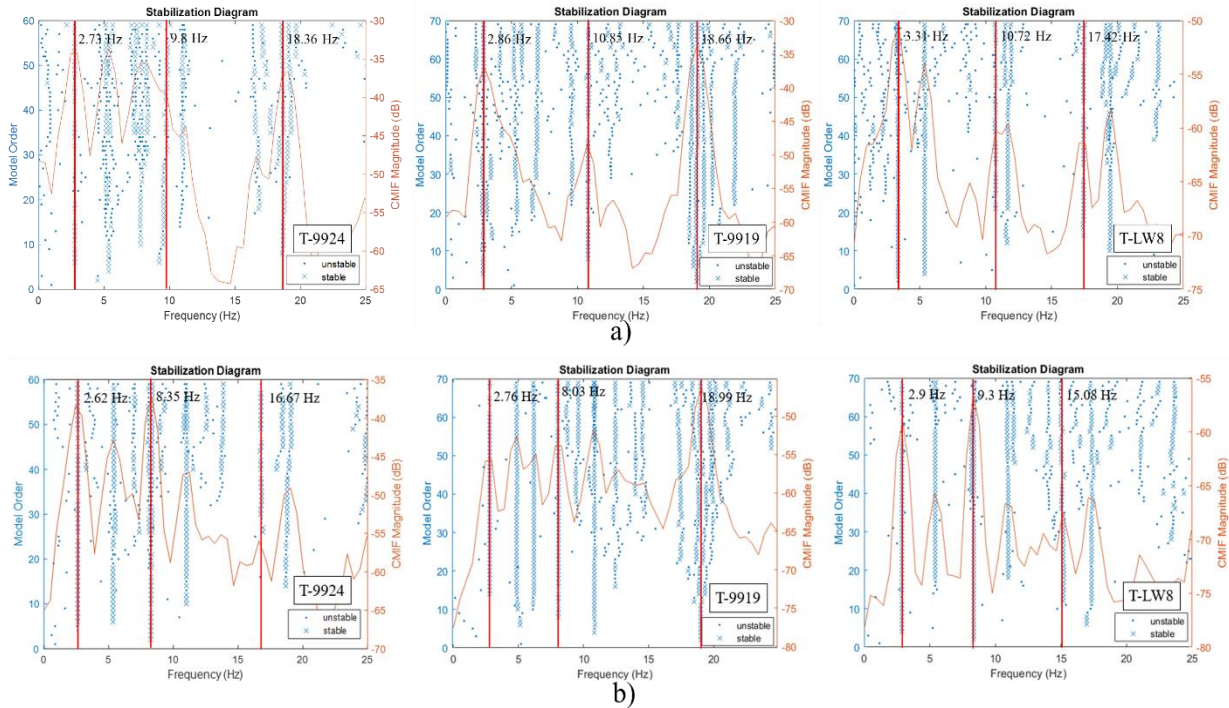
Figure 26. Stabilization diagrams associated with the SSI-COV technique through the free decay measured of bridge B1 after the train passage; a) Vertical direction, b) Transverse direction.
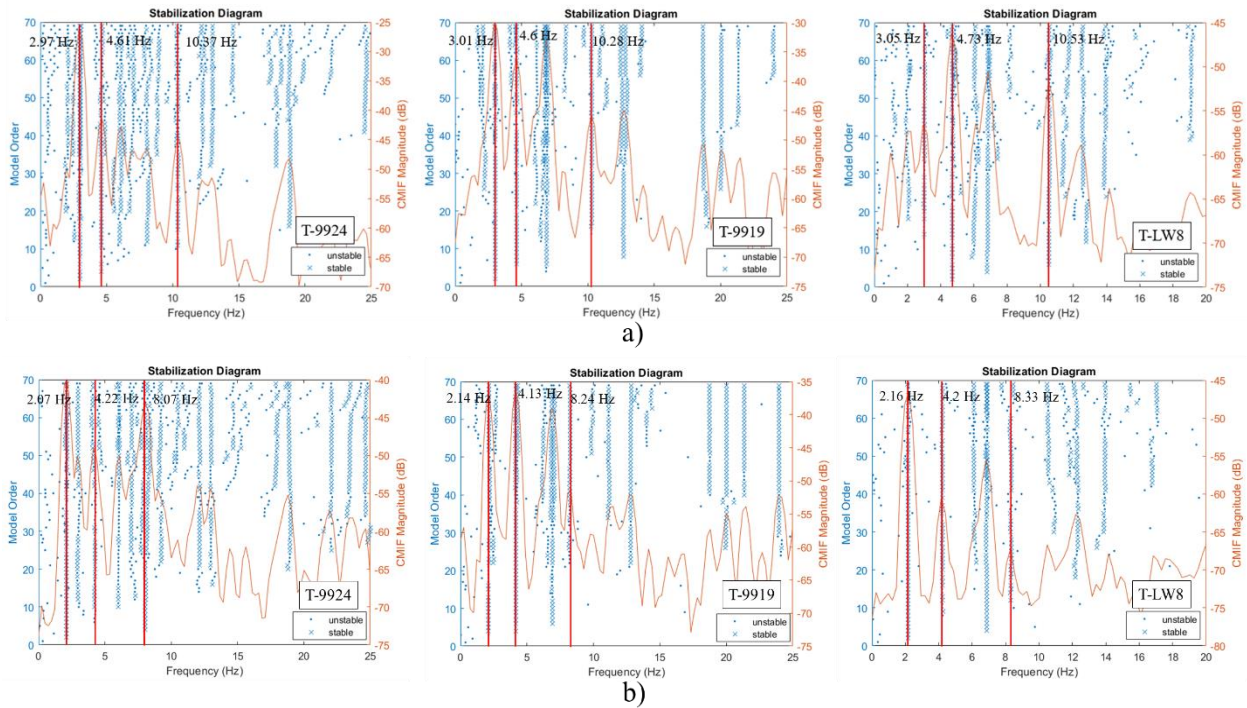
Figure 27. Stabilization diagrams associated with the SSI-COV technique through the free decay measured of bridge B2 after the train passage; a) Vertical direction, b) Transverse direction.

Identified frequencies extracted through all train crossings and both OMA techniques are summarized in Figure 28-31. The figures provide a comparative overview of identified frequencies. Information presented in these figures is the identified frequencies for each of the 23 train crossings as well as the mean frequency and the mean ± standard deviation (std) for each train crossing group. For some train crossings, both methods missed some modes, particularly for bridge B2 in the case of the passage of the lightweight vehicle. Of the 8 lightweight vehicle crossings for bridge B2, just the use of 3 of them resulted in modal identification. The fact that the number of missing modes of bridge B2 among lightweight vehicle crossings is much greater than those among loaded and unloaded train crossings can stem from the weak amplitudes of the acceleration specifically in sensors far from that end of the bridge where the train is leaving (see Section 4.3.3.2 and Figure 23).

a)   b)

Figure 28. Identified frequencies for bridge B1 using the FDD method through free decay responses after the train crossing; a) vertical direction, b) transverse direction.

a)   b)
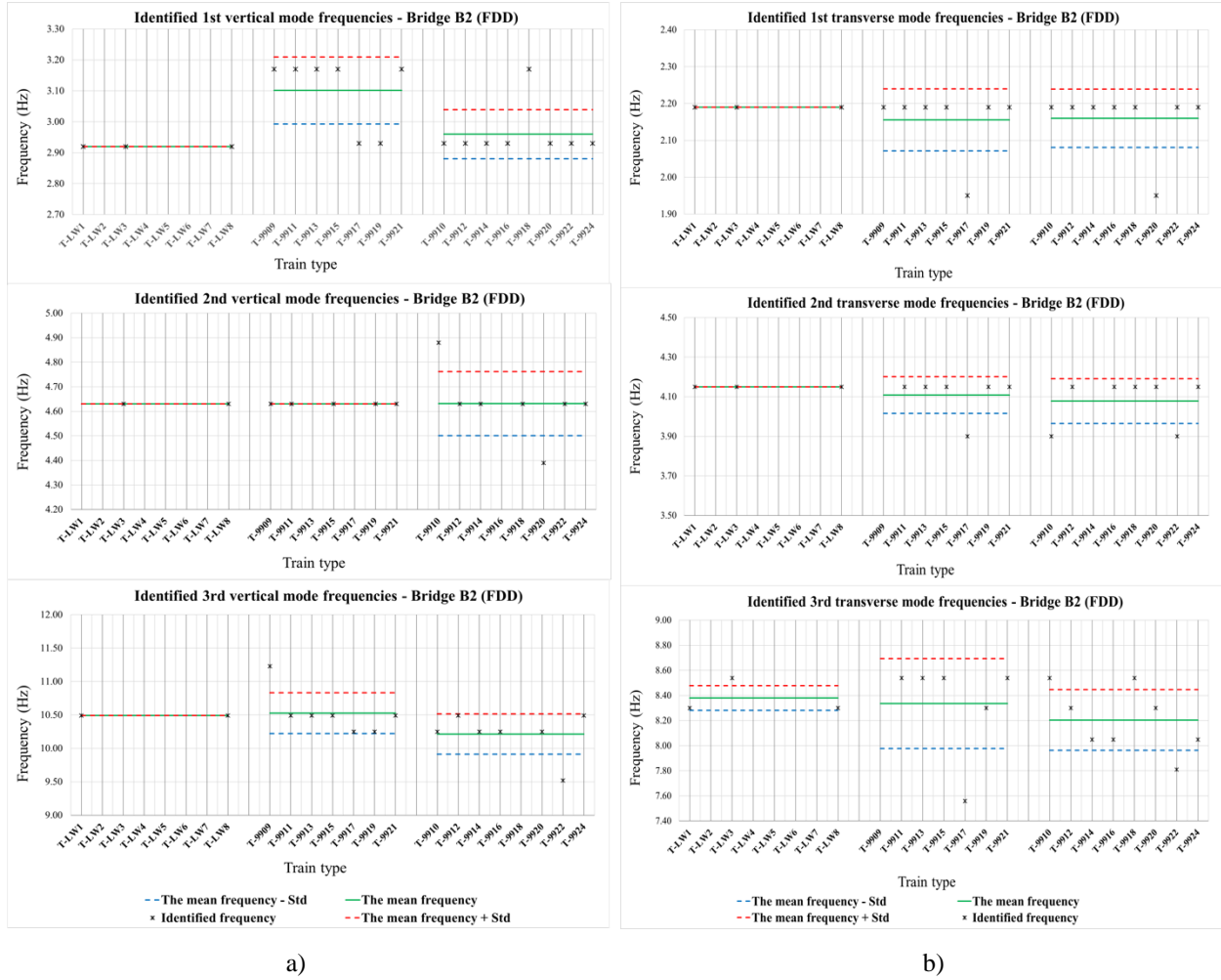
Figure 29. Identified frequencies for bridge B2 using the FDD method through free decay responses
after the train crossing; a) vertical direction, b) transverse direction.
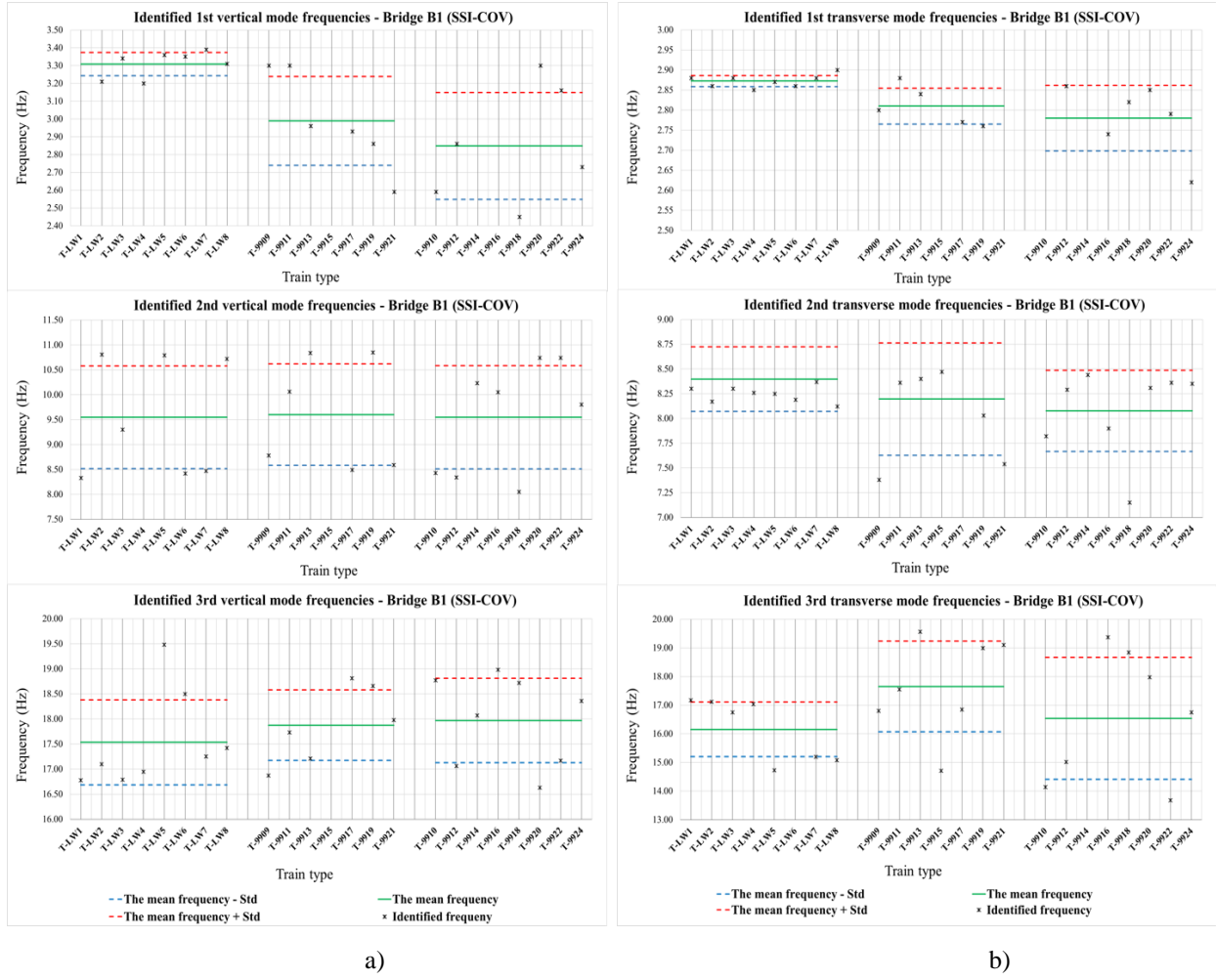
Figure 30. Identified frequencies for bridge B1 using the SSI-COV method through free decay responses after the train crossing; a) vertical direction, b) transverse direction.
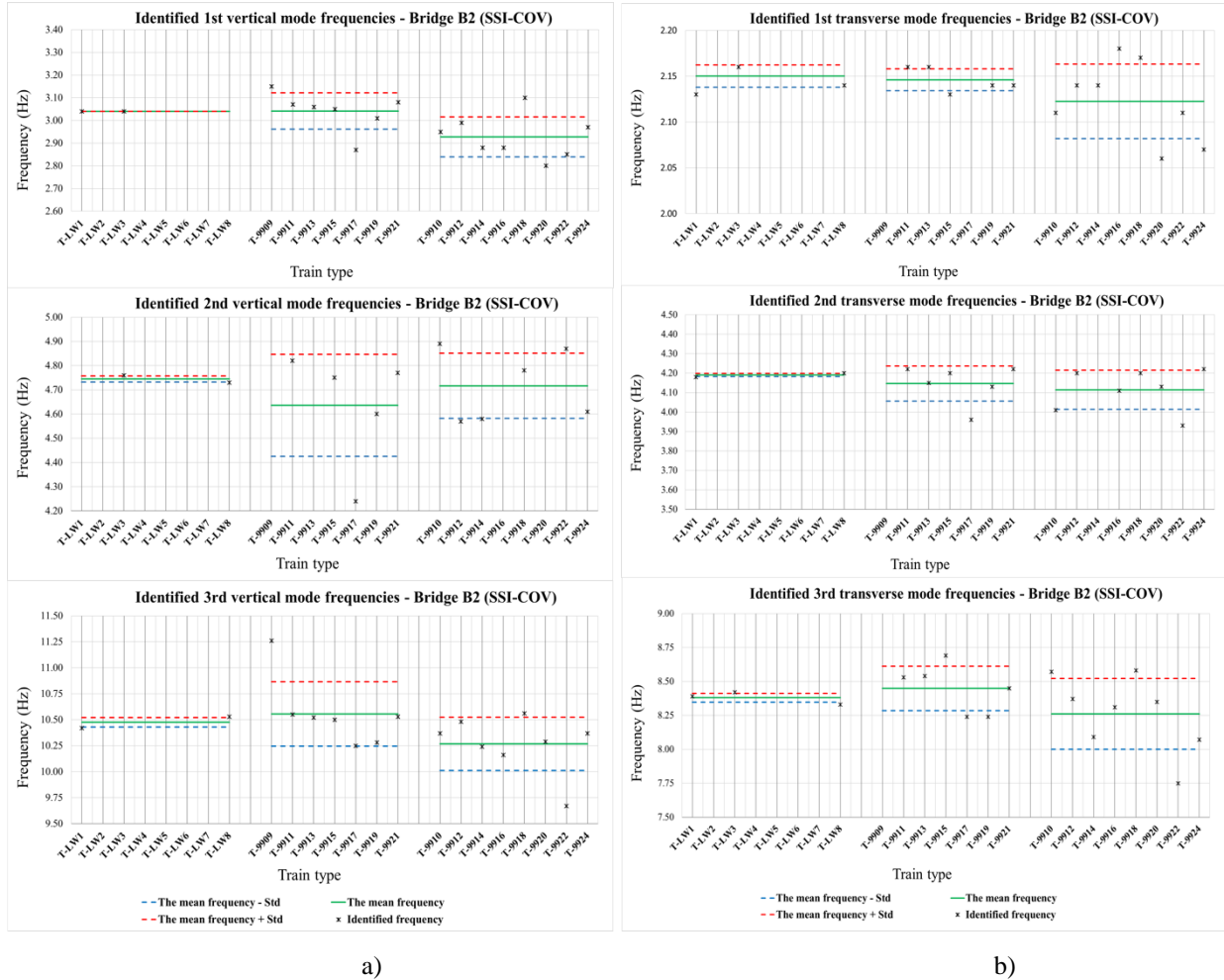
Figure 31. Identified frequencies for bridge B2 using the SSI-COV method through free decay responses after the train crossing; a) vertical direction, b) transverse direction.

4.4.2 Identified mode shapes of the bridges

Identified mode shapes can be considered a useful parameter as they can provide localized information of the structure as well as global information. Localized insight can be valuable since it assists in a better understanding of the dynamic behavior of the structure compared with global information [29].

Figure 32 and Figure 33 present a comparison of the identified mode shapes for bridge B1 using the SSI-COV and FDD techniques, while Figure 34 and Figure 35 show those for bridge B2. Each row in these figures illustrates one of the mode shapes, while each of the first three columns depicts the mode shapes identified by one group of the passing train. The images on the fourth column

depict the mean mode shapes identified by each group of excitation cases to enable the comparison of the results from different excitation sources.

Since one of the aims of this study is evaluation of the boundary condition behavior of the railway bridges, the plotted mode shapes at the ends of the bridges as well as the column in the middle of the bridge B2, are considered as movable supports and they are not considered as fixed points with no translation as shown in Figure 32-35. For the sake of simplicity, idealized boundary conditions and supports can be considered as a pin or roller that allows the rotation but no translation. Considering this assumption for supports means no translational movements that may create unrealistic translational stiffness of the bearings that leads to different mode shapes especially close to supports.

To obtain the complete mode shape curves, the curve fitting process was utilized in MATLAB using the normalized displacement of each sensor to find the best-fitted curve to the series of data points. This can be the reason for some variations, especially at the support locations. During the data recording of bridge B2 the data from the sensor close to the support, left end of bridge B2 in figures, was missing. Therefore, the curve fitting process provided dramatically unrealistic shapes for the left end of bridge B2. To avoid these unreal mode shapes for bridge B2, due to mentioned problem, the support for this end is perforce assumed as the pinned support with no translation. Although using the lightweight vehicle crossing was as successful as using two other train crossings to identify the mode shapes of bridge B1, most of the mode shapes are missing for bridge B2 through the lightweight vehicle crossing as the excitation source.

a)
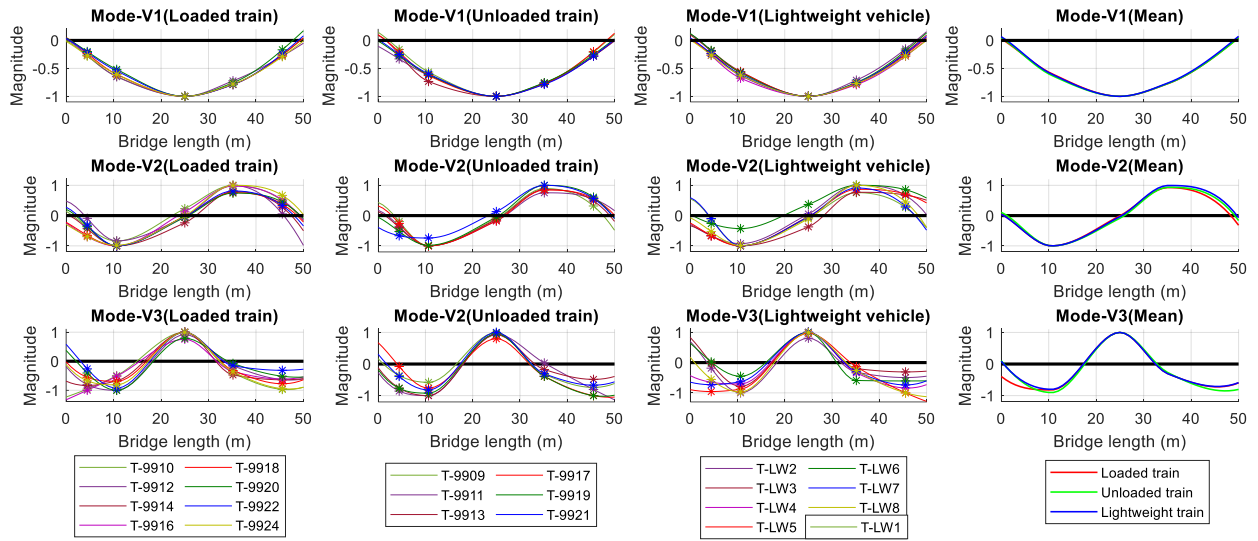
b)

Figure 32. The identified mode shapes for bridge B1 using the SSI-COV method through free decay
responses after the train crossing; a) vertical direction, b) transverse direction.

Vertical mode shape - Bridge B1 (FDD)

a)
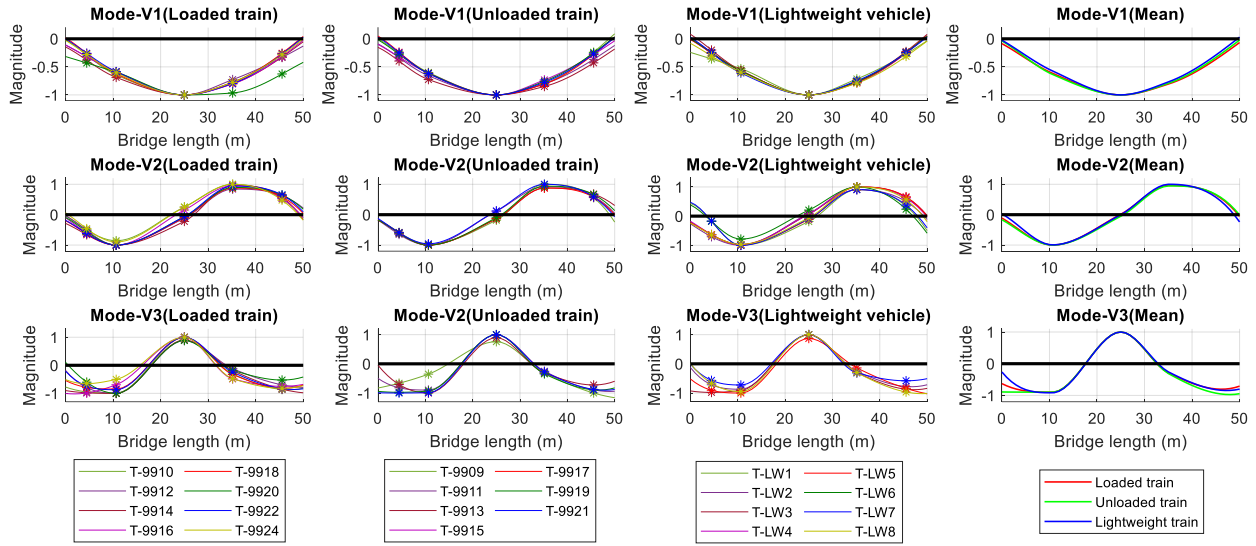
Transverse mode shape - Bridge B1 (FDD)
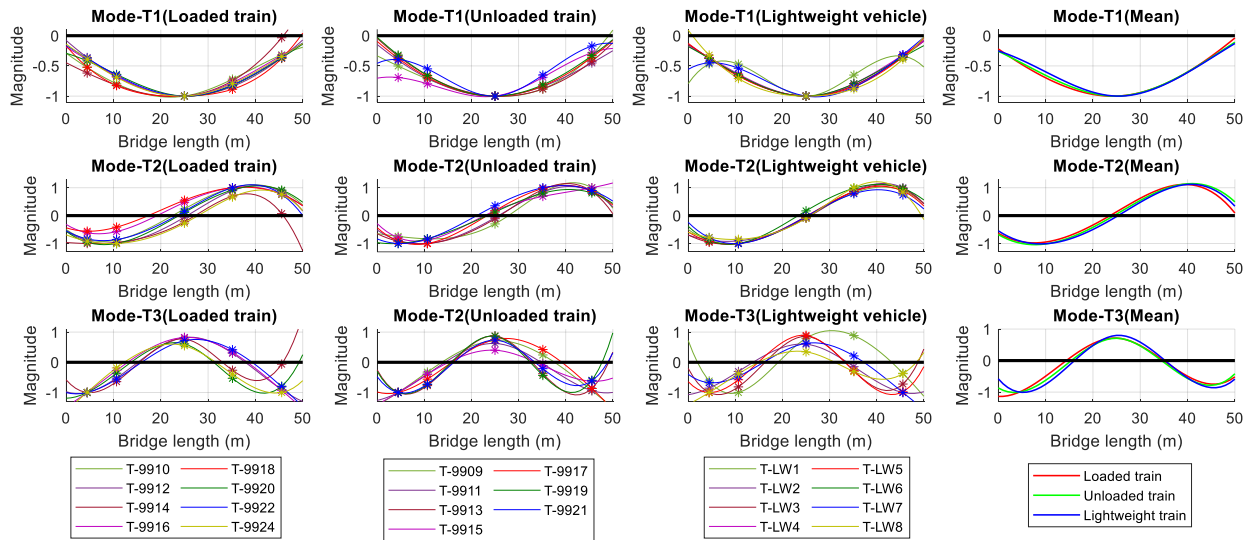
b)

Figure 33. The identified mode shapes for bridge B1 using the FDD method through free decay responses after the train crossing; a) vertical direction, b) transverse direction.

Vertical mode shape - Bridge B2 (SSI-COV)

a)
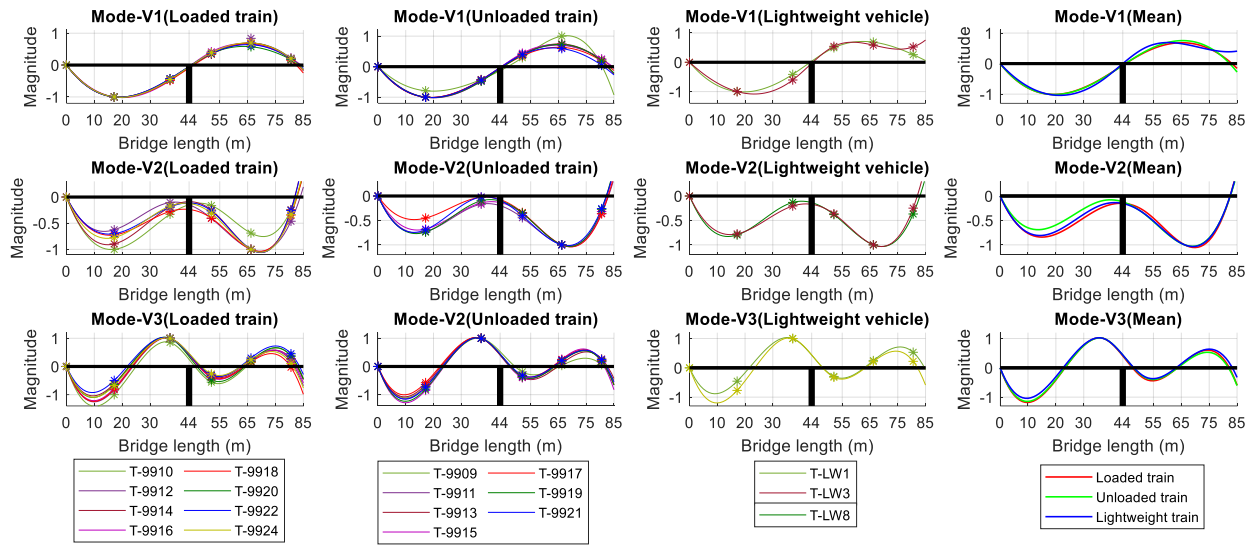
Transverse mode shape - Bridge B2 (SSI-COV)
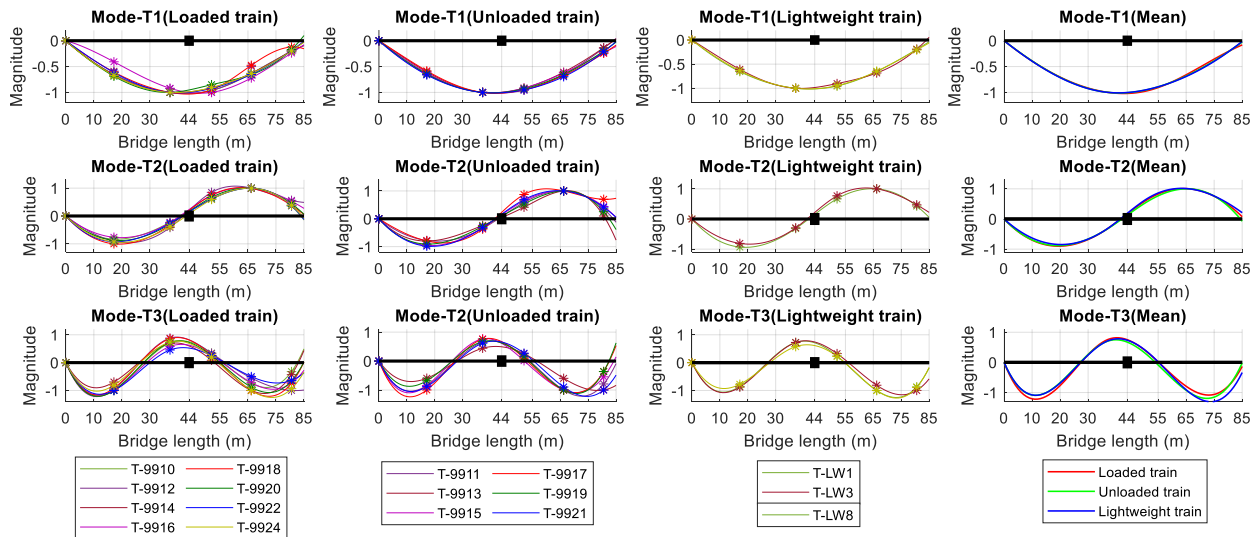
b)

Figure 34. The identified mode shapes for bridge B2 using the SSI-COV method through free decay responses after the train crossing; a) vertical direction, b) transverse direction.

a)
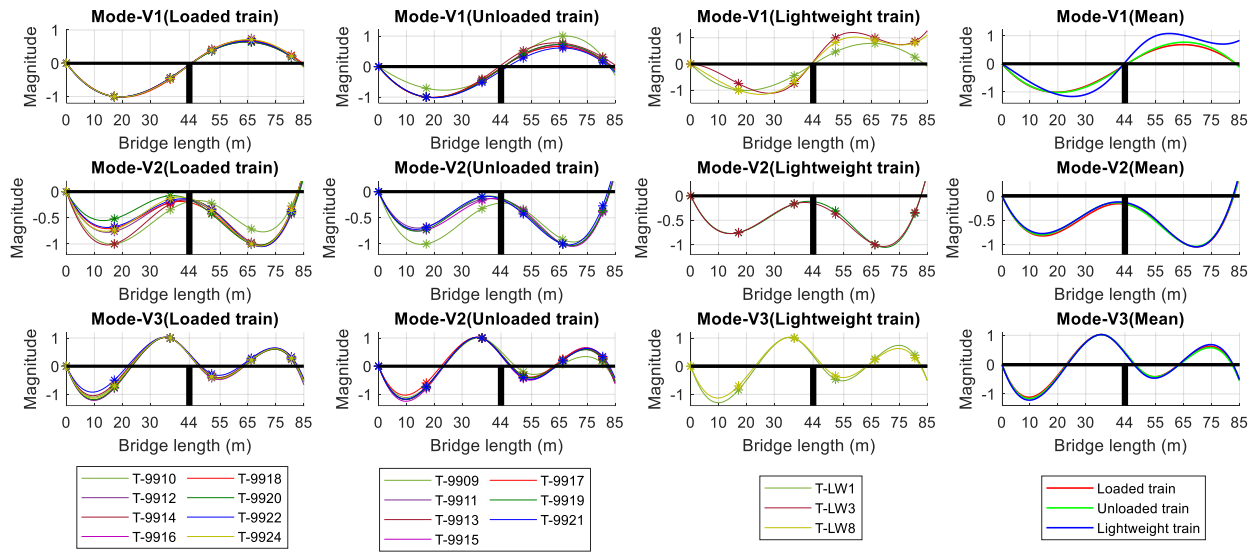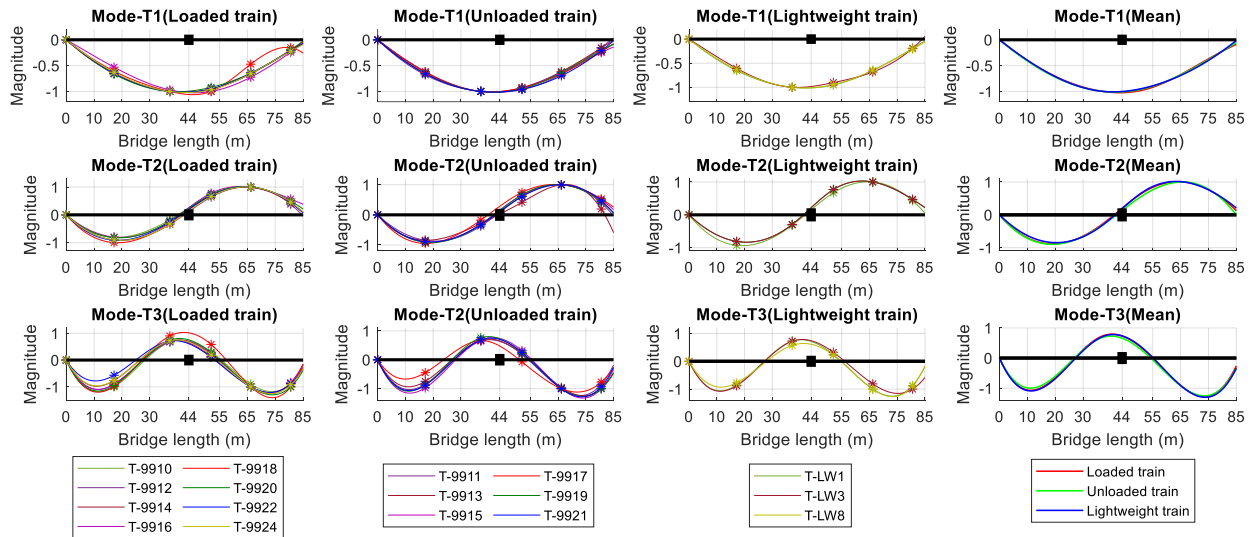
b)

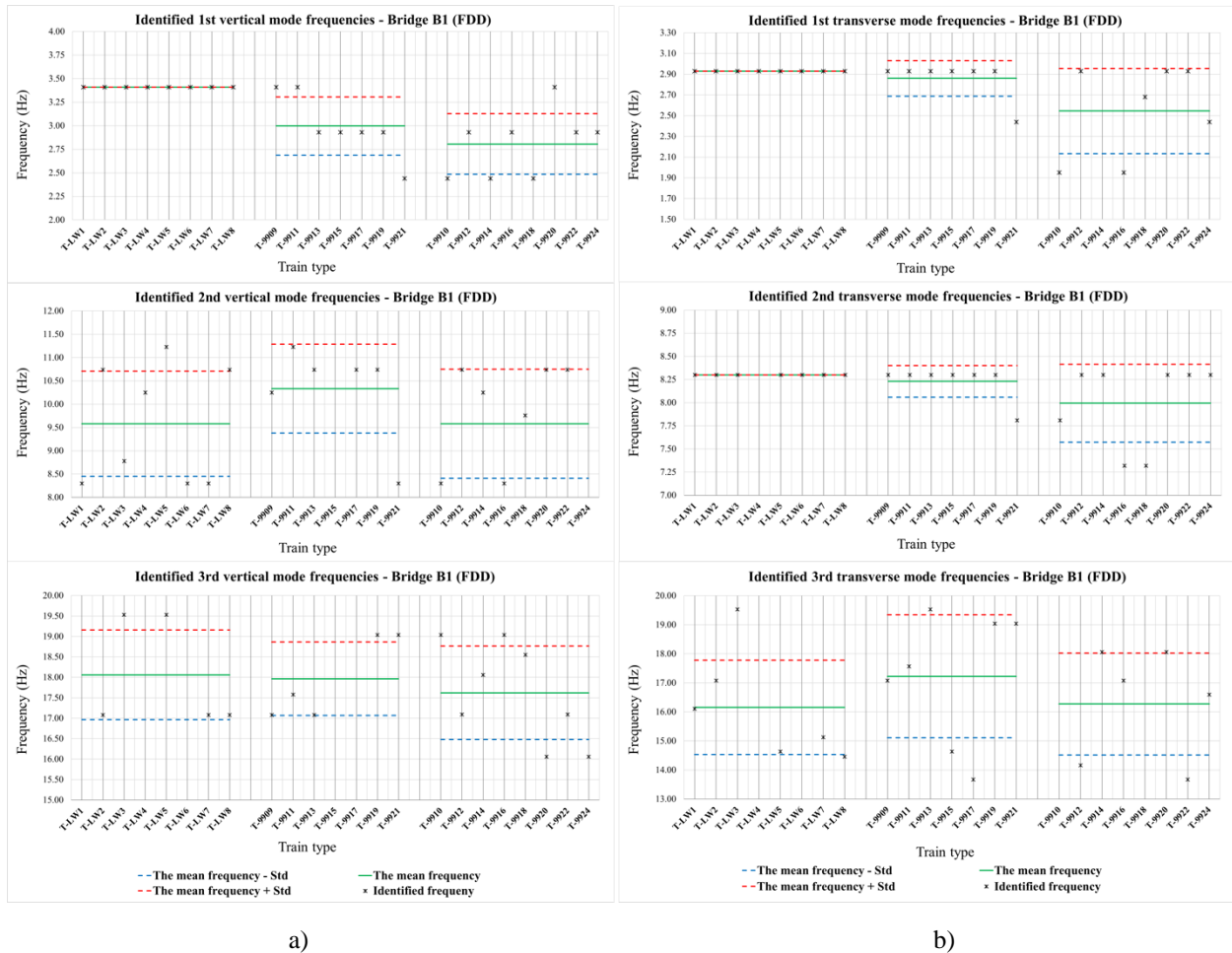Figure 35. The identified mode shapes for bridge B2 using the FDD method through free decay responses after the train crossing; a) vertical direction, b) transverse direction.

4.4.3 Identified modal damping of the bridges

The damping ratios of the first six modes of both bridges were identified using the SSI-COV method and summarized in Table 2, where the mean and standard deviation of damping values are presented. The range of identified damping ratios is between approximately 1.2% and 5.77%. The difference in the identified damping ratios through different excitation sources can be easily observed. Since damping ratio identification is not the main aim of this thesis, this parameter is less evaluated compared with frequency and mode shape. Generally, more significant variation can be observed in identified damping ratios compared with corresponding identified frequencies as mentioned in literature [29,34,35].

Table 2. Modal damping ratio identified by SSI-COV for the bridges.

| Mode | Bridge B1 | | | | | | Bridge B2 | | | | | |
| | Loaded train | | Unloaded train | | Lightweight train | | Loaded train | | Unloaded train | | Lightweight train | |
	Mean (%)	Std (%)	Mean (%)	Std (%)	Mean (%)	Std (%)	Mean (%)	Std (%)	Mean (%)	Std (%)	Mean (%)	Std (%)
V1	4.13	1.25	5.77	2.02	3.25	1.66	2.42	0.64	1.56	0.57	2.99	0.76
V2	2.85	0.96	2.42	1.53	2.43	1.02	3.05	1.56	2.15	0.72	1.98	0.15
V3	1.91	0.45	1.87	0.98	1.21	0.72	1.37	0.44	1.39	0.25	1.26	0.04
T1	3.79	2.96	3.6	1.36	1.52	0.44	2.46	1.28	2.75	0.88	1.60	0.17
T2	1.43	0.55	3.39	2.55	2.01	1.51	3.27	1.68	2.61	2.48	1.24	0.07
T3	2.08	0.49	1.99	0.74	1.68	1.19	2.45	0.95	2.52	0.81	1.71	0.36

4.5 Discussion and comparison of identified modal parameters

4.5.1 Natural frequencies and damping ratios

As presented in Figure 28-31, all of the six modes of interest could be identified by two OMA algorithms for each bridge, however, by use of some train crossings, some modes are missed. The reason can be the relatively low participation of these modes in the bridge vibration responses. The missing modes are more highlighted for bridge B2 in the case of the lightweight vehicle crossing as the excitation source. Of the 48 cases of lightweight vehicle crossings for bridge B2 (six modes and eight lightweight vehicle crossings), FDD could successfully identify just 17 cases with a success rate of 35.4%, while SSI-COV could successfully identify 14 cases with a 29.1% success rate. This can be potentially attributed to the weak excitation caused by the passage of the

lightweight vehicle and low signal-to-noise ratios recorded by sensors specifically for those sensors far from the excitation source (where the train is leaving the bridge) as explained in Section 4.3.3.2. Conversely, considering all loaded and unloaded train crossings, this success rate for bridge B2 is 92.2% and 91.1% for FDD and SSI-COV methods respectively that can imply the higher amount of energy of the excitation caused by these two types of trains crossings.

Regarding bridge B1, although crossing of the lightweight vehicle produced weak excitation compared with two other types of passing trains, the identification process using lightweight vehicle crossing was as successful as using the loaded and unloaded train crossings. For bridge B1, the FDD and SSI-COV methods have the same success rate of 89.8% and totally, of the 138 train crossing cases (six modes and 23 train crossings), each method missed just 14 modes. Also, the number of identified transverse modes is approximately equal to those of vertical modes for both bridges, which shows that modes in the transverse direction can be excited as well as vertical modes by the passage of the trains.

In Table 3 and Table 4, mean identified frequencies for both bridges are presented among different excitation sources and algorithms. In the tables, the modes are indicated by the symbols V and T for vertical and transverse direction. For both bridges, for the first vertical (V1) and transverse mode (T1), a descending trend in the mean identified frequency is observed with the increase in the mass of the passing train. But the same trend is not always observed in higher modes. This observation implies that identified frequencies, especially fundamental modes, are affected by the mass of the train crossings. Moreover, the vertical modes are affected more than transverse modes by the mass of the train crossing. The train mass has a greater effect on the identified frequencies for the single-span bridge as evidenced by the difference in the frequencies identified from the crossing of the lightweight vehicle and the loaded iron ore train for this bridge.

For bridge B1, the identified frequency of the mode V1 is reduced from 3.31 Hz for the lightweight vehicle to 2.85 Hz for the loaded iron ore train (frequencies extracted from SSI-COV). This difference for bridge B2 is from the frequency of 3.04 Hz for the lightweight vehicle to 2.93 Hz for the loaded iron ore train, although identified results from the lightweight train crossing for bridge B2 suffer from insufficient samplings and they are likely to be unreliable due to weak excitation and low SNRs. It is difficult to consolidate the confidence in the identified frequencies for bridge B2 using excitation induced by lightweight vehicle crossings. As for comparison of the

identified frequencies across the loaded train and unloaded train for bridge B2, the reducing effect of the train mass on the identified frequencies is clearly observed.

An increasing trend in the standard deviation of the identified frequencies is observed with the increase in mass of the train crossings, there is also a more standard deviation for higher modes. It can be observed that the variation of identified frequencies for bridge B1 (single-span bridge) is higher than those of bridge B2 (two-span bridge). This observation can demonstrate that identified frequencies of the stiffer bridges with shorter spans can be more prone to uncertainties.

With respect to the effect of the train mass, it can imply that identified parameters from free decay responses induced by those trains that have less mass can be more reliable to be used for model updating since the results are less affected by the mass of the train crossing.

Table 3. Means and standard deviations (in parentheses) of the identified frequencies for bridge B1 across different excitation cases and methods.

| Mode | Natural frequency (Hz) | | | | | |
| | Loaded train | | Unloaded train | | Lightweight train | |
	FDD	SSI-COV	FDD	SSI-COV	FDD	SSI-COV
T1	2.54 (0.41)	2.78 (0.08)	2.86 (0.17)	2.81 (0.04)	2.93 (0.00)	2.87 (0.01)
V1	2.81 (0.32)	2.85 (0.30)	3.00 (0.31)	2.99 (0.25)	3.41 (0.00)	3.31 (0.06)
T2	7.99 (0.42)	8.08 (0.41)	8.23 (0.17)	8.20 (0.57)	8.30 (0.00)	8.40 (0.33)
V2	9.58 (1.17)	9.55 (1.04)	10.33 (0.95)	9.60 (1.02)	9.58 (1.13)	9.55 (1.03)
T3	16.27 (1.75)	16.54 (2.09)	17.22 (2.12)	17.56 (1.58)	16.16 (1.62)	16.16 (0.95)
V3	17.62 (1.15)	17.97 (0.84)	17.96 (0.90)	17.88 (0.70)	18.06 (1.10)	17.53 (0.85)

Table 4. Means and standard deviations (in parentheses) of the identified frequencies for bridge B2 across different excitation cases and methods.

| Mode | Natural frequency (Hz) | | | | | |
| | Loaded train | | Unloaded train | | Lightweight train | |
	FDD	SSI-COV	FDD	SSI-COV	FDD	SSI-COV
T1	2.16 (0.08)	2.12 (0.04)	2.16 (0.08)	2.15 (0.01)	2.19 (0.00)	2.14 (0.01)
V1	2.96 (0.08)	2.93 (0.09)	3.10 (0.11)	3.04 (0.08)	2.92 (0.00)	3.04 (0.00)
T2	4.08 (0.11)	4.11 (0.10)	4.11 (0.09)	4.15 (0.09)	4.15 (0.00)	4.19 (0.01)
V2	4.63 (0.13)	4.72 (0.13)	4.63 (0.00)	4.64 (0.21)	4.63 (0.00)	4.75 (0.01)
T3	8.21 (0.24)	8.26 (0.26)	8.34 (0.36)	8.45 (0.16)	8.38 (0.10)	8.38 (0.03)
V3	10.21 (0.3)	10.27 (0.26)	10.53 (0.31)	10.56 (0.31)	10.49 (0.00)	10.48 (0.04)

In terms of the performance comparison among the FDD and SSI-COV techniques, more frequency discrepancy across the FDD method was observed compared with SSI-COV. The highest discrepancy in terms of standard deviation was 2.12 Hz using the FDD method observed in mode T3 for bridge B1 across the unloaded train crossing. Generally, both FDD and SSI-COV techniques were successful in the identification of all modes in the frequency range of interest. Due to the lack of a comparative benchmark, the performance evaluation of the FDD and SSI-COV is not possible to determine superior performance.

Regarding identified damping ratios, the mean values were almost below 3.5%, although in some cases like mode V1 for bridge B1, under excitation of the unloaded train crossing, the damping ratio was identified at 5.77%. It can also be observed that identified damping ratios among the crossing of the lightweight vehicle are rather smaller than those of two other types of train crossings that can be related to the smaller bridge displacements caused by the lightweight vehicle crossing. Mostly identified damping ratios are smaller than damping ratios assumed in the seismic design of the bridges. This can be attributed to the amplitude of the displacements. Basically, when displacements become larger as expected during earthquakes, damping ratios can be higher [56]. The scattering observed for identified damping ratios is substantially larger than those for the corresponding frequencies. This large variance for identified damping ratios is well-known and reported in the structural identification literature [30,55].

4.5.2 Mode shapes

A considerable variation in mode shapes caused by different train crossings showing the importance of considering the various free vibration responses to achieve a mean mode shape. The mean mode shapes using different train crossings, for both bridges, are rather close to each other while, the most significant differences in mean mode shapes were observed at the ends of bridges, more specifically for bridge B1 for modes V3 and T3 that confirms the importance of sensor installation at supports to identify the boundary conditions behavior. It should be mentioned that due to the problem of missing data from the sensor close to the left end of bridge B2, this end is perforce assumed as a pinned support, which is in contrast to what this research is looking for and the aim of this thesis. This assumption may be providing unreliable observation on the mode shapes for bridge B2 specifically for the boundary conditions at the left end of the bridge.

Figure 36-38 present the correlation of the identified mode shapes for bridge B1 between the FDD and SSI-COV method, using the MAC values. Due to the aforementioned problem related to missing data for bridge B2, MAC values for this bridge are not calculated. The MAC values for bridge B1 are higher for the lower order modes than the higher modes values, showing a high level of correlation between the identified fundamental modes, indeed the MAC values reach as high as above 98% for modes V1 and T1. The MAC values for modes V2 and T2 are also above 90%. It is evident that there are more challenges in the identification of higher-order modes as the lower MAC values are observed for modes V3 and T3. There is an unsatisfactory correlation between FDD and SSI-COV results for mode T3 among the crossing of the unloaded train since the MAC value is 55.7%. Since there is no benchmark to be used, a decisive comment on the best performance between FDD and SSI-COV is difficult.

Identified mode shapes using unloaded train crossing indicate considerable differences specifically at the two ends of the bridge for mode T3 (see Figure 32b and Figure 33b). For the third transverse mode shapes across all train crossings, obtained MAC values range from 55% to 95% that have the largest variation compared with other mode shapes. The lower MAC value for higher modes can stem from the complex vibration mechanisms of these modes, and this complexity can be governed by nonlinearity in material properties and structural characteristics, and measurement errors [55].

For bridge B2, less variation is observed between mode shapes among different train crossings using both identification methods compared with bridge B1, the same results were observed earlier for identified frequencies. Even a good agreement is found between the mean mode shapes at the right end of bridge B2, at the support location that is not considered as a pinned or roller support.

Although for the mean mode shapes of bridge B2, a significant variation for mode V1 is observed between the mean obtained from lightweight vehicle crossing and the mean obtained from two other train crossings, particularly through the FDD method (see Figure 35a), this observation cannot be reliable. Generally, the extracted results from the lightweight vehicles crossing bridge B2 require more cases to be analyzed. Also, the low SNRs may result in erroneous parameter identification.

a)   b)
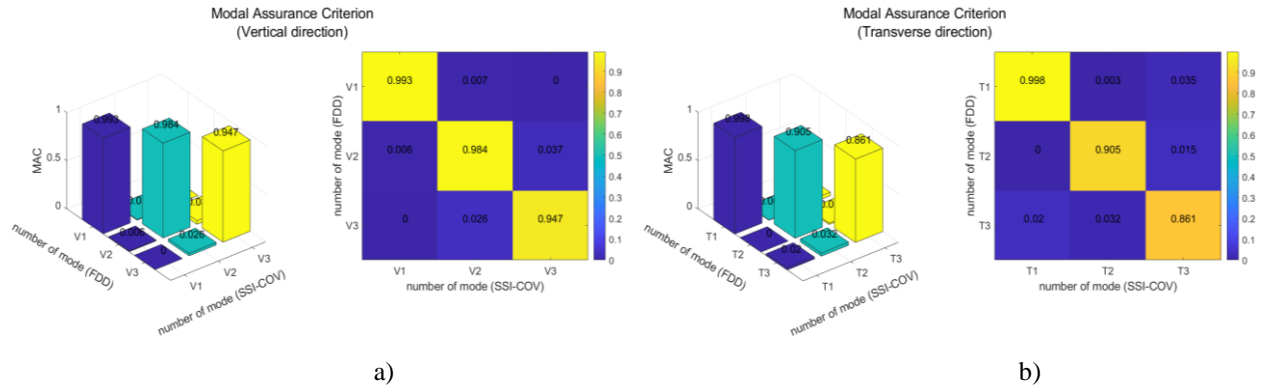
Figure 36. Correlation between the mean mode shapes identified through the FDD and SSI-COV for bridge B1 using the free vibration after the lightweight vehicle crossing; a) Vertical modes, b) Transverse modes.

a)   b)
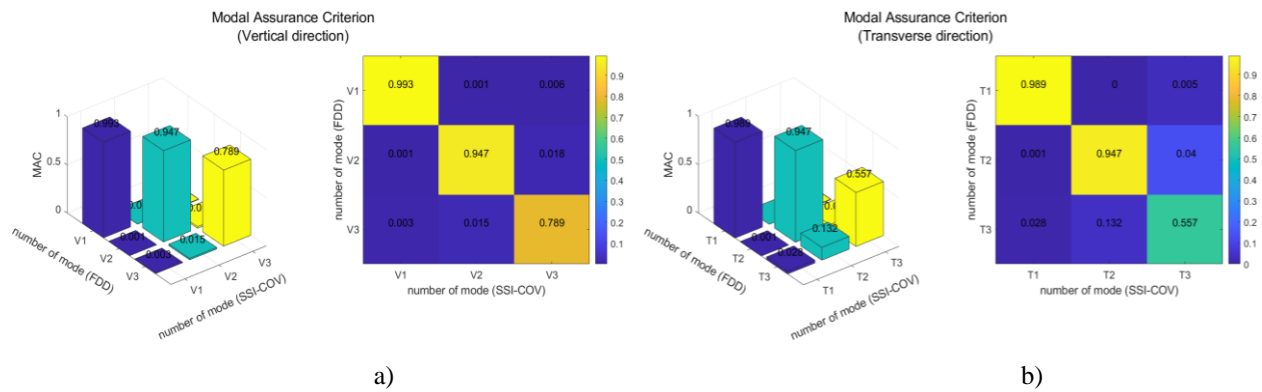
Figure 37. Correlation between the mean mode shapes identified through the FDD and SSI-COV for bridge B1 using the free vibration after the unloaded train crossing; a) Vertical modes, b) Transverse modes.

a)   b)
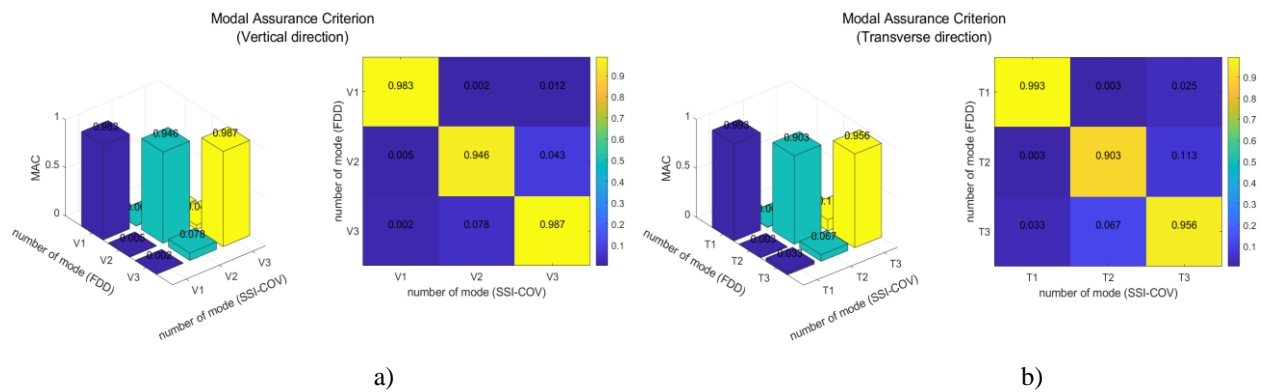
Figure 38. Correlation between the mean mode shapes identified through the FDD and SSI-COV for bridge B1 using the free vibration after the loaded train crossing; a) Vertical modes, b) Transverse modes.

In the end, based on mentioned observations and the problem of data recording for bridge B2, it is decided that model updating is just performed for bridge B1, and concluded that the results from the lightweight vehicle crossing are more likely to be close to the real modal parameters of the bridge. Also, the extracted parameters from the SSI-COV method are used for FE model updating since this method is introduced as a robust OMA algorithm in the identification literature [29,30].

Chapter 5

Finite Element Model Updating

5.1 Introduction

In this chapter, the details are presented on the model calibration of bridge B1. Due to before mentioned problem for bridge B2, updating the finite element (FE) model of this bridge with a pinned support does not fulfill the aim of this research. An initial FE model of bridge B1 was developed based on the available drawings and site visits. Different updating parameters are considered for model updating, and a sensitivity analysis is performed to determine the most effective parameters and examine their effective range of the parameters for the model updating process. To develop an efficient method for FE model updating, the artificial neural network (ANN) is used since it is a robust computing tool to model complex relationships between a set of data. The FE modeling is performed in SAP2000, and Python is used to train the ANN to identify the updating parameters. The natural frequencies of bridge B1 ($f_{v1}, f_{v2}, f_{v3}, f_{t1}, f_{t2}, f_{t3}$) are inputs, and bridge parameters are the outputs of the network.

As discussed in Section 4.5, the identified modal parameters across lightweight vehicle crossing using the SSI-COV technique can be more reliable to be considered as the field-measured parameters to validate the success of the model updating process and quantify the accuracy of parameter estimation.

5.2 Initial FE model of the bridge B1

The bridge is single-span with a length of 50m as introduced in Section 4.2, the slab is supported by two T-beames with the bearing under each T-beam, the dimension of the cross section was measured manually on the initial drawing and presented in Figure 39. Since the bridge is completely straight and symmetric and sensors were installed on one side of the deck in a straight line (see Figure 13), the beam element is used for the simulation of the bridge. For simplicity, the parapets and other non-structural elements are not considered in FE modeling as they have no effect or at least negligible effect on the bridge stiffness. The FE model of the bridge is presented in Figure 40.

The common bridge boundary conditions in FE modeling for the sake of simplicity are often assumed ideal rollers or hinges, that their behavior can be far from the actual behavior of the supports. Therefore, in this thesis, it is tried to simulate the boundary conditions introducing the real behavior of the bearings as explained in Section 5.3.1.

The concrete class is considered C45/55 with an elasticity modulus of 36GPa based on available information in the drawings. Also, the weight per unit volume of the concrete is assumed 25 KN/m^3 including all the reinforcements, tendons, and prestressing cables.

a)   b)
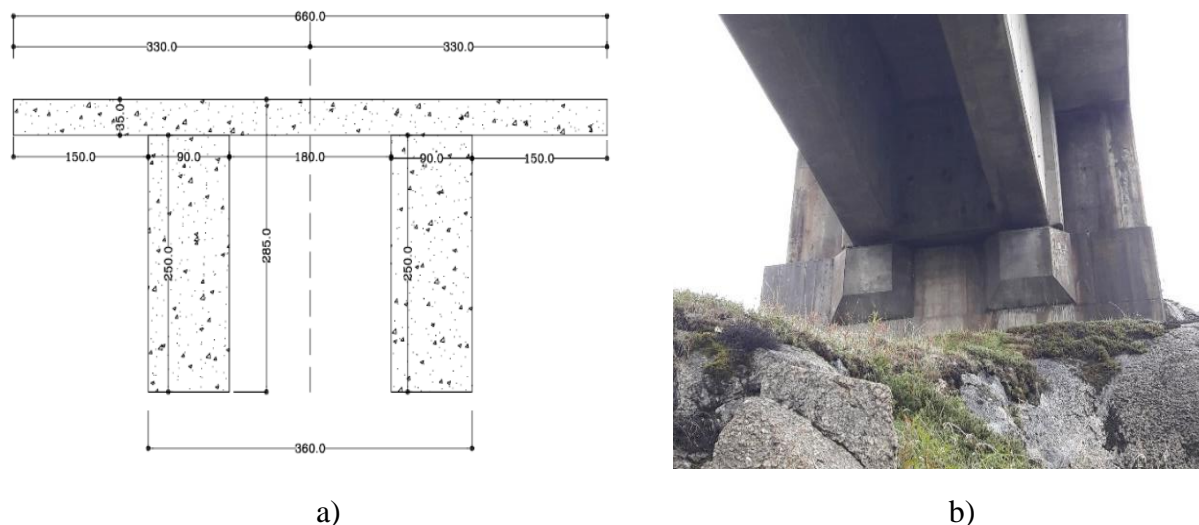
Figure 39. Bridge B1; a) The cross section (unit:cm), b) bridge support.

In addition to the concrete bridge deck, other factors including parapets, ballast, and other railway track equipment causing significant changes in the mass of the bridge. Since accurate dimensions of the bridge deck and information related to the bridge pavement were unavailable, it was difficult

to determine the participation of all these factors separately in the total mass of the bridge. Therefore, it was decided that the total mass of the bridge is determined by multiplying the mass per unit volume of the concrete by a coefficient larger than 1.0 to account for the other factors in the total mass. For this, it is assumed that the bridge deck pavement is distributed uniformly with the same properties along the bridge deck. Based on initial investigation the low limit of this coefficient is assumed 1.15.

a)   b)
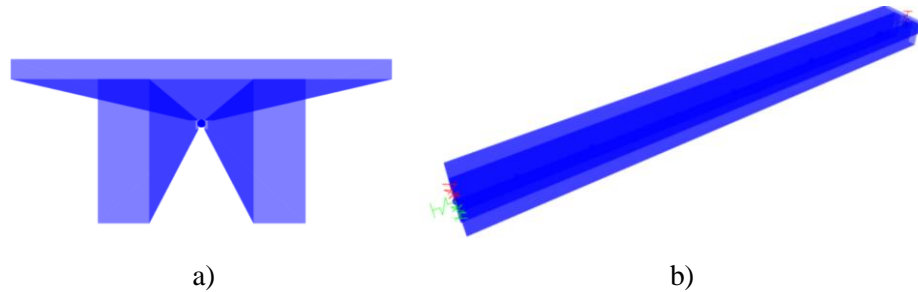
Figure 40. FE model of bridge B1; a) cross-section view, b) 3D view.

5.3 Selection of the updating parameters and sensitivity analyses

Identification of the updating parameters is of great importance for the success of the model updating process. There is a large set of updating parameters mostly affecting the local responses of the bridge. Identification of the updating parameters affecting the global responses is a significant step for model calibration of the bridges. The parametric investigation revealed that for the bridge critical updating parameters, affecting the dynamic responses significantly, are boundary conditions, elasticity modulus of the concrete, and mass of the bridge deck.

5.3.1 Boundary conditions considering rotational stiffness

Since the behavior of the boundary conditions is complex, in many studies, for simplicity, rollers and pinned supports are assumed as the ideal boundary condition presenting infinite translational stiffness. This assumption can be completely different from the real behavior of the supports since real supporting connections have certain resistance and stiffness. Hence in this study at each support, the translational springs are defined in three perpendicular directions with different spring stiffnesses K_v, K_t, K_l corresponding to the vertical, transverse, and longitudinal directions respectively. In addition to the translational stiffness, an additional constraining effect of boundary conditions is assumed as the rotational stiffness. Therefore, two rotational springs with stiffnesses

KR_t and KR_v about transverse and vertical directions are defined, so that KR_t is affecting vertical modes while KR_v is affecting transverse modes. Figure 41 shows a 2D view of the theoretical model of the bridge with mentioned translational and rotational springs.

It should be noted that the properties of the two bridge supports are considered to be similar and the restraining effects of two elastomers at each end are grouped and allocated to a single point at each end.
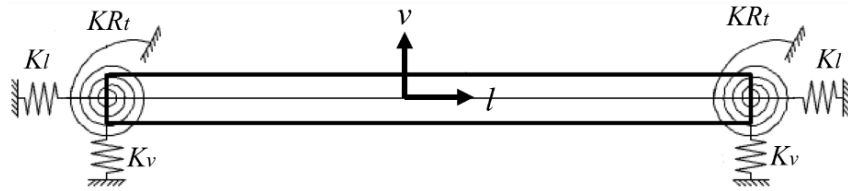
Figure 41. The 2D view of the theoretical bridge model with translational and rotational springs at two ends.

To determine the effective range of a parameter, this parameter is changing while the other parameters are kept constant. For this, to determine the effective range of each spring stiffness, the frequencies of the six studied modes of the bridge are recorded while considered spring stiffness is taking values from low to very high stiffness until no significant change is observed in the mode frequencies. The results are presented in Figure 42 and Figure 43 for translational and rotational stiffnesses respectively. Just in the case of rotational spring about vertical direction (KR_v), Figure 43b, since obtained frequencies during the sensitivity analysis were much higher than the identified frequency for mode T1 through OMA, the recording stopped. The identified frequency for mode T1 through OMA is 2.87 Hz while the obtained frequency in sensitivity analysis reached more than 4.1 Hz. Therefore higher stiffnesses for KR_v are not considered.

Figure 42 and Figure 43 show that vertical and transverse translational spring stiffnesses affect the higher mode frequencies more than low-order mode frequencies, while higher-order modes are not as sensitive as the low-order mode to the rotational spring stiffnesses. It should be noted that in case of consideration of the boundary conditions as a pinned with no translational movement, the frequency of the first vertical mode reaches 1.96 Hz that is far from identified field-measured frequency for mode V1 for bridge B1 that is 3.31 Hz. It shows that additional constraining effects of boundary conditions should be applied to increase the frequency and reflect the real behavior of the supports. Otherwise, other factors like elasticity modulus should have unreal large values to increase the frequency. Also, Figure 42c manifests that frequencies are not sensitive to the stiffness

of the longitudinal spring. Therefore, this parameter can be removed from the FE model updating process.

Figure 42. The change of the natural frequencies of the bridge FE model based on translational spring stiffnesses; a) vertical stiffness, b) transverse stiffness, c) longitudinal stiffness.

It can be observed that frequencies of V2 and V3 are highly sensitive to vertical spring stiffnesses (K_v) between 10^5 KN/m and approximately 10^9 KN/m, and frequencies of T2 and T3 are sensitive to transverse spring stiffness (K_t) between 10^5 KN/m and approximately 10^8 KN/m. It should be noted that unrealistic displacements, rigid body deformation, were observed in the case of low

values for K_v and K_t as shown in Figure 44. Therefore, the low limit for translational stiffness in both transverse and vertical is determined 10^5 KN/m. Also, for KR_t and KR_v the sensitive range is restricted to the range of 10^5-10^8 KN.m/rad. Although the values higher than 10^8 KN.m/rad for KR_v could increase the frequency of the first transverse mode, these values were ignored since obtained frequencies were much higher than identified frequency from OMA.

That is to say, during changing the stiffness values, the order of modes may switch or even new modes may appear depending on the value of the existing stiffness. For instance, it can be observed that in very low values of the vertical spring stiffness, K_v (see Figure 42a) the order of the third vertical mode (V3) is lower than the second and third transverse modes (T2, T3) while by increasing values of K_v, the order of the modes is changing. Hence, it is of utmost importance to ensure that the order of experimental and analytical modes are equivalent not just in terms of frequency values, but also in terms of mode shape similarity. Finally, four parameters of the boundary condition including K_v, K_t, KR_t, and KR_v are selected as the updating parameters.
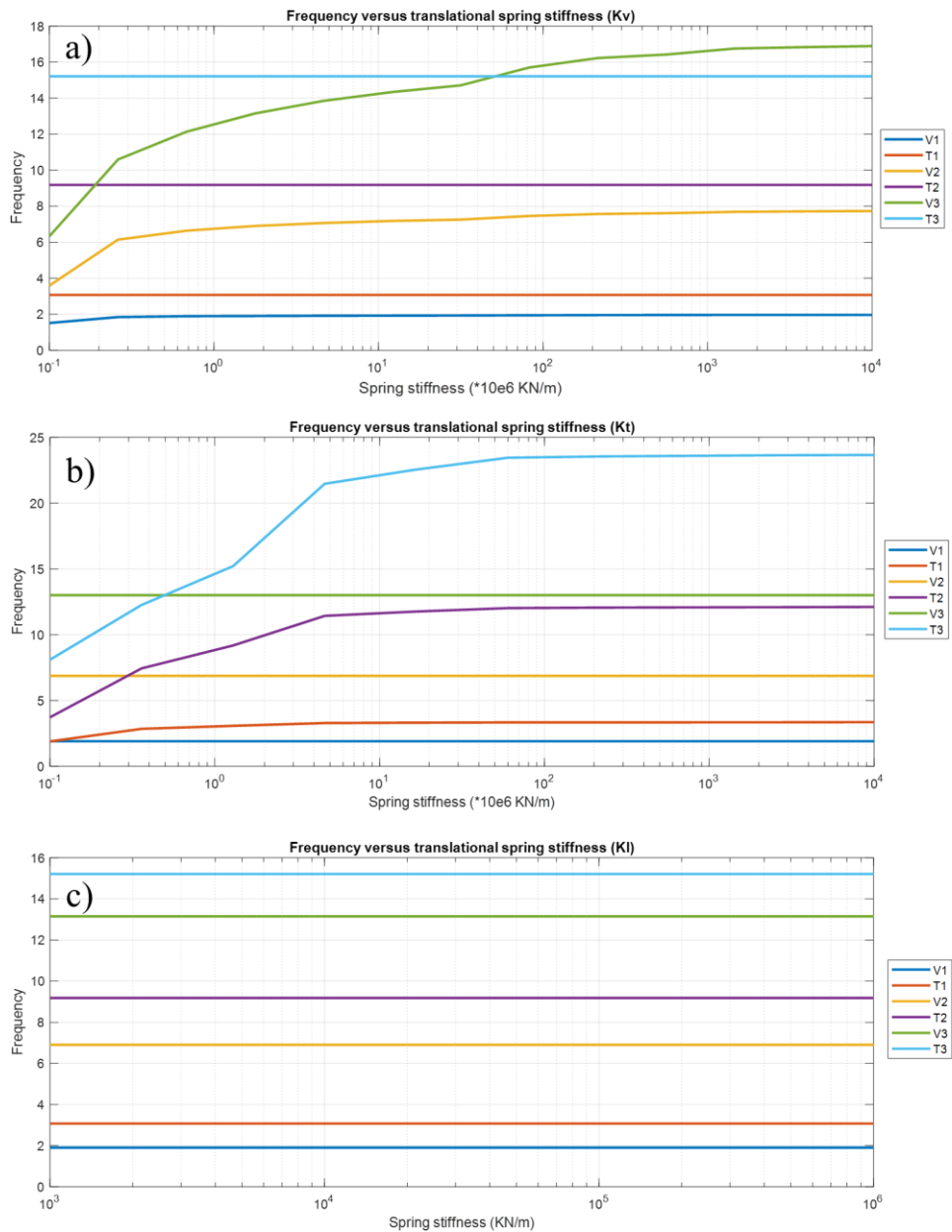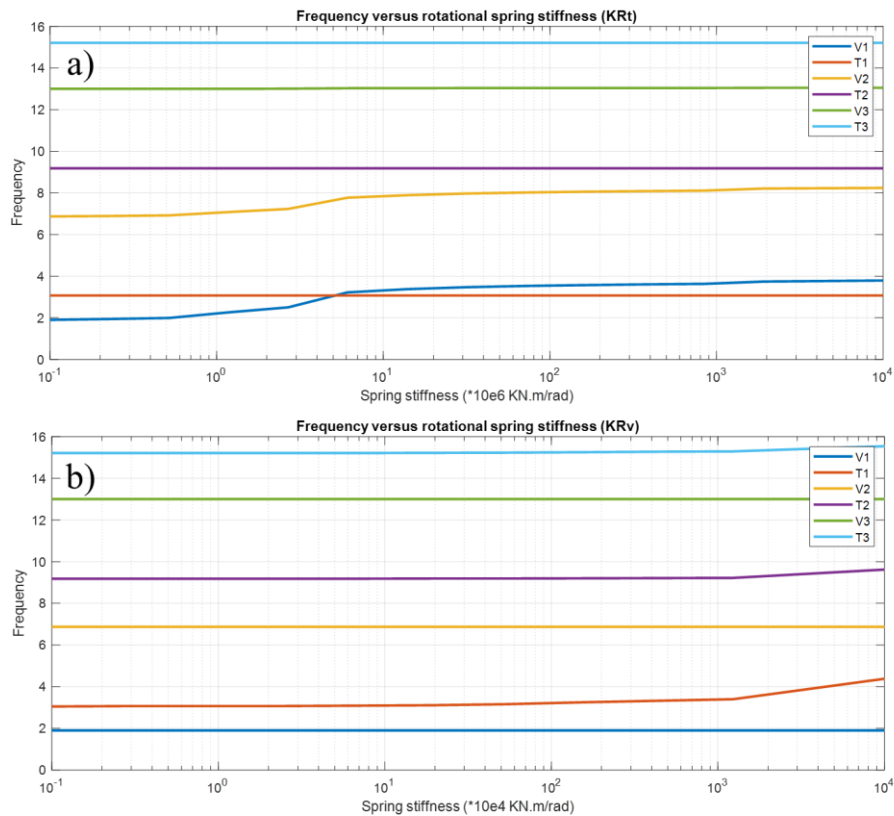

Figure 43. The change of the natural frequencies of the bridge FE model based on rotational spring stiffnesses; a) about transverse direction, b) about vertical direction.
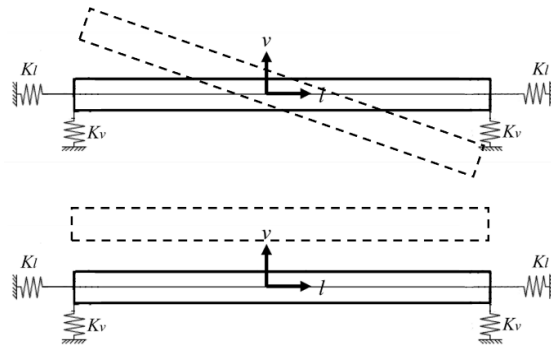
Figure 44. Rigid body displacements of the bridge with the low values of the translational spring stiffness.

5.3.2 Elasticity modulus of concrete

Elasticity modulus of the concrete (E) is another decisive factor in modal parameters estimation. The increase in this parameter leads to a stiffer structure and increases the frequencies. It should be highlighted that a single value of elasticity modulus is considered for whole the bridge in FE modeling, although the local variation of this parameter is more likely caused by damages, deterioration, or non-homogenous property of the concrete. This single parameter is representing a general condition of the concrete in an overall sense. Although the information related to the concrete class was available in the drawings, due to the lack of material tests on the concrete of the bridge a large variation is considered for this parameter to count the effect of aging, deterioration, and other unknown factors changing the concrete properties. For this purpose, a modification factor ranging from 0.5 to 1.5 multiplied by the pre-assumed concrete elasticity modulus. The variation range of this parameter is set as 18-54 GPA as shown in Figure 45.
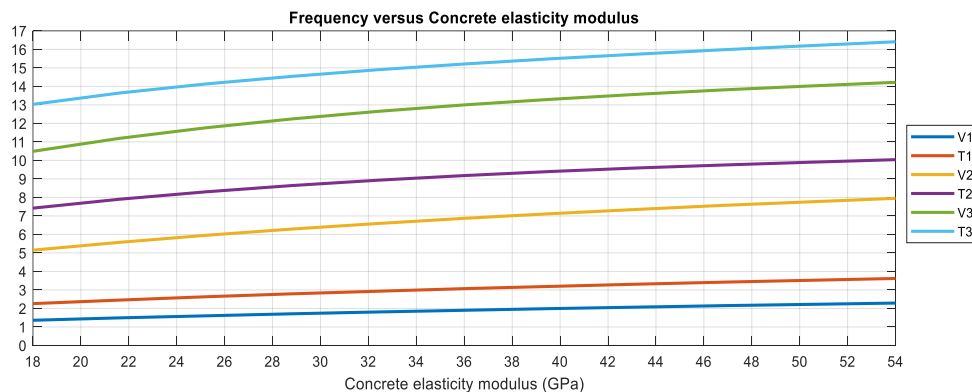
Figure 45. The change of natural frequencies based on concrete elasticity modulus.

5.3.3 Mass of bridge deck

It was mentioned that due to the lack of the accurate dimensions of the bridge deck and information related to the pavement over the bridge deck, it was decided that the total mass of the bridge is determined as a single parameter presenting the total mass of the bridge including concrete parts, ballast, sleepers, and other railway equipment on the bridge contributing to the modal mass. The initial mass of the bridge deck pavement is assumed 15% of the concrete part of the bridge, therefore an increasing factor (C_m) in the range of 1.15-1.40 was multiplied by the density of the concrete to count the mass of the other factors. It is mentioned that the distribution of the surface overlay of the bridge deck is assumed uniformly. Figure 46 is presenting the frequency changes versus mass modification factor (C_m).
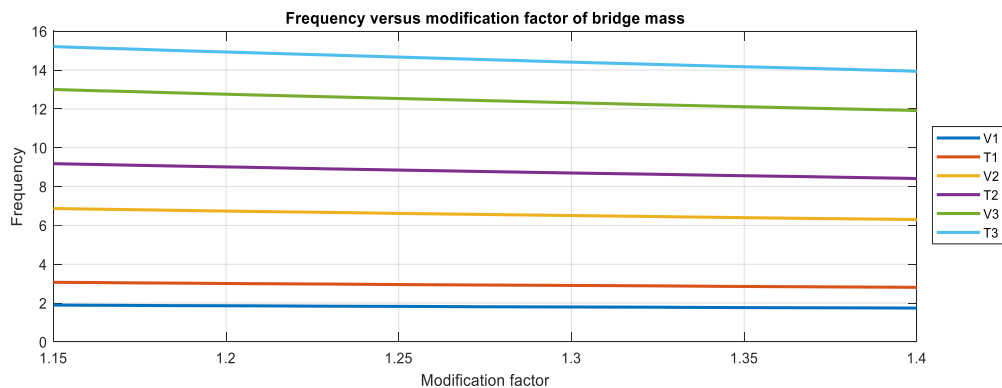
Figure 46. The change of natural frequencies based on the mass modification factor.

5.4 Neural network based model updating

The neural network based model updating is involved in the procedure as follows:

1. Determination of the updating parameters (i.e. K_v, K_t, KR_v, KR_t, E, C_m) and their effective range.

2. Identification of the bridge modal parameters from the field test.

3. Generating a training dataset by repeated FE analyses, by changing the values of the updating parameters in their effective range, and obtaining the FE model responses.

4. Choosing the suitable network and training the network by use of the training dataset, to learn the relationship between inputs (f_{v1}, f_{v2}, f_{v3}, f_{t1}, f_{t2}, f_{t3}) and outputs (K_v, K_t, KR_v, KR_t, E, C_m).

5. Feeding the identified modal parameters of the bridge into the trained network, and obtaining the predicted parameters.

6. Updating the FE model according to predicted parameters and analyzing the FE model to obtain the responses.

8. Comparison of the field-measured responses with simulated responses to quantify the accuracy of the updated model and the success of the updating process.

The following subsections present further details and implementation of the model updating process.

5.4.1 Generating dataset for neural networks

After performing the sensitivity analysis, six bridge parameters are selected as the most important parameters affecting the natural frequencies, i.e. K_v, K_t, KR_v, KR_t, E, and C_m. Two sets of training data are generated after the identification of the updating parameters. In the first training dataset, only one parameter is changing within its predefined ranges while others are constant and a total of 550 FE models are created. The second dataset is generated by a total of 100 FE models while all parameters are changing randomly within their effective ranges.

To validate the trained neural network, each dataset is divided into two subsets of the training set and the cross-validation set. The training set is used to identify the inverse relationships between frequencies (inputs) and parameters (outputs) and it consists of both input and output, while the cross-validation set is used to prevent over-fitting. Over-fitting occurs when the errors are reducing to very small values but the network loses its capacity to generate excellent predictions for those data not included in the training set [57]. The cross-validation set consists of just inputs (frequencies) and predicts the parameters. It should be noted that predicted parameters in this level are available in the training dataset and they are not final updating parameters and this prediction is just performed to validate the trained network results. For this purpose, 20% of the training dataset is selected as the cross-validation set.

5.4.2 Training process

The training process is an iterative procedure that involves identifying a set of weights in the network. This process is developed step by step with small changes in the weights during each iteration, resulting in the change of the network performance in each iteration. The performance of the network highly depends on the network architecture and parameters chosen. The network parameters can be chosen according to the nature of the problem and former studies'

recommendations. To choose the suitable network architecture, no specific recommendation is outlined in former studies and it requires trial and error to reach the most suitable network architecture. For this, various networks with one and two inner layers are evaluated considering the set of network parameters listed below.

- Share of training sets: 80%.
- Share of cross-validation sets: 20%.
- Number of input layer neurons: 6.
- Number of output layer neurons: 6.
- Activation functions: Sigmoid, Relu function.
- Normlization range: (0.0- 1.0).

The networks with one and two hidden layers are evaluated while the number of neurons in the hidden layer(s) is varied from 8 to 12 to generate different network architectures, totally ten different cases. Then each network is trained and field-measured frequencies are fed into the network to predict the parameters. Then FE model is updated according to the predicted parameters and the responses from the FE model are compared to the field-measured frequencies. The best performance of the network is obtained with one hidden layer including eight neurons. Hence, the architectural form of the network is 6-8-6 as illustrated in Figure 47. Also, the activation function of Sigmoid had a better performance compared to the results of the Relu activation function.
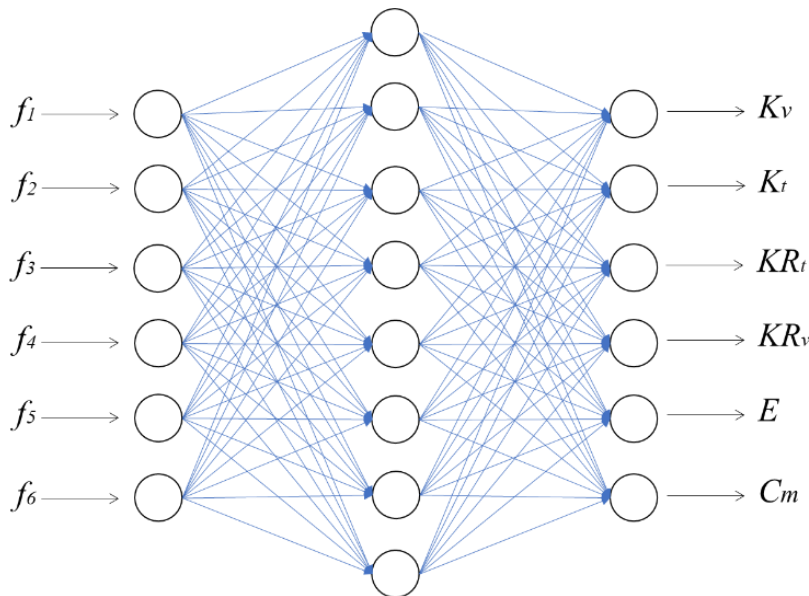
Figure 47. The network architecture used for the model updating process.

5.4.3 Trained network and estimation of updated parameters

The training of the network is performed by two datasets. In the case of using just the first dataset (one updating parameter is changing), the network was not able to predict the proper output that is a combination of all parameres, this deficiency was due to the unsuitable training dataset. Then the second dataset, in which all parameters are changing randomly, was added to the first one and the training process was performed by use of both datasets, the network was trained properly to find the relationships between inputs (frequencies) and outputs (bridge parameters).

According to the explanation in CHAPTER 4, it is decided that the identified frequencies from the crossing of the lightweight vehicle using the SSI-COV method are introduced to the trained network as the inputs. The predicted parameters (K_v, K_t, KR_v, KR_t, E, C_m), or outputs of the network, are presented in Table 5, then the FE model is updated according to these parameters. The natural frequencies of the updated FE model are presented in Table 6 in which transverse and vertical directions are indicated by t and v indexes.

Table 5. Estimated bridge properties by ANN.

K_v (KN/m)	K_t (KN/m)	KR_t (KN.m/rad)	KR_v (KN.m/rad)	E (GPa)	C_m
24.238 E+6	1.485 E+6	7.613 E+7	5.863 E+5	32.716	1.302

Table 6. The natural frequencies obtained from the updated model and field-measured data
(Numbers in parentheses are the order of mode).

	f_{t1}(1st)	f_{v1}(2nd)	f_{t2}(3rd)	f_{v2}(4th)	f_{t3}(5th)	f_{v3}(6th)
Field-measured responses	2.87	3.31	8.40	9.55	16.16	17.53
Analytical responses by SAP2000	2.86	3.36	9.09	9.15	15.70	17.32
Diff. (%)	-0.35%	1.51%	8.21%	-4.09%	-2.55%	-1.2%

It is essential to ensure that analytical and experimental modes are equivalent not just in terms of frequency values, but also in terms of mode shapes. As such, in addition to frequency matching, modal assurance criterion (MAC) is used to quantify the degree of similarity between experimental and analytical mode shapes. In Figure 48 the analytical mode shapes are correlated with field-measured mode shapes. In addition, a comparison of the mode shapes from the updated FE model and field-measured data is presented in Figure 49.

Figure 48. Correlation between analytical and experimental mode shapes using MAC; a) Vertical direction, b) Transverse direction.

a)

b)

Figure 49. Comparison of the analytical and field-measured mode shapes for bridge B1; a) vertical direction, b) transverse direction.

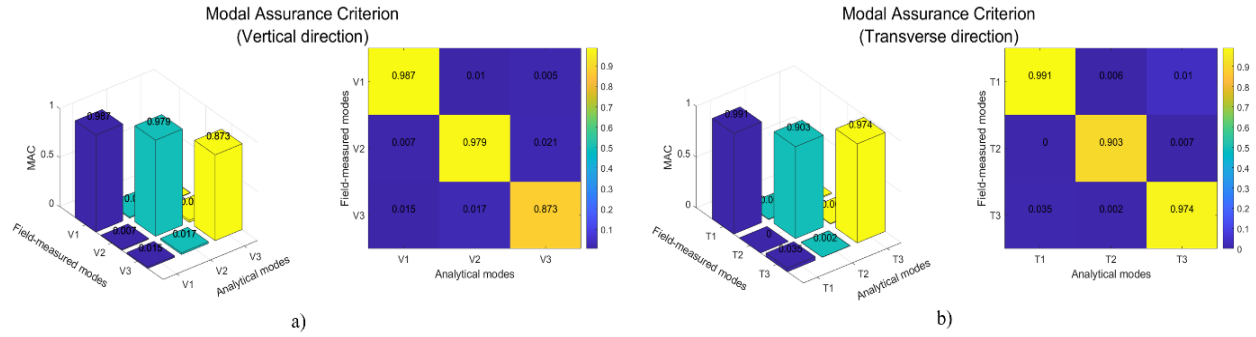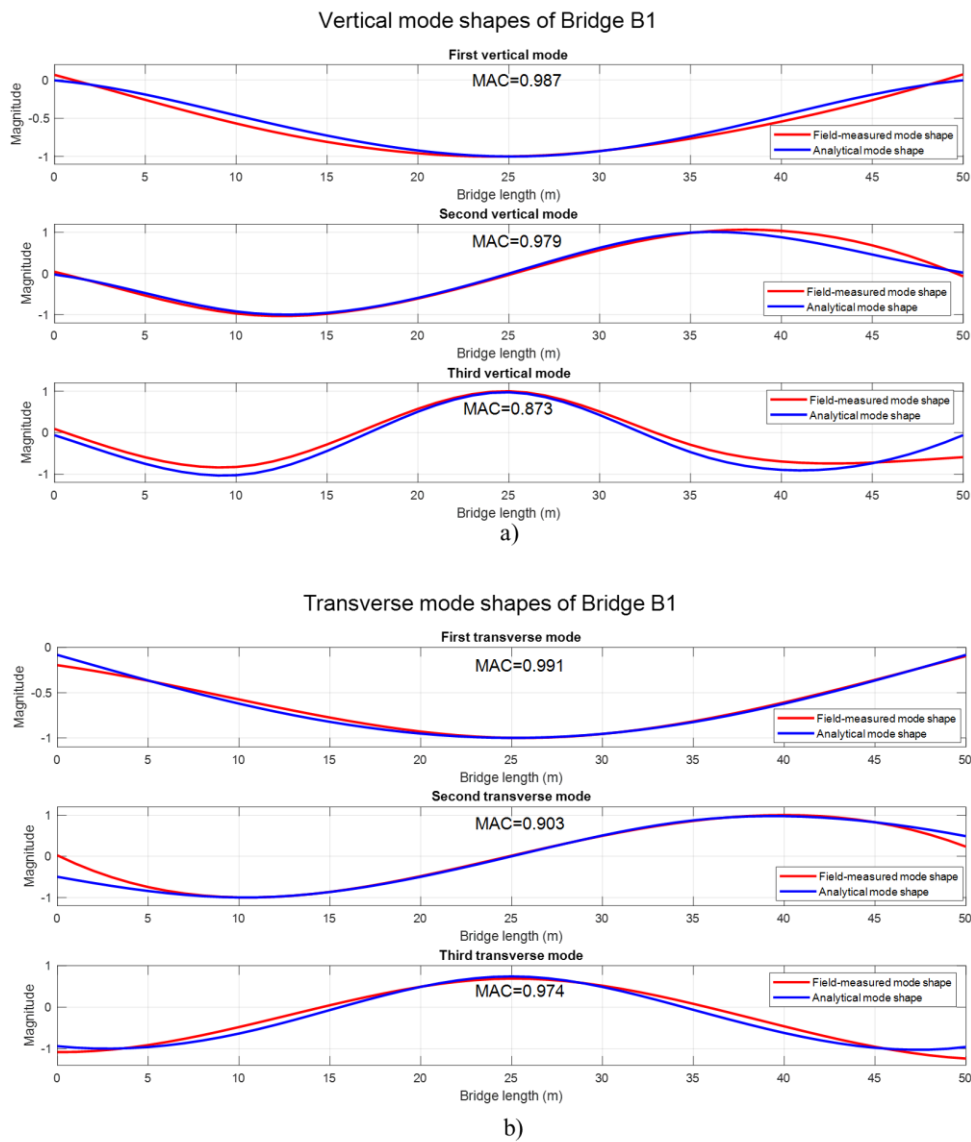## 5.5 Discussion and analysis of the results

Identification of the critical updating parameters and using the proper training dataset play a substantial role in the proper training process of the neural networks. The training dataset should contain all updating parameters in their effective ranges. The best training process was performed with the use of a dataset created by randomly selecting different combinations of updating parameter values within their effective ranges as reported by Atalla and Inman [58]. Also, using the more complicated network architecture cannot ensure the best performance of the network. For this, a trial and error process is inevitable to find the best network architecture.

The first six modes of bridge B1 are identified by OMA and compared with their counterparts from the updated FE model. The average order of error for all estimated frequencies turns out to be 2.98% with a maximum error of 8.21% for the second transverse mode while a more satisfactory level of agreement is observed between other frequencies specifically for the first modes in both transverse and vertical direction. Considering various FE modeling assumptions and a high level of uncertainties, this accuracy level can be acceptable for the dynamic responses of the updated model.

The physical implications of the updated bridge parameters for translational stiffnesses can be interpreted in a way that (i) the bridge is restrained in the vertical direction effectively with the high vertical stiffness of $K_{v=}$24.238 E+6 KN/m (24238 KN/mm); (ii) the transverse stiffness, $K_{t=}$1.485 E+6 KN/m (1485 KN/mm), is much less than vertical stiffness and also displacement at two ends of the bridge in the transverse direction, particularly for the third transverse mode, can prove it. It can be also in contrast to the design assumption assuming the support movement in the transverse direction is fully constrained by shear keys.

It was mentioned that even by considering the bridge boundary conditions as the pinned supports in the FE model, the first vertical mode reaches 1.96 Hz that is far from identified frequency of the first vertical mode for bridge B1 through field measurements. The results indicate that the estimated value for KR_t can fill this gap since by applying the rotational stiffness of KR_t the first vertical mode from the FE model reaches 3.36 Hz, very close to the field-measured counterpart. As such, in addition to translational stiffness, the vertical frequencies are substantially affected by the rotational stiffness of KR_t, but the transverse modes are less affected by the rotational stiffness of KR_v in the considered sensitivity range.

As for comparison of the mode shapes, 5 out of the 6 modes have a MAC greater than 0.90, while the lowest MAC value is observed for mode V3 with the value of 87.3% that can be counted as an acceptable level. The lower MAC value for the mode V3 may be attributed to the larger variation of the mode shape at the supports, specifically the right end, compared to other mode shapes. This variation can be caused by the error in FE modeling, modal identification, and also the curve fitting process. Therefore, recording the bridge responses at the support locations can play a vital role to increase the accuracy of the model updating process.

The estimated modification factor of the bridge mass (C_m) is 1.302, as presented in Table 5, indicating considerable participation of the bridge paving in the total mass of the bridge affecting the global bridge responses. By applying this coefficient to the factor of concrete unit weight, this factor is obtained 32.55 KN/m^3 and used in the updated FE model, and based on this the total weight of the bridge is approximately 22.61 t/m.

Also, the predicted parameter for elasticity modulus shows a reduction of 9.12% in the concrete elasticity modulus can be caused by deterioration, aging, and possible damages. Since a single elasticity modulus is assumed for the entire bridge, it is presenting a general situation of the concrete, not a localized evaluation. Further investigation is required to identify the local variation of the elasticity modulus in different parts of the bridge that is out of the scope of this thesis.

Based on results from the updated FE model, the modal mass participation of the identified modes is 87% and 98% in vertical and transverse direction respectively, representing high participation and the highlighted role of the identified modes in the results of the bridge modal analysis.

Chapter 6

Conclusion and future research

6.1 Conclusion

This chapter reports some general results and the highlighted observations arising from the research conducted during this master thesis. The thesis was divided into two main parts: (i) the quality evaluation of the identified modal parameters through the different modal identification methods and various train-induced excitations, performed on two prestressed concrete bridges; (ii) finite element (FE) model updating with a focus on the aging and constraining effect of the boundary conditions presented by both translational and rotational stiffness at the supports to establish a more accurate FE model.

This thesis presents results of the modal parameter identification of two railway bridges in Northern Norway, located on the Ofot line (*Ofotbanen)*, using the free vibration responses after different train crossings. The bridges are crossed by various types of trains ranging from iron ore trains carrying very high loads to regular trains. The vibration test was conducted using five triaxial accelerometers during a 24-hour period for each bridge in August 2020. The bridge modal parameters were identified using two OMA algorithms, FDD and SSI-COV, for 23 different train crossings while they were categorized according to the train weight into three groups including loaded iron ore train, unloaded iron ore train, and lightweight railway vehicle. The identified parameters were analyzed to evaluate the variation in modal identification results.

This thesis paid specific attention to the bridge boundary condition in the FE model updating process. The rotational stiffness was introduced to the boundary conditions in addition to the translational stiffness. The artificial neural network (ANN) is used to find the relationship between FE model responses and bridge parameters. After training the suitable network, identified parameters from experimental tests are fed to the network to estimate the real parameters of the existing bridge.

Based on the research work carried out in this thesis, it can be concluded, that:

- The identified frequencies show a significant variance, specifically for higher modes, from one train crossing to another. In addition, a higher standard deviation was observed for identified frequencies through the loaded iron ore train crossings, while the identified frequencies through the lightweight vehicle crossings showed the lowest discrepancies. Also, a rather higher standard deviation was observed for identified frequencies for the single-span bridge compared to bridge B2 (two-span bridge). This observation can demonstrate that identified frequencies of the stiffer bridges with shorter spans can be more prone to uncertainties.

- The mass of the train creating the excitation seems to have an outstanding effect on the identified frequencies for both bridges, particularly for the one-span bridge (bridge B1). A decreasing trend in the mean identified frequencies is observed with the increase in the mass of the train crossing the bridges. It should be noted that the extracted results from the lightweight vehicle crossings for bridge B2 (two-span bridge) may not be reliable due to the lack of evaluated cases and low signal-to-noise ratios.

- The mean identified natural frequencies through the different techniques (FDD and SSI-COV) were in good agreement, with a difference of less than 3% in most cases. A relatively larger frequency discrepancies were observed for the frequencies identified by the FDD method compared to their counterparts extracted by SSI-COV. Generally, the necessity to apply more than one identification technique to obtain convincing experimental results is an important recommendation worth reiterating.

- The mean identified mode shapes through the various train crossings are, generally, close to each other, indicating that mode shapes can be reliably extracted from a population of train crossings. As for comparison of the identified mode shapes, the quality of the mean mode shapes from the FDD and SSI-COV are very close. The evaluation of the extracted mean

mode shapes revealed that the SSI-COV and FDD techniques identified consistent mode shapes as evidenced by MAC values higher than 0.90 in most cases, the lowest MAC values were observed for the third vertical and transverse mode shape (V3 and T3) among passage of the unloaded train for bridge B1. Due to the lack of a comparative benchmark, the evaluation of the qualitative performance of the FDD and SSI-COV is not possible to determine the superior performance.

- For both bridges, the number of identified transverse modes is approximately equal to identified vertical modes, which shows that modes in the transverse direction can be excited as well as vertical modes by the passage of the trains, therefore train passage can be completely useful to identify the modes in both directions.

- The identified damping ratios (identified only from the SSI-COV method) can be stated as the most challenging parameter to be identified due to the large variation observed from train crossing to crossing. The same as identified frequencies, the larger standard deviations were observed for damping ratios identified across the loaded and unloaded train crossings compared to those of the lightweight vehicle crossings for both bridges. Also, there was a higher variation in identified damping ratios for bridge B1 (stiffer bridge).

- For single-span bridges with a short or medium span, free decay responses of the bridge caused by the passage of the train can be reliably used to identify the modal parameters even under weak excitation or poor signal-to-noise ratios (SNRs), but in terms of the bridges with the longer or more span(s), under weak excitation caused by passing train, identification analysis may not lead to the satisfactory and acceptable results.

- The high variation of the identified mode shapes and frequencies from one train crossing to another can show a disadvantage of the damage detection techniques that rely on the modal parameter changes such as modal curvature and modal energy.

- On the one hand, the observed variation in the identified mode shapes at the location of the bridge supports can be a sign of the importance of the sensor installation at these points to identify the accurate support behavior. On the other hand, the mode shapes at the support location reveal that the real behavior of the supports can be in contrast to the design assumptions considering the supports as the pinned or roller supports that are of utmost importance in the model updating process.

- FE model calibration using ANNs would be inaccurate and misleading if an inappropriate training dataset is used to train the network and definitely it is not due to incapability or deficiency of the ANNs. The best training dataset can be consist of a combination of all parameters which are randomly selected in their effective ranges.

- The sensitivity analyses demonstrated that translational stiffness affected significantly the higher modes (V3 and T3), while fundamental modes (V1 and T1) were affected more by rotational stiffness. Therefore, both translational and rotational stiffnesses of the boundary conditions were selected as the parameters representing the actual bridge support behavior.

- This research clearly indicated the significance of boundary conditions considering the rotational stiffnesses. The crucial role of the rotational stiffness was confirmed since the frequency of mode V1 for bridge B1 with idealized pinned support was far from the field-measured frequency. Therefore, the model updating with pinned support assumption would result in erroneous parameter estimations such as a very high concrete elasticity modulus to increase the frequency of the FE model.

- The average order of error between frequencies of the field-measured data and updated FE model is 2.98% that shows the acceptable parameter predictions by the neural network based model updating process. The maximum error was 8% for the frequency of the second transverse mode while errors for the first vertical and transverse modes were considerably less and just 1.51% and 0.35% respectively.

- The MAC values between mode shapes of the field test and updated FE model were mostly higher than 0.95, indicating that the mode shapes extracted by the updated FE model and experimental test are at a satisfactory level of agreement, in addition to an acceptable level of accuracy for natural frequency estimations. The two lowest MAC values were 0.873 and 0.903 for third vertical and second transverse mode shapes respectively, which can be considered as the high degree of similarity. For these cases, more deviation in mode shapes at support location can be observed compared with other mode shapes.

- The variation of the mode shapes at the supports can be caused by the error in FE modeling, modal identification, and also the curve fitting process. Therefore, recording the responses of the bridge at the supports during the vibration tests can be highly beneficial to identify the real behavior of the boundary conditions.

6.2 Future works

Despite the promising results obtained and presented in the current thesis, further studies are required to improve and enhance the modal identification and model updating process of the railway bridges. In the following, just some further works and suggestions are listed:

- Evaluation of the variation in the identified modal parameters of the railway bridge through other train properties like velocity.

- The modal parameter identification of the studied bridges through the ambient or artificial dynamic excitation to compare with the results obtained from this research to provide a deeper insight into the effect of train crossings on the identified modal parameters.

- Determination of the optimal sensor locations and evaluation of the effect of different sensor locations on the quality of the identified parameters.

- Performing the model updating process considering nonlinearity in boundary conditions and material properties. In addition, comparison the other structural responses such as deflections, curve radius, and rotational angles at the supports.

- Evaluation of the boundary conditions behavior at each support separately. Since properties of the elastomeric bearings that the bridge rests on may be different from each other and may result in an asymmetry in the bridge behavior.

- Generating a 3D FE model, using shell or solid elements, representing the complete geometry of the bridge. The use of a 3D visualization can provide the opportunity for more accurate modal identification such as evaluation of the torsional modes. Also, for this, more sensors are required to be installed on 2 sides of the bridge.

References

[1] Rainieri, C. and G. Fabbrocino, Operational modal analysis of civil engineering structures. Springer, New York, 2014. 142: p. 143.

[2] He, J. and Z.-F. Fu, Modal analysis. 2001, Butterworth-Heinemann: Oxford;,Boston.

[3] Ghiassi, B. and P.B. Lourenço, Long-term performance and durability of masonry structures: degradation mechanisms, health monitoring and service life design. 2019, Woodhead Publishing, an imprint of Elsevier: Duxford, United Kingdom.

[4] Fu, Z.F. and He, J., 2001. Modal analysis. Elsevier.

[5] Grosel, J., W. Sawicki, and W. Pakos, Application of Classical and Operational Modal Analysis for Examination of Engineering Structures. Procedia Engineering, 2014. 91: p. 136-141.

[6] Cunha, A. and Caetano, E., 2006. Experimental modal analysis of civil engineering structures.

[7] Mbarek, A., et al., Comparison of experimental and operational modal analysis on a back to back planetary gear. Mechanism and machine theory, 2018. 124: p. 226-247.

[8] Chauhan, S., Parameter estimation and signal processing techniques for operational modal analysis. 2008, University of Cincinnati.

[9] Avitabile, P., Modal testing: a practitioner's guide. 1st ed. ed. 2017, Hoboken, NJ: Hoboken, NJ: Wiley.

[10] Peeters, B. and G. De Roeck, Stochastic system identification for operational modal analysis: a review. J. Dyn. Sys., Meas., Control, 2001. 123(4): p. 659-667.

[11] Masjedian, M. and M. Keshmiri, A review on operational modal analysis researches: classification of methods and applications. Proc. of the 3rd IOMAC, 2009: p. 707-718.

[12] Bendat, J.S. and A.G. Piersol, Random data: analysis and measurement procedures. Vol. 729. 2011: John Wiley & Sons.

[13] de Souza, J.T. and N. Barbieri, COBEM-2017-2347 Modal parameters identification methods based on output-only.

[14] Ghalishooyan, M. and A. Shooshtari. Operational modal analysis techniques and their theoretical and practical aspects: A comprehensive review and introduction. in 6th International Operational Modal Analysis Conference IOMAC 2015. 2015.

[15] Reynders, E., 2012. System identification methods for (operational) modal analysis: review and comparison. Archives of Computational Methods in Engineering, 19(1), pp.51-124.

[16] Bendat, J. S., Piersol, A. G., *Engineering applications of correlation and spectral analysis 2nd ed.*, Wiley Interscience, New York USA, 1993.

[17] Shih, C.Y., Tsuei, Y.G., Allemang, R.J., Brown, D.L., *Complex Mode Indicator Function and its Applications to Spatial Domain Parameter Estimation*, Proc. of IMAC XII 1989, Las Vegas, Nevada USA.

[18] Brincker, R., L. Zhang, and P. Andersen, *Modal identification of output-only systems using frequency domain decomposition.* Smart materials and structures, 2001. 10(3): p. 441.

[19] Brincker, R. and Zhang, L., 2009, May. Frequency domain decomposition revisited. In Proc. 3rd Int. Operational Modal Analysis Conf. (IOMAC'09) (pp. 615-626).

[20] Strang, G., Linear algebra and its applications 4th, Cengage Learning, 2005.

[21] Pioldi, F., Ferrari, R. and Rizzi, E., 2014, September. A refined FDD algorithm for Operational Modal Analysis of buildings under earthquake loading. In *Proceedings of the 26th International Conference on Noise and Vibration Engineering, Leuven, Belgium* (Vol. 1, pp. 3353-3368).

[22] Binda, L., Condoleo, P., Tiraboschi, C., Rigamonti, P., *On-site investigation and crack monitoring of an ancient bell tower*, Proc. of SFR 2012 (1-10), July 3-5, Edinburgh, Scotland.

[23] Pastor, M., Binda, M. and Harčarik, T., 2012. Modal assurance criterion. Procedia Engineering, 48, pp.543-548.

[24] Jin, B., Zhu, C., Yu, K., Li, Z. and Bai, Y., 2020, July. Comparison and application of two time-domain methods analysis to modal parameter identification of Songhuajiang River highway-railway bridge. In *IOP Conference Series: Materials Science and Engineering* (Vol. 892, No. 1, p. 012035). IOP Publishing.

[25] Zahid, F.B., Ong, Z.C. and Khoo, S.Y., 2020. A review of operational modal analysis techniques for in-service modal identification. *Journal of the Brazilian Society of Mechanical Sciences and Engineering*, *42*(8), pp.1-18.

[26] Brincker, R. and Andersen, P., 2006. Understanding stochastic subspace identification. In *Conference Proceedings: IMAC-XXIV: A Conference & Exposition on Structural Dynamics*. Society for Experimental Mechanics.

[27] Ho, B., Kalman, R.E. (1966), "Efficient Construction of Linear State Variable Models from Input/Output Functions", Regelungstechnik 14.

[28] Wu, C., Liu, H., Qin, X. and Wang, J., 2017. Stabilization diagrams to distinguish physical modes and spurious modes for structural parameter identification. Journal of Vibroengineering, 19(4), pp.2777-2794.

[29] Chen, G.-W., P. Omenzetter, and S. Beskhyroun, *Operational modal analysis of an eleven-span concrete bridge subjected to weak ambient excitations.* Engineering Structures, 2017. 151: p. 839-860.

[30] Lorenzoni, F., et al., Ambient and free-vibration tests to improve the quantification and estimation of modal parameters in existing bridges. Journal of Civil Structural Health Monitoring, 2019. 9(5): p. 617-637.

[31] Silva, M.S. and F.A. Neves, Modal identification of Bridge 44 of the Carajás Railroad and numerical modeling using the finite element method. Revista IBRACON de estruturas e materiais, 2020. 13(1): p. 39-68.

[32] Jin, B., et al. Comparison and application of two-time domain methods analysis to modal parameter identification of Songhuajiang River highway-railway bridge. in IOP Conference Series: Materials Science and Engineering. 2020. IOP Publishing.

[33] Pedrosa, B., et al., Modal Identification and Strengthening Techniques on Centenary Portela Bridge. Structural Engineering International, 2019. 29(4): p. 586-594.

[34] Magalhães, F., E. Caetano, and Á. Cunha, *Challenges in the application of stochastic modal identification methods to a cable-stayed bridge.* Journal of Bridge Engineering, 2007. 12(6): p. 746-754.

[35] He, X., et al., System identification of Alfred Zampa Memorial Bridge using dynamic field test data. Journal of Structural Engineering, 2009. 135(1): p. 54-66.

[36] Gönen S, Soyöz S. Dynamic Identification of Masonry Arch Bridges Using Multiple Methodologies. In Special Topics in Structural Dynamics & Experimental Techniques, Volume 5 2021 (pp. 37-47). Springer, Cham.

[37] Farrar, C.R. and Worden, K., 2007. An introduction to structural health monitoring. *Philosophical Transactions of the Royal Society A: Mathematical, Physical and Engineering Sciences*, *365*(1851), pp.303-315.

[38] Saadat, S., Noori, M.N., Buckner, G.D., Furukawa, T. and Suzuki, Y., 2004. Structural health monitoring and damage detection using an intelligent parameter varying (IPV) technique. *International Journal of Non-Linear Mechanics*, *39*(10), pp.1687-1697.

[39] Sanayei, M., Khaloo, A., Gul, M. and Catbas, F.N., 2015. Automated finite element model updating of a scale bridge model using measured static and modal test data. *Engineering Structures*, *102*, pp.66-79.

[40] Sehgal, S. and Kumar, H., 2016. Structural dynamic model updating techniques: A state of the art review. *Archives of Computational Methods in Engineering*, *23*(3), pp.515-533.

[41] Alkayem, N.F., Cao, M., Zhang, Y., Bayat, M. and Su, Z., 2018. Structural damage detection using finite element model updating with evolutionary algorithms: a survey. *Neural computing and applications*, *30*(2), pp.389-411.

[42] Collins JD, Hart GC, Hasselman TK, Kennedy B (1974) Statistical identification of structures. Am Inst Aeronaut stronaut J 12(2):185–190.

[43] Moravej, H., Jamali, S., Chan, T. and Nguyen, A., 2017. Finite element model updating of civil engineering infrastructures: A literature review. In Proceedings of the 8th International Conference on Structural Health Monitoring of Intelligent Infrastructure 2017 (pp. 1-12). International Society for Structural Health Monitoring of Intelligent Infrastructure (ISHMII).

[44] Tran-Ngoc, H., Khatir, S., De Roeck, G., Bui-Tien, T. and Wahab, M.A., 2019. An efficient artificial neural network for damage detection in bridges and beam-like structures by improving training parameters using cuckoo search algorithm. Engineering Structures, 199, p.109637.

[45] Chang CC, Chang TYP, Xu YG. Adaptive neural networks for model updating of structures. Smart Mater Struct 2000;9:59‑68.

[46] Bekdaş, Gebrail and Sinan Melih Nigdeli, and Melda Yücel. Artificial Intelligence and Machine Learning Applications in Civil, Mechanical, and Industrial Engineering. Hershey, PA: IGI Global, 2020.

[47] Hasançebi, O. and Dumlupınar, T., 2013. Linear and nonlinear model updating of reinforced concrete T-beam bridges using artificial neural networks. Computers & Structures, 119, pp.1-11.

[48] https://sebastianraschka.com/

[49] Mosavi, A.A., Sedarat, H., O'Connor, S.M., Emami-Naeini, A. and Lynch, J., 2014. Calibrating a high-fidelity finite element model of a highway bridge using a multi-variable sensitivity-based optimization approach. *Structure and Infrastructure Engineering*, *10*(5), pp.627-642.

[50] Park, Y.S., Kim, S., Kim, N. and Lee, J.J., 2017. Finite element model updating considering boundary conditions using neural networks. Engineering Structures, 150, pp.511-519.

[51] Maity, D. and Saha, A., 2004. Damage assessment in structure from changes in static parameter using neural networks. *Sadhana*, *29*(3), pp.315-327.

[52] Chang CC, Chang TYP, Xu YG. Adaptive neural networks for model updating of structures. Smart Mater Struct 2000;9:59–68.

[53] Zapico JL, Gonzlez-Buelga A, Gonzlez MP, Alonso RA. Finite element model updating of a small steel frame using neural networks. Smart Mater Struct 2008;17:1‑11.

[54] Ülker-Kaustell, M. and Karoumi, R., 2011. Application of the continuous wavelet transform on the free vibrations of a steel-concrete composite railway bridge. *Engineering structures*, *33*(3), pp.911-919.

[55] Chen, G.W., Chen, X. and Omenzetter, P., 2020. Modal parameter identification of a multiple-span post-tensioned concrete bridge using hybrid vibration testing data. Engineering Structures, 219, p.110953.

[56] Gomez HC, Ulusoy HS, Feng MQ. Variation of modal parameters of a highway bridge extracted from six earthquake records. Earthquake engineering & structural dynamics. 2013 Apr 10;42(4):565-79.

[57] Hristev RM. The ANN book. GNU public license; 1998.

[58] Atalla MJ, Inman DJ. On model updating using neural networks. Mech Syst Signal Process 1998;12:135‑61.